The Dissertation Committee for Caitlin Reese Schlagal Certifies that this is the

approved version of the following dissertation:

Impact on Endogenous Neural Stem Cells and Neurogenesis by Drugs of Abuse:

From Fetal Neurodevelopment to the Adult Brain

Committee:

Ping Wu, MD, Ph.D.

Kathryn Cunningham, Ph.D.

Jonathan Hommel, Ph.D.

Shelly Buffington, Ph.D.

Kimberly Nixon, Ph.D.

Impact on Endogenous Neural Stem Cells and Neurogenesis by Drugs of Abuse:

From Fetal Neurodevelopment to the Adult Brain

by

Caitlin Reese Schlagal, B.S.

Dissertation

Presented to the Faculty of the Graduate School of

The University of Texas Medical Branch

in Partial Fulfillment

of the Requirements

for the Degree of

Doctorate of Philosophy

The University of Texas Medical Branch

July 21, 2020

Dedication

I would like to thank my best friend and heart, Dan. There are no words to describe how your support and encouragement have helped me get here. Not only were you my rock through this whole process but the one who always reminded me to smile, laugh and fully embrace the experience.

To my Mom, who was always there for me and provided me with guidance when I was feeling overwhelmed. You have always encouraged me to pursue my passions. To my sister, Katherine, you challenged me to think outside the box and explore all avenues.

To my Grandma, you inspired my love of art and taught me patience that has helped me innumerable times during my studies. The same patience that is needed to carefully rip seam after seam, I applied when met with roadblocks in my project. To my Grandpa, you have always been my example of strength and perseverance. Thank you for always being there for me and supporting me.

To the memory of my Dad. Though you could not be here to witness the completion of my doctorate, I will always remember how proud you were when I was accepted into the Neuroscience graduate program. You inspired me to become the scientist I am today. I know I was able to finish with you looking down on me from above. Rest in peace.

Impact on Endogenous Neural Stem Cells and Neurogenesis by Drugs of Abuse:

From Fetal Neurodevelopment to the Adult Brain

Publication No._____

Caitlin Reese Schlagal, PhD

The University of Texas Medical Branch, 2020

Supervisor: Ping Wu, MD, PhD

Neural stem cells (NSCs) are a subpopulation of cells, found within the fetal and adult brain, that are integral to brain development, maintenance, and repair. Neurogenesis is the process through which NSCs proliferate and differentiate to create new neural cells within the central nervous system. These cells are vulnerable to drugs of abuse by decreasing self-renewal and subsequent differentiation, during adult or prenatal exposure. Recently, there has been an increase in the number of prescriptions written for opioids, leading to the current opioid epidemic. Further, prescription opioid use by women during pregnancy has risen dramatically since 2004. This rise was accompanied by a striking increase in the prevalence of neonatal opioid withdrawal syndrome and other long-term neurological deficits. Some of these drugs of abuse also include cocaine and alcohol, and the combination of which is the third leading cause of drug overdose deaths in the United States. While the effects of cocaine and alcohol, individually, on NSCs has been studied, the combined effects, whether additive or synergistic, remains unknown. This dissertation aimed to examine the effects of drugs of abuse on endogenous neural stem

cells and neurogenesis in two translationally relevant novel murine models of substance

use; in the developing and adult brain.

TABLE OF CONTENTS

List of Tables

List of Figures

List of Illustrations

List of Abbreviations

UTMB	University of Texas Medical Branch
GSBS	Graduate School of Biomedical Science
TDC	Thesis and Dissertation Coordinator
NSC	Neural stem cell
NPC	Neural progenitor cell
SGZ	Subgranular zone
SVZ	Subventricular zone
TL	Tanycyte layer
HtNSCs	Hypothalamic neural stem cells
BrdU	Bromodeoxyuridine
CSF	Cerebrospinal fluid
MBH	Mediobasal hypothalamus
DNA	Deoxyribonucleic acid
EdU	5-Ethynyl-2'-deoxyuridine
eYFP	Endogenous Yellow Fluorescent Protein
GFP	Green Fluorescent Protein
CUD	Cocaine Use Disorder
AUD	Alcohol Use Disorder
SUD	Substance Use Disorder
GABA	Gamma-aminobutyric acid
CES1	Carboxylesterase 1
CNS	Central nervous system
SAMHSA	Substance Abuse and Mental Health Services Administration
OUD	Opioid use disorder

DSM-5	Diagnostic Statistical Manual of Mental Health Disorders 5
NOWS	Neonatal opioid withdrawal syndrome
MAT	Medication-assistance treatment
RELN	Reelin
LC-MS	Liquid chromatography coupled to mass spectrometry
COC	Cocaine
BCE	Benzoylecgonine
CE	Cocaethylene
DCX	Doublecortin
GFAP	Glial fibrillary acidic protein
oRMS	Origin of the rostral migratory stream
NeuN	Neuronal nuclear antigen
BEC	Blood ethanol concentration
PCR	Polymerase chain reaction
ADHD	Attention-deficit/hyperactivity disorder
E18.5	Embryonic day 18.5
BUP	Buprenorphine
VTA	Ventral tegmental area
OXY	Oxycodone
OXY+BUP	Oxycodone plus buprenorphine
CRL	Crown-rump length
SOX2	Sex determining region y-box 2
Tbr2	T-box brain protein
VZ/SVZ	Ventricular zone/subventricular zone
ROI	Region of interest

SATB2	Special AT-rich sequence binding protein
Ctip2	COUP-TF-interacting protein 2
Cux1	Cut-like homeobox 1 protein
PND	Postnatal day
TH	Tyrosine hydroxylase
FST	Force swim test
ICV	Intracerebroventricular
Agrp	Agouti-related peptide
MSG	Monosodium glutamate
MRI	Magnetic resonance imaging
PFC	Prefrontal cortex
DAT	Dopamine transporter
D4R	Dopamine 4 receptor
qRT-PCR	Real-time quantitative reverse transcription polymerase chain reaction

CHAPTER 1: INTRODUCTION

Neural Stem Cells during Fetal Neurodevelopment

Neuroepithelial cells, known as neural stem cells, line the neural tube in the layer closest to the ventricular space and give rise to all lineages of cells in the central nervous system [2,3]. One of the first processes to begin in an embryo, neural development results in one of the most complex structures within the body and is one of the last completed after birth. Vertebrate embryology is unified, chronologically, using Carnegie stages, which allows for the comparison of developmental milestones across different vertebrate species [4]. Following fertilization and blastula formation, gastrulation occurs resulting in the different germ layers known as the endoderm, mesoderm and ectoderm [5]. Highly controlled and regulated, the central part of the ectoderm will form the neural plate (Carnegie stage 9), which begins to fold over the notochord. This folding will continue to form the neural groove, which will then begin to fuse, proceeding in both rostral and caudal directions [5]. This process, known as neurulation, will result in the formation of the neural tube, open at both ends by the anterior neuropore and caudal neuropore [6]. The anterior neuropore will close before the caudal neuropore, and a failure to close can result in complications known as neural tube deficits [6].

The neural tube will give rise to both the brain and spinal cord, in a developing embryo [6]. Following this is the formation of three primary vesicles, which include the prosencephalon, mesencephalon and rhombencephalon that will become the forebrain, midbrain and hindbrain, respectively [5]. At Carnegie stage 14, approximately week 5 in a human and 11.5 days in a mouse, five secondary vesicles begin to form from the primary vesicles including the telencephalon, diencephalon, mesencephalon, metencephalon, and myelencephalon [7](**Table 1**).

	Primary Vesicles	**Secondary Vesicles**	**Brain Structures**
Neural Tube	Prosencephalon (forebrain)	Telencephalon	Cerebral hemispheres
		Diencephalon	Caudal forebrain; thalamus, hypothalamus, third ventricle
	Mesencephalon (midbrain)	Mesencephalon	Midbrain
	Rhombencephalon (hindbrain)	Metencephalon	Pons, Cerebellum, 4th ventricle
		Myelencephalon	Medulla oblongata

Table 1: **Brain Structures Formed from Developing Neural Tube.**

Next is the formation of the ventricular system, which forms from the hollow space within the neural tube, and will lead to the development of the ventricles in the brain, as well as the central canal of the spinal cord [8]. Found in the ventricular layer, NSCs will give rise to progenitor cells known as neuroblasts and glioblasts [9,10]. Neuroblasts will migrate out along radial glial cells to incorporate into the cortical plate. Glioblasts will differentiate into different glial cells within the central nervous system including radial glia, oligodendrocytes and astrocytes.

Development of cortical layers begin with formation of the pre-plate in the embryo brain [11]. The pre-plate is formed from Cajal-Retzius cells which will become Layer I in the cortical plate [12]. Layer I cells secrete many signals which help to drive the correct organization and migration of subsequent layers and one example of this is a glycoprotein called reelin (RELN) [12]. A well-characterized animal model with mutated Reelin expression, *reeler* mice, show a dramatic effect in the disorganization of the cortical plate

[11,13]. Forming next is layer VI, which is the deepest layer in the cortical plate. Cells from the ventricular zone will migrate to the pre-plate and will then divide to form the subplate and marginal zone. Subsequent layers, starting with V and proceeding sequentially to II, will pass through the subplate until reaching the upper marginal zone, where they will stop and divide [11,14] (**Illustration 1**). Perturbations in cortical layer development can lead to learning disabilities, seizures and mood disorders [15-19].
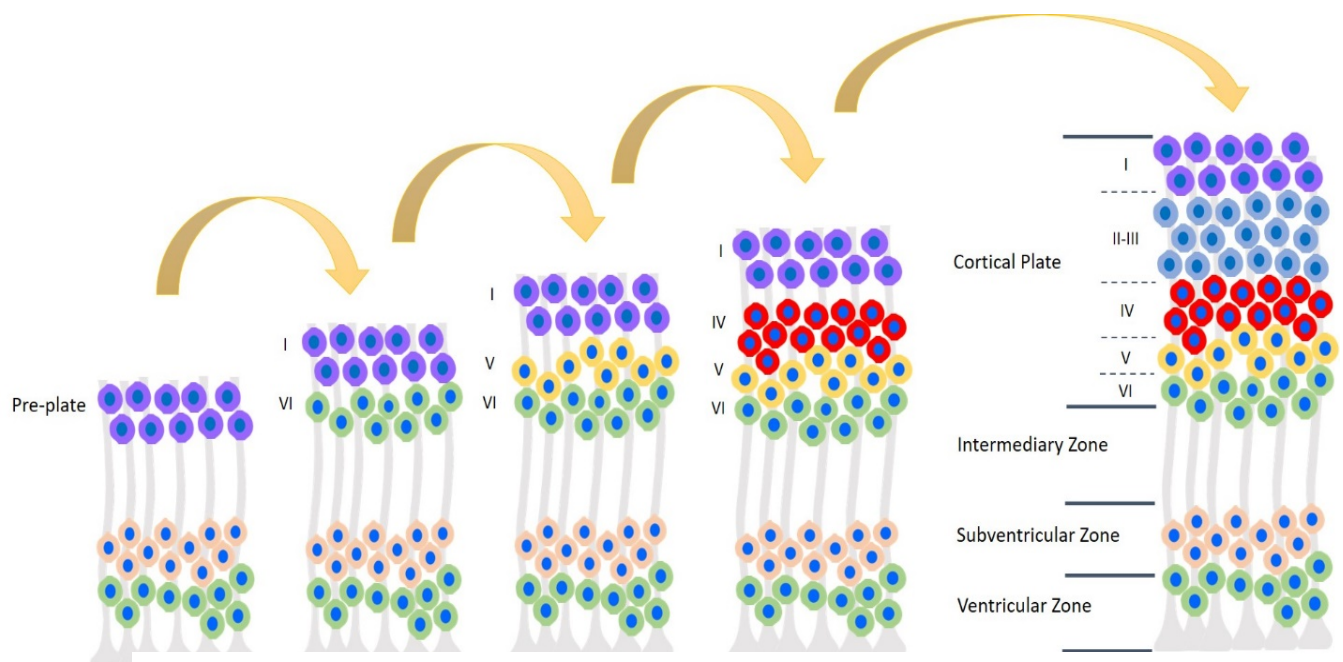
Illustration 1: Development of Cortical Layers in Fetal Brain.

Neural Stem Cells in the Adult Brain

Neurogenesis was first proposed in 1962 by Joseph Altman, not without debate, and launched an ever-expanding field that showed new neurons could be born from the adult brain [20]. Since then, neurogenesis has been extensively examined in both development and adulthood [21,22]. This phenomenon is crucial not only during development, where it drives the formation of neural connections and brain growth, but

also throughout life to generate new neurons in several key regions of the brain. Neural stem cells (NSCs) play an integral role in brain maintenance and repair in the adult brain [23]. NSCs are characterized by two main features, self-proliferation and differentiation into new neurons, astrocytes and oligodendrocytes. Differentiation into new neurons is called neuronogenesis while differentiation into astrocytes and oligodendrocytes is, more broadly, called gliogenesis [24].

Most NSCs are quiescent and wait for physiological cues, to proliferate or differentiate [25-27]. NSCs will undergo either symmetrical or asymmetrical division [28]. Symmetrical division is when NSCs divide into two new progenitor cells which will have the same committed cell fate. While asymmetrical division is when NSCs divide into a progenitor cell, as well as a daughter NSC which will go back to repopulate the NSC pool. Neural progenitor cells (NPCs) maintain cellular markers for a quiescent NSC state but are now primed to differentiate into either neuronal or glial cells [28,29]. The route of differentiation also depends on cues, sensed through the surrounding environment [25,27]. For example, pro-inflammatory states, within the brain, can increase the differentiation ratio of NPCs towards glial lineages versus neuronal [30-32]. The two most studied neurogenic regions, where this occurs in the adult brain, are the subgranular zone (SGZ) of the hippocampus and the lateral ventricles of the subventricular zone (SVZ) [21,25,33].

The SGZ has been shown to play a role in memory and learning due to the close association within the inner layer of the dentate gyrus of the hippocampus [34-36].Within this region, NSCs will be incorporated into the dentate gyrus as new neurons or astrocytes. These cells undergo a well characterized differentiation into new, mature neurons [37]. Mice with deficits in SGZ neurogenesis show impairments in multiple behavioral tasks, related to learning and memory, including; novel object recognition, marble burying, and fear condition context discrimination, to name a few [35,36,38]. The second well-characterized

region for NSCs, is the SVZ. Progenitor cells born from this population will travel down the rostral migratory stream and be integrated in the olfactory bulb [36,39].

More recently, a new population of NSC-like cells, found in the tanycyte layer (TL) of the third ventricle, have been under investigation. In 1954, Ernst Horstmann discovered tanycytes lining the third ventricle and named them for the Greek word 'tany' meaning drawn out [40]. This was due to the morphology of the cells and the long tail-like processes that extended away from the ventricle. Later on tanycytes were divided into subpopulations due to their morphology, and they are known as alpha1, alpha2, beta1, and beta2 [41] (**Illustration 2**).
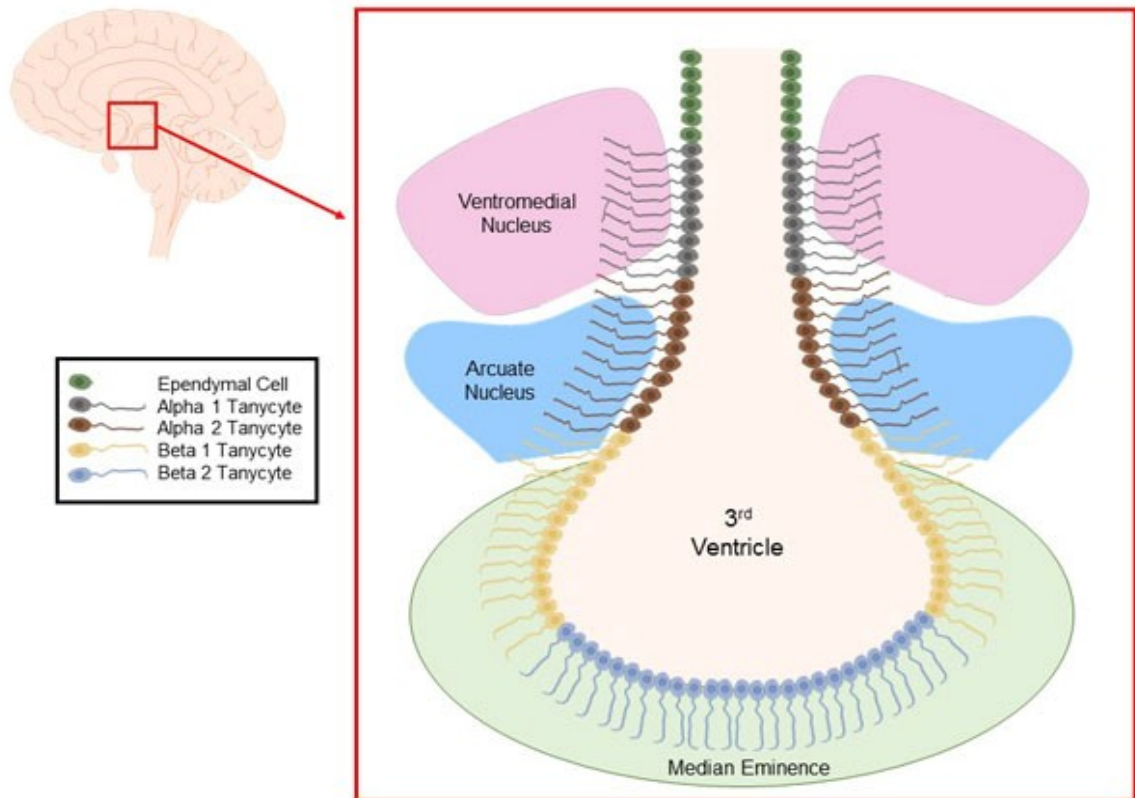
Illustration 2: Hypothalamic Neural Stem Cells lining the Third Ventricle. Accessed from: Schlagal C.R., Wu P. Tipsy Neural Stem Cells. Neural Regeneration Research[1]

It was more recently that tanycytes were shown to have neurogenic capabilities via bromodeoxyuridine (BrdU) staining and other advanced molecular techniques [42,43].

Robins et al., showed that it was the alpha2 subpopulation, that expressed NSC-like capabilities, with these cells differentiating into primarily new astrocytes and less frequently, new neurons [42]. However in 2013, Haan et al., showed that the beta1 cells were also capable of differentiating into new neurons, however this was a temporal increase between P4-P28 in mice [43]. Since then, other groups have confirmed the neurogenic properties of tanycytes which led to them being identified as hypothalamic neural stem cells (htNSCs) [44-49].

Due to their location along the third ventricle, htNSCs have been primarily studied for their role in energy homeostasis and neuroendocrine functions [50-53]. HtNSCs lining the third ventricle are directly exposed to cerebrospinal fluid (CSF) and therefore act as sensors, relaying information back to the mediobasal hypothalamus (MBH) [50]. Additionally, researchers have further expounded upon the role of htNSCs in energy homeostasis by investigating the role of taste receptors found on the surface of these cells [54]. Also found on the tongue, these taste receptors are G-protein coupled receptors, which can send secondary signals to the cell to modulate the hypothalamus [55].

The subpopulation of alpha-htNSCs lack tight junctions between the cells, allowing CSF to permeate the arcuate nucleus of the hypothalamus, and therefore making it a circumventricular organ [44]. This is crucial because circulating neurotoxins can therefore pass through and detrimentally impact cells lining the ventricle or within the arcuate nucleus. The subpopulation of beta-htNSCs, on the other hand, have tight junctions between the cells which prevents this from happening [50]. One group has shown that ablation of htNSCs results in decreased locomotion, impaired learning and memory, as well as expression of an advanced aging phenotype [45]. This could suggest that htNSCs play a large role in energy homeostasis, by sending key signals to the hypothalamus to regulate cell aging processes.

Tools of the Trade

Traditionally, neurogenesis was investigated using tracers such as ^{3}H-thymidine and BrdU to label cells [22]. BrdU is a thymidine derivative that is incorporated into the deoxyribonucleic acid (DNA) of dividing cells, and as such was the gold standard to labeling NSCs for an extended period of time [56]. However, BrdU can cause DNA damage upon incorporation, so other, less toxic, derivatives have become more commonplace, such as 5-ethynyl-2'-deoxyuridine (EdU). Another alternative approach available today are transgenic mouse models, tools which can allow us to better study disease states such as addiction. In 2007, Lagace et al., produced a reliable Cre/Lox bi-transgenic mouse model which allowed for fate-tracking of NSCs across time [57] (**Illustration 3**).
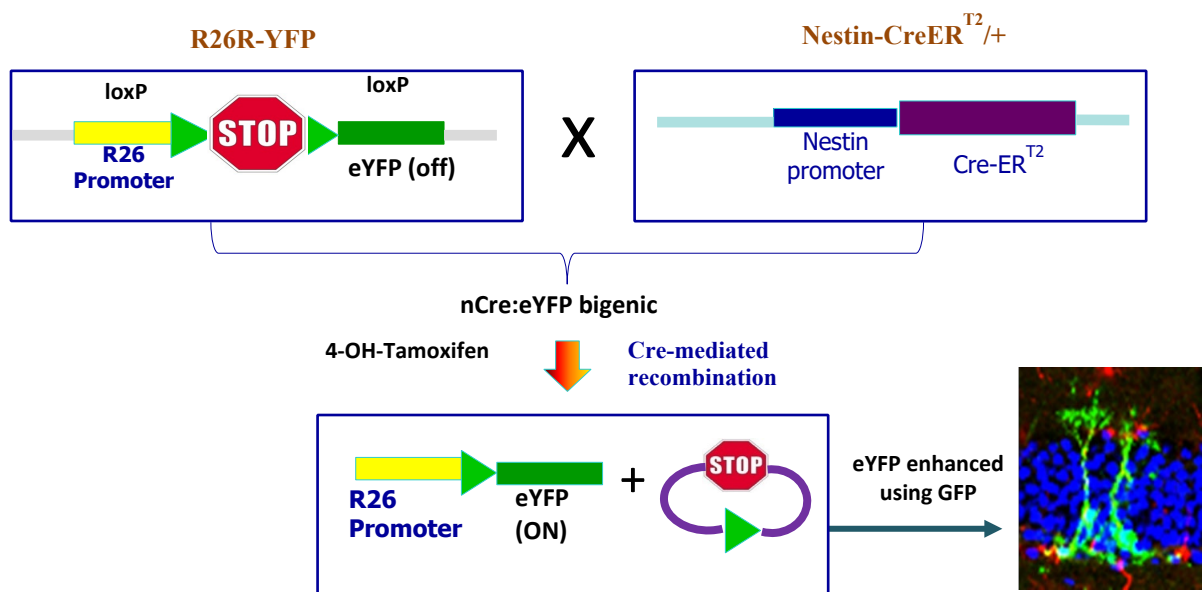
Illustration 3: Diagram for Cre/Lox Bi-transgenic Mice. Upon induction, tamoxifen will bind to the Cre recombinase coupled to the estrogen receptor (Cre-ER). The fusion protein will translocate to the nucleus where it will cleave the stop codon, allowing for constitutive expression of eYFP in all nestin expressing cells.

This model works by crossing R26R-YFP mice, which have the endogenous yellow fluorescent protein (eYFP) floxed by two lox-P sites under control of the Rosa26 promoter,

with Nestin-Cre mice to produce Cre/YFP offspring. Nestin is an intermediary filament that is expressed in quiescent and active NSCs. Upon administration, 4-hydroxy-tamoxifen, a prodrug which is metabolized to tamoxifen, will bind to the mutated estrogen receptor found in all nestin-expressing cells. Upon binding, Cre will then relocate to the nucleus, cleaving the Lox-P sites, enabling constitutive YFP expression in all Nestin expressing cells. The YFP can then be immune-enhanced using a green fluorescent protein (GFP) primary antibody and specific NSC populations can be investigated over time. This model allows for temporal investigation of endogenous NSCs, despite proliferation or differentiation.

Another alternative mouse model which can be used to study NSCs was created by Enkipolov et al. and is a Nestin-GFP model [58]. These mice have constitutive GFP expression in all Nestin expressing cells. Our lab has used this model to study embryonic disease states such as Zika infection and maternal opioid use. Utilizing this model, we can therefore track NSC development and differentiation in a developing embryo, as well as through adolescence and even into adulthood. New genetic manipulations and tools provide researchers with beneficial models to study different disease states. It has been shown that different activities can promote neurogenesis including exercise, learning new skills and even fasting [59-61]. Additionally, these models can also give us unique insight into disease states, which can negatively impact neurogenesis during development or adulthood, such as addiction.

NEURAL STEM CELLS AND DRUGS OF ABUSE

OPIOID EPIDEMIC IN THE UNITED STATES

Recently, an opioid epidemic has been on the rise in the United States [62]. In 2012, there was a dramatic increase in the number of prescriptions written for opioids, with over 250 million prescriptions being written in one year alone [63]. This amount is enough for every adult American to receive their own bottle of opioids. Along with the rise in opioid prescription availability there was also a rise in misuse, abuse and dependence on prescription opiates [63]. In 2015, the Substance Abuse and Mental Health Services Administration (SAMHSA) reported two million people were diagnosed with opioid use disorder (OUD) [64]. It is important to distinguish between opioid misuse and opioid use disorder. Opioid misuse can encompass improper use of prescriptions, such as taking opioids that had been prescribed to a family member or taking more than what was prescribed. Opioid use disorder is defined in the diagnostic statistical manual of mental health disorders 5 (DSM 5), and individuals can be diagnosed by meeting a minimum of 2 out of the 11 criteria, which could be increased cravings or tolerance, for example [65]. Furthermore, this trend of opioid misuse has continued with the National Survey on Drug Use and Health reporting 9.4 million people were misusing pain relievers, 92% of which was opioid misuse [66].

Oxycodone, or known by its brand name OxyContin®, is a semisynthetic opioid prescribed for the treatment of moderate to severe pain [67]. SAMHSA reported that oxycodone is one of the most commonly prescribed opiates for pain [64]. Additionally, groups have shown that rodents will self-administer oxycodone, which provides evidence for the reinforcing effects of the drug [68]. Oxycodone has high potency due to its active influx across the blood brain barrier [69]. Females are more sensitive to the analgesic effects of oxycodone and are more likely to develop OUD [70]. Therefore, along with the rise in prescription availability, there was also a documented increase in the number of prescriptions written for pregnant women [71]. However, OUD in pregnant females has been

shown to lead to the development of neonatal opioid withdrawal syndrome (NOWS) [72-75]. Indeed, in 2018, there was a reported 433% increase in the prevalence of NOWS [72].

Clinical cases have documented dramatic health and developmental consequences for offspring from pregnant women taking opiates, such as oxycodone. This led to the implementation of medication-assistance therapy (MAT) in the clinic [76-80]. MAT with methadone, a full opioid agonist, or buprenorphine, a partial opioid agonist, are the most common. However, increasing evidence shows negative health and developmental effects for the fetus including: low birth weight, NOWS, cardiac complications and CNS deficits [81-89]. Clinical studies have shown methadone increases the likelihood for the development of NOWS, compared to buprenorphine, which shows less post-delivery complications [75,89-92]. However, few preclinical studies have investigated the role of buprenorphine on fetal neurodevelopment and adolescent behavior, despite multiple clinical studies showing a detrimental impact of MAT with BUP on learning and attention in offspring [93-95]. Additionally, very little is known regarding the effects of MAT in pregnant women on embryonic NSCs.

ALCOHOL AND COCAINE POLY-DRUG USE

The role of drugs of abuse on NSCs has been studied, extensively, due to the crucial role of NSCs in brain maintenance and repair. Multiple groups have shown that drugs of abuse such as alcohol, cocaine, or opiates can impact the endogenous neural stem cells in the adult brain [96-102]. Research has shown that individual use of these drugs can affect the quiescent NSC pool, and the loss of NSCs can affect behavior leading to learning or memory deficits and, possibly, the development of psychiatric illnesses [98]. While studying the individual effects of drugs, on NSCs, helps to tease apart the direct effects; translationally, it is also important to study combined drug abuse since most users will abuse two drugs to ameliorate the negative side effects of a single drug. Cocaine use

disorder (CUD) and alcohol use disorder (AUD) are highly prevalent substance use disorders (SUDs) in the United States, which are associated with long-term use and high risk for relapse [97,103]. All SUDs cost the US $440 billion annually, with 12 million Americans co-abusing cocaine and alcohol each year [62].

Poly-drug abuse, of cocaine and alcohol, represent a significant problem due to the synergist effects when two drugs of abuse are combined [104-110]. Cocaine acts by blocking monoamine transporters, thereby increasing extracellular levels of dopamine commonly associated with feelings of euphoria, excitement, and increased energy [111]. Conversely, alcohol is a common 'depressor' which acts on many neurotransmitter systems, primarily through the activation of gamma-Aminobutyric acid (GABA) and inhibition of glutamate [112] [113]. While there is a 'high' associated with alcohol, this occurs only at low to moderate doses and exceeding this results in impaired cognition and motor control as well as increased depressive-like emotions [1]. Cocaine and alcohol are frequently co-abused due to the amelioration of common negative side effects of the individual drugs [114,115].

Chronic consumption of cocaine or alcohol can result in impaired cognition, psychological symptoms, and advanced aging [106]. Also documented, are memory deficits following chronic combined use, which persist even after abstinence from cocaine use [97,116]. Interestingly, it has also been documented that females have greater euphoria when cocaine and alcohol are combined, compared to males [117]. When these two drugs are combined, they are metabolized by carboxylesterase 1 (CES1) to create a new psychoactive compound known as cocaethylene [118]. Cocaethylene has a half-life three times that of cocaine and has been shown to be ten times more cardio-toxic [104]. One study has shown negative consequences on the central nervous system (CNS) following cocaethylene administration [119]. It is known that individual use of cocaine or alcohol can have deleterious effects on the endogenous neural stem cell population [48,96,97,100,102,120]. It

is unknown if this destruction is driven by the production of cocaethylene, a toxic metabolite.

Attention-Deficit/Hyperactivity Disorder in Adolescence

Neurodevelopmental disorders can arise during adolescence and can detrimentally impact learning, memory and social behaviors in young children. Some of these disorders include attention-deficit/hyperactivity disorder (ADHD), autism spectrum disorder (ASD), depression, and others. Maternal opioid use has been linked to neurodevelopmental disorders in adolescent offspring, including ADHD [93,121-124]. ADHD is a neurodevelopmental disorder classified by hyperactivity, inattention, impulsivity, and altered social behaviors [125,126]. Multiple studies have also shown a sex-dependent manifestation of symptoms, where males presenting with ADHD are more likely to have hyperactivity/impulsivity than females [127-129]. Indeed, studies show that males are more likely to develop ADHD than females, however some clinicians argue this could be due to females presenting with less obvious symptomology [129].

Clinical studies have shown that patients with ADHD are more likely to have a significantly smaller brain size than matched healthy controls [126,130-132]. There have also been studies showing a decrease in white matter in young patients with ADHD [126,132]. One group posed the theory that these observed brain changes are a delay in development rather than a permanent alteration [131]. Along with changes in brain structure, ADHD has also been linked to an imbalance in neurotransmitters, specifically dopamine and norepinephrine [133,134]. Dopamine deficits have been observed in multiple ADHD animal models, specifically in the prefrontal cortex, as well as, altered dopamine transporter (DAT) levels [135-137]. Indeed, the most commonly prescribed treatments for ADHD including, methylphenidate or amphetamine, have DAT as a principal target [132,136-139]. This led to a prevailing dopamine deficit theory, or hypo-dopamine, that by name is misleading [125]. Multiple reports have shown that there is in fact a higher baseline tone of dopamine in the

animal models of ADHD and alterations of dopamine neurons within the ventral tegmental area (VTA) [134,137,140-142].

The VTA is found in the midbrain, next to the substantia nigra, where the dopaminergic neurons of the brain reside [143-145]. The VTA has been linked, via projections to the nucleus accumbens and prefrontal cortex, to behaviors dealing with reward and motivation, as well as, cognitive and executive functioning, respectively [145-147]. The VTA has been implicated in ADHD, due to these crucial dopamine projections and associated behaviors which are altered in ADHD [134,140,141].

Specific Aims

Few studies have investigated the role of opioid administration in pregnant dams on fetal NSCs. Clinical studies have shown that opioid use during pregnancy can increase the chance for development of NOWS, cardiac complications, and later developmental disorders in offspring [72,75,78,93,121,148]. Moreover, preclinical studies investigating this have failed to take into consideration the clinical presentations of opioid use in pregnant females [149]. Specifically, prescription opioids during pregnancy are prescribed to women who come into the clinic with opioid use disorder prior to pregnancy and are placed on MAT to avoid negative withdrawal symptoms and relapse.

Specific aim 1 was designed to address some of these critical gaps in knowledge in a novel murine model, that is simulated based on clinical presentations of maternal opioid use. We established opioid dependency in female mice [68], prior to pregnancy, and then transitioned to BUP MAT following pregnancy confirmation. We investigated changes in overall size and cortical development at E18.5, as well as, changes in emerging adulthood behavior and neuronal ontogenesis at PND60. We hypothesized we would see

reductions in brain size, alterations in cortical development and a depressive-like behavioral phenotype in prenatally opioid-exposed offspring.

Additionally, single administration of cocaine or alcohol has been well characterized, however the effects of poly-drug administration, with a specific emphasis on endogenous neural stem cells and neurogenesis in the adult brain, has yet to be explored. Therefore, the goal of specific aim 2 was to investigate the effects of poly-drug use on NSCs in three neurogenic regions; the SVZ, SGZ and TL. To accomplish this, we used a transgenic fate-mapping animal model to track NSCs, across a chronic administration paradigm, despite proliferation or differentiation. We also investigated behaviors which could be affected following reductions of neurogenesis, in these key regions. We hypothesized that combined drug administration would be more detrimental than single drug use and would negatively affect memory in animals who received poly-drug administration.

CHAPTER 2: PRENATAL OPIOID EXPOSURE AFFECTS FETAL NEURODEVELOPMENT AND CONTRIBUTES TO HYPERACTIVE PHENOTYPE IN ADOLESCENCE

INTRODUCTION:

Opioid misuse is garnering increased scrutiny due to the national opioid epidemic currently unfolding in the United States [64]. The opioid crisis has been fueled by over-prescription of opioid-based pain medications as well as socioeconomic circumstances that have together resulted in increased prevalence of opioid use disorder (OUD), including among pregnant women [64,71]. The increased prevalence of OUD in pregnant women has been paralleled by a staggering increase in neonatal opioid withdraw syndrome (NOWS), which can be caused by either illicit or prescription opioid use. To note the scale of this problem, between 2004 and 2014, there was a documented 433% rise in NOWS [72]. In addition to NOWS, fetal consequences of maternal opioid use include decreased birth weight, increased duration of hospital stay following delivery, as well as other defects such as, microcephaly and reduced cortical thickness in the central nervous system [81-83,86,88,93,122]. Furthermore, maternal opioid use has been associated with short- and long-term behavioral alterations in adolescent offspring, including learning and memory deficits, hyperactivity, and impulsivity [93,123,124].

Despite overwhelming evidence that maternal opioid use can cause birth defects, 1.2% of women reported using an opioid during pregnancy in 2016 [64]. In an effort to curb negative health effects of opioids, women diagnosed with OUD are prescribed opioid substitution therapy, also known as medication-assisted treatment (MAT), to manage opioid withdrawal and craving symptoms [76,79]. The most frequently prescribed MAT substitution is the long-lasting receptor opioid receptor agonist methadone or the partial

opioid agonist buprenorphine [76]. While prescribed with the intent of improving maternal and fetal short- and long-term health outcomes, methadone and buprenorphine, like addictive opioids themselves, can also prove harmful to the fetal development[76,78-80].

Increased compliance rates with buprenorphine (BUP) usage, the second most commonly prescribed treatment for maternal opioid use following methadone, has resulted in a recent surge in BUP prescriptions during pregnancy [79]. Benefits of BUP treatment over methadone include shorter duration of infant hospitalization and decreased prevalence of NOWS-associated complications in affected infants [75,90-92,150]. While pregnant women diagnosed with OUD and presenting at an obstetric clinic are prescribed BUP, little is known about the short- and long-term effects of MAT BUP on pregnancy outcomes and long-term child health outcomes. To date, most studies of the effects of maternal opioid use and OUD in animal models have not followed the standard of care for pregnant women with OUD [149]. Furthermore, previous animal OUD models did not address crucial components in fetal neurodevelopment, such as neural stem cell and cortical development. Our novel model of OUD and maternal MAT addresses these gaps in knowledge by using an innovative transgenic mouse model with translational potential that allows for precise tracking of neural stem cell (NSC) lineage, migration, and maturation.

Neuroepithelial cells, also known as neural stem cells (NSCs), line the neural tube and give rise to all neural cells within the developing central nervous system, through proliferation, differentiation, and maturation [29]. NSCs also play a critical role in the organization of cortical layers. Furthermore, dysregulation of cortical neuron migration and differentiation have been linked to developmental disorders [151]. NSCs differentiate to become Cajal-Retizus cells, which will form layer I in the developing neocortex. These cells secrete reelin which directs proper migration of subsequent cortical layers as well as the organization of cells in other regions, such as dopamine neurons in the ventral tegmental area (VTA) [152]. Intriguingly, altered dopamine neurotransmission in the VTA has

been shown to lead to attention deficit hyperactivity disorder (ADHD)-like behavioral phenotypes such as hyperactivity and impulsivity [153], reminiscent of those children affected by maternal OUD [93].

In this study, we established a model in which female mice received oxycodone, one of the most commonly prescribed opioids for pain management [64], prior to mating and, following pregnancy confirmation, switched dams to oral BUP, similar to clinical presentations [72,93,122]. We then collected embryonic day 18.5 (E18.5) or adolescent brains to document changes in neurodevelopment following maternal opioid use. Adolescent mice were assayed for spontaneous motor activity and depressive-like behaviors. Our study showed teratogenic effects of BUP MAT, which is detrimental to fetal neurodevelopment and can promote a hyperactive phenotype in male adolescent offspring.

RESULTS:

Novel Murine Model of Prenatal Opioid Use Reflects the Clinical Standard of Care

To determine whether MAT for OUD affects offspring neurodevelopment and behavior, we designed a treatment course (**Fig. 1A**) that mimics the standard therapy of MAT in pregnant women using opioids, as seen in clinical presentation [79,80]. *Nestin*-GFP homozygous females were crossed with wildtype C57/Bl-6J males to produce heterozygous *Nestin*-GFP offspring, allowing tracing of neural stem cells [58]. Females received subcutaneous injections of oxycodone or vehicle, twice daily for seven days; injections were terminated the day before caging with a male. Following confirmation of the presence of the vaginal plug, designated as E0.5, females received liquid diet with or without BUP, orally. BUP was administered in a ramping regimen, over several days, to reach the desired dose, similar to clinical practice [148]. BUP was dissolved in Ensure high

protein liquid diet in custom feeding dishes and administered once daily (**Fig. 1B**). This dosing protocol reduced additional stress by eliminating daily injections, due to voluntary oral administration of the drug. Female dams treated with oxycodone plus BUP (OXY+BUP) showed no significant differences in home cage behavior during prenatal treatment, including grooming behaviors, such as coat maintenance and posture. There was no significant difference in weight gain between control and OXY+BUP dams. At E10.5, there was an increase in body weight of approximately 1 g, a trend we observed on each of the following days in both treatment groups (**Fig. 1C**). Additionally, there was no difference in the number of embryos per litter between the two treatment groups (**Fig. 1D**). The percentage of viable embryos did not significantly differ between control and OXY+BUP treated dams (**Fig. 1E**). Representative morphological features are shown for normal (**Fig. 1F**), resorbed (**Fig. 1G**), and miscarried embryos (**Fig. 1H**).
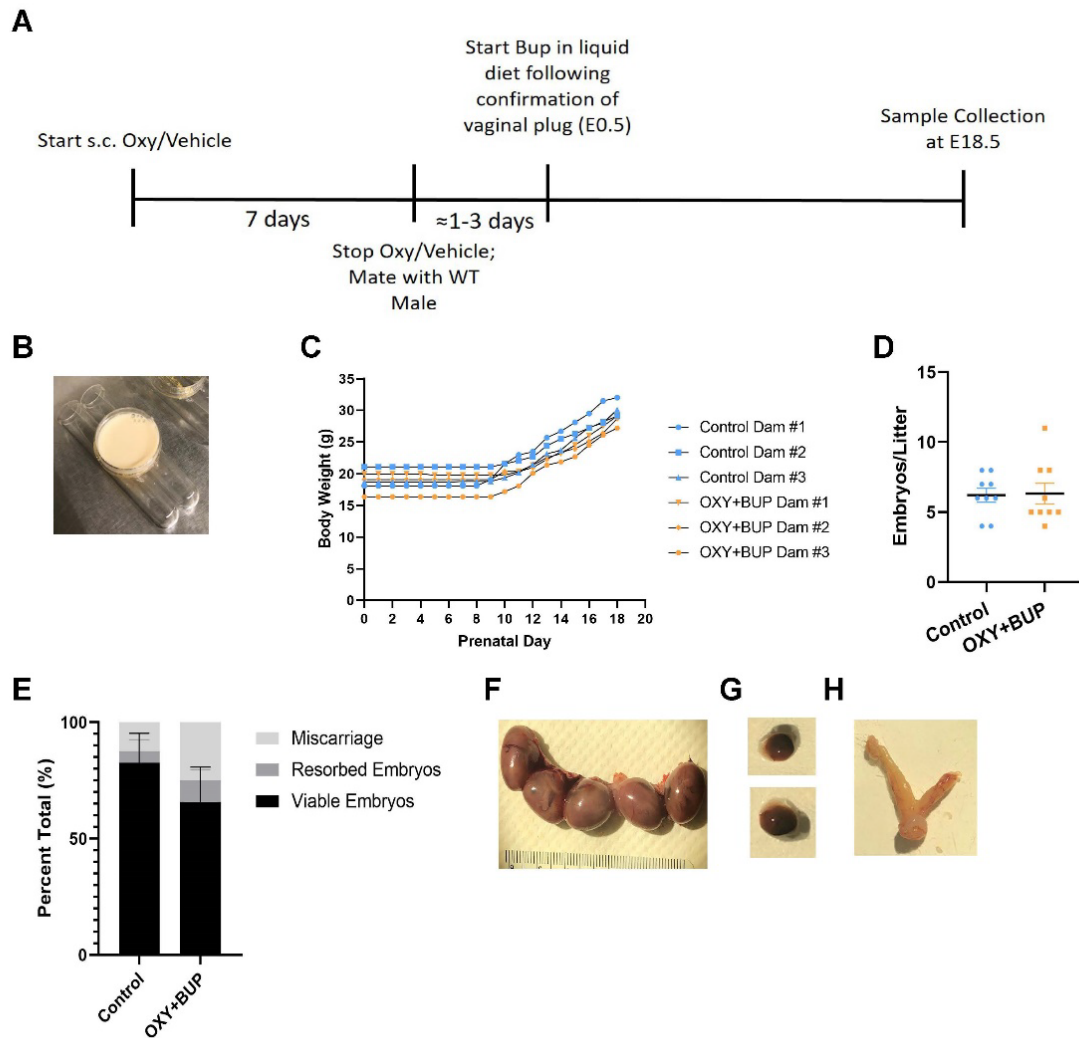
Figure 1. Experimental Timeline and Maternal Demographics

(A) Timeline for drug administration and sample collection for E18.5 samples and (B) example of liquid diet food dish. (C) Daily body weights of dams following confirmation of vaginal plug, n=3/treatment group. (D) Average number of embryos per litter (n=6 litters/treatment group) and (E) percent total number of intact embryos (n=6 litters/treatment group) (F), resorbed embryos (G), and miscarriage (H) from each treatment group. Quantitative data are represented as mean ± SEM.

Maternal Opioid Substitution Therapy Alters Embryo Gross Phenotype

Embryos were collected at E18.5 from control or OXY+BUP treated dams and photographed to analyze their gross phenotype (**Fig. 2A, 2B**). The size of OXY+BUP embryos, as measured by crown-rump length (CRL, **Fig. 2C,**) and width (**Fig. 2D,** P<0.05), was significantly decreased relative to controls without change in apparent placenta size (**Fig. 2A**). A dramatic 25% reduction (P<0.001) in CRL was observed in the OXY+BUP embryos relative to controls (**Fig. 2C**). The brain was then removed and measured to document changes in brain width and length (**Fig. 2E**). A significant decrease in brain length (**Fig. 2F,** P<0.05) and brain width (**Fig. 2G,** P<0.05) was detected in the OXY+BUP offspring vs. controls. The sex of all offspring was determined by standard PCR for lysine-specific demethylase 5c (Kdm5c, a gene specific to the X-chromosome) and lysine-specific demethylase 5d (Kdm5d, specific to the Y-chromosome) [154] (**Fig. 2H**). A two-way ANOVA indicated a main effect of sex ($F_{(1,18)}$ = 8.984, P=0.0077), and an interaction between sex X treatment ($F_{(1,18)}$ = 6.976, P=0.0166), but not a main effect of treatment ($F_{(1,18)}$ = 0.3884, *n.s.*), on the number of embryos/litter (**Fig. 2I**). Tukey's multiple comparisons analyses demonstrated significantly higher male, relative to female, embryos/litter from females treated with OXY+BUP vs. controls. Taken together our results show that prenatal opioid exposure detrimentally impacts overall body size, brain growth and sex of embryos.
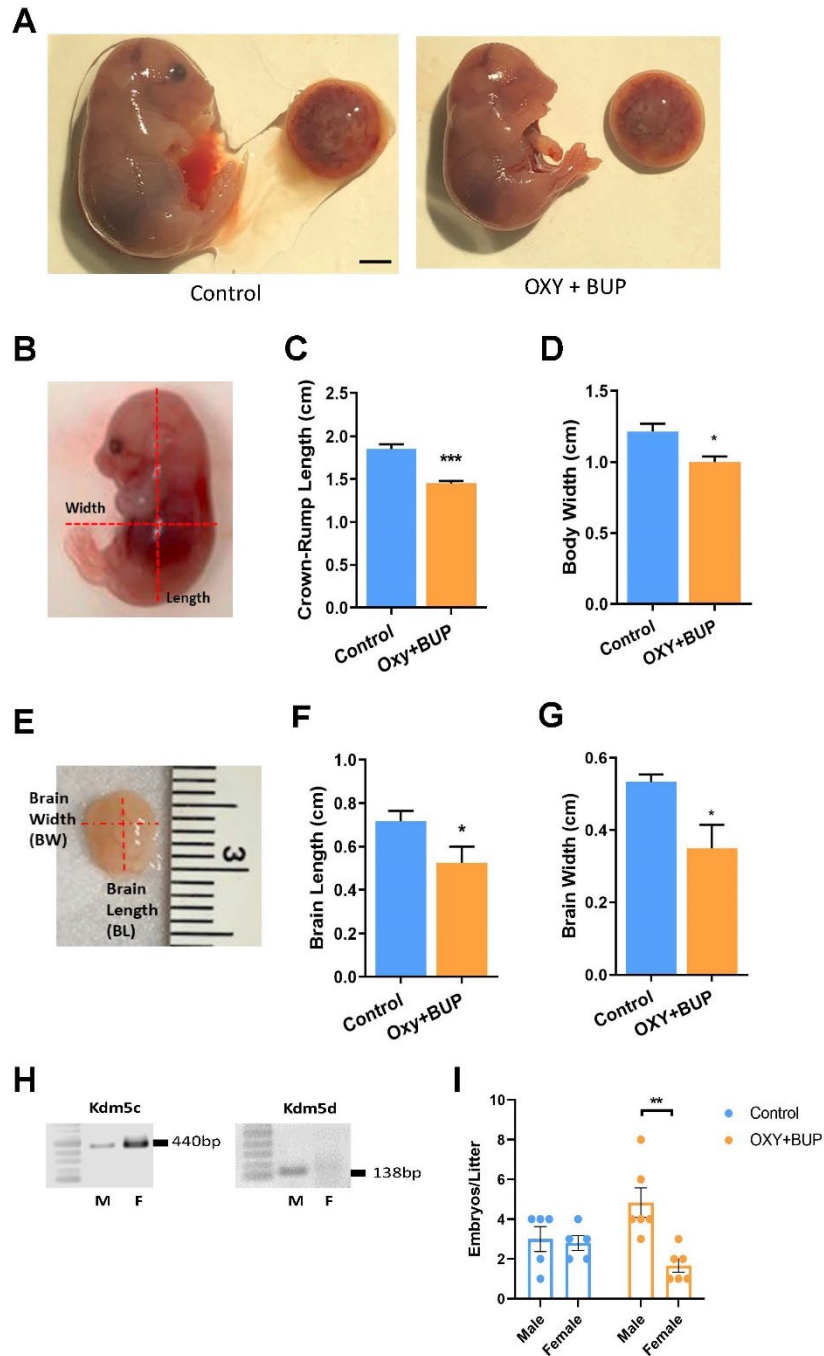
Figure 2. E18.5 Gross Phenotype and Measurements

(A) Representative images of overall body size between control (left) and OXY+BUP treated (right) embryos and placenta. (B) Representative image showing how crown-rump length (CRL) (C) and body width (D) measurements were taken, n=2 embryos/litter with 4 litters/treatment group. (E) Representative image showing how brain length (F) and brain width (G) measurements were taken, n=2 embryos/litter with 4 litters/treatment group. (H) Representative gel image showing positive identification of X- (Kdm5c) and Y-specific (Kdm5d) chromosomal markers used to determine embryo sex. (I) Graph showing the number of male or female embryos per litter, taken from 8 litters/treatment group. Scale bars, 3 mm. Data are represented as mean ± SEM with *p<0.05, **P<0.01, ***P<0.001, two-tailed *t*-test and two-way ANOVA with Tukey's test.

Maternal Opioid Substitution Therapy Alters Neural Stem/Progenitor Cell Proliferation at E18.5

Offspring generated in the experiment were heterozygous for Nestin-GFP [58]. Nestin is an intermediary filament and often used as a marker for NSCs or radial glia [49]. During development, since the neural cells generated arise from the NSCs, widespread GFP staining was visible in the brains of these animals. Due to this expression, GFP was sometimes excluded from representative images to emphasize the staining pattern of interest. To determine whether proliferation of NSCs and intermediate progenitor cells (together as NS/PCs) differed between the two treatment groups, we immunostained control versus OXY+BUP offspring brains at E18.5 for Ki67, a marker of proliferating cells. Additionally, cortical layer-specific proteins sex-determining region y-box 2 (Sox2) and T-box brain protein 2 (Tbr2) were used to investigate changes in the ventricular zone/subventricular zone (VZ/SVZ) (**Fig 3A**, red outline). Sox2 is a well-characterized marker for NS/PCs in the ventricular zone of E18.5 embryos, and Tbr2 is expressed by intermediate progenitor cells in the SVZ of the cortex. To demonstrate the regions selected for analyses, we included a lower magnification image from our own samples, along with comparable NISSL staining (image credit: Allen Institute [155,156]) (**Fig 3B**). There was a significant decrease in the number of Ki67$^+$ cells (approximate 50% reduction, $P<0.01$) in OXY+BUP-treated embryos, when compared to control (**Fig. 3C, 3D**). However, the number of Sox2$^+$ cells did not significantly differ between the two treatment groups (**Fig. 3E, 3F**). Quantification of Sox2$^+$ cells in VZ/SVZ was then established. The thickness of the Sox2-labeled layer within the VZ/SVZ of embryos did not differ between control or OXY+BUP treatment (**Fig. 3G**). By measuring the thickness of each layer, we aimed to determine whether the differences between maternal treatment groups were due to changes in cell migration. Additionally, neither the number (**Fig. 3H, 3I**) nor the thickness

(**Fig. 3G**) of Tbr2$^+$ cells in the SVZ differed between control and OXY+BUP-treated offspring.
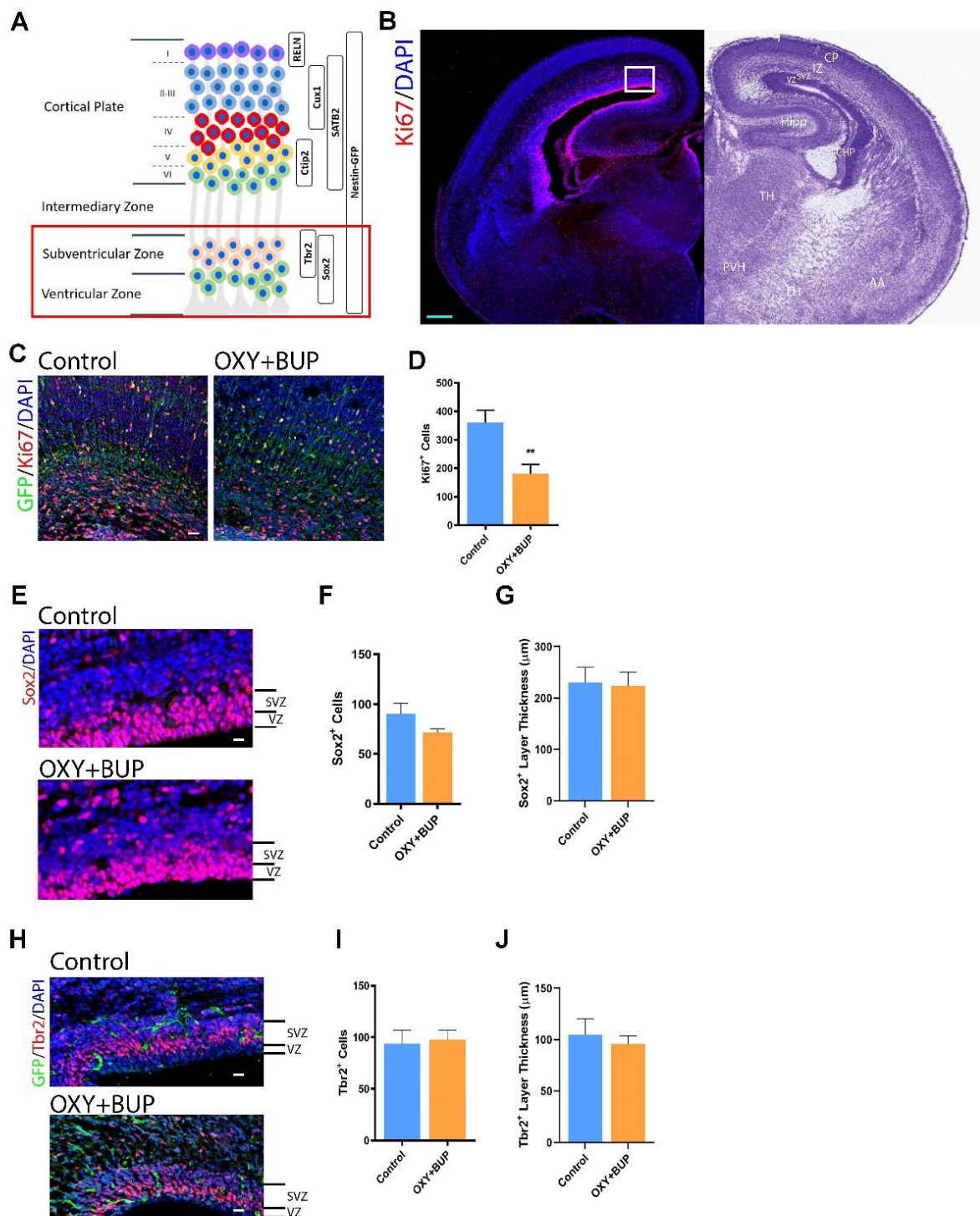
Figure 3. Altered NSC Proliferation during Prenatal Opioid Exposure

(A) Representative diagram showing cortical markers in mouse E18.5 embryos. Red box highlights specific markers for emphasis. (B) Left: 4x magnification of Ki67 staining for location reference. White box shows the selected ROI for quantification. Right: NISSL stained image provided by Allen Brain Atlas for reference. (C) Ki67 and GFP labeled, image at 20x magnification (D) Graph showing quantification of Ki67$^+$ cells. (E) Sox2 and GFP labeled, of Control and OXY+BUP E18.5 brains. (F) Graph showing number of Sox2$^+$ cells per ROI (G) Sox2 cell migration quantified. (H) Tbr2$^+$ staining in E18.5 with (I) graphing the number of positive cells. (J) Tbr2$^+$ cell migration quantification. Light blue scale bars are 500 μm. White scale bars are 100μm. Data are represented as mean ± SEM, n=2 embryos/litter with 4 litters/treatment group with *p<0.05, ***P<0.001, two-tailed *t*-test. AA- anterior amygdala, CHP- choroid plexus, CP- cortical plate, Hipp- hippocampus, IZ- intermediary zone, LH- lateral hypothalamus, PVH- paraventricular hypothalamus, SVZ- subventricular zone, TH- thalamus, VZ- ventricular zone.

Maternal Opioid Substitution Therapy Alters Corticogenesis at E18.5

Given our observation of reduced brain length and width in OXY+BUP embryos relative to controls (**Fig. 2F, 2G**), we first investigated changes in overall cortical thickness (**Fig. 4A**, yellow line). A significant reduction in cortical thickness (approximately 33%, P<0.0001) was observed in the OXY+BUP embryos at E18.5 (**Fig. 4B**). This opioid-mediated thinning of the cortex was accompanied by a significant increase in ventricle width (**Fig. 4A**, white line) that is almost doubled in the OXY+BUP embryos as compared to control (P<0.001) (**Fig. 4C**), indicating an opioid-induced ventricular enlargement.

We next explored the effects of maternal opioid exposure on cortical plate development, or corticogenesis. Corticogenesis is a highly regulated process and results in the formation of well-characterized cortical layers, I-VI, which can be investigated using specific markers [157] (**Fig. 4D**, red outline). The analyses were conducted by both quantifying the total number of cells in a set region of interest (ROI) for each layer and the distance of cell spread in a specific layer. In addition, we also measured the percent area of positive cells within the ROI to measure changes in cell density or size. Robust labeling of special AT-rich sequence-binding protein (SATB2), an upper-layer neuronal marker, was observed through layers II-VI with the OXY+BUP-treated group exhibiting a significant

decrease (approximately 40%, $P<0.01$) relative to controls (**Fig. 4E, 4F**). A significant decrease in the thickness of SATB2-labeled layers was also observed (**Fig. 4G, 4H,** $P<0.0001$). Finally, the percent of cells positively labeled for SATB2$^+$ in this area was significantly reduced in OXY+BUP vs. control, which was consistent with the decrease in total SATB2$^+$ cells within the ROI (**Fig. 4I,** $P<0.05$).

Next, immunostaining for COUP-TF-interacting protein 2 (Ctip2), a deep-layer neuronal marker corresponding to layers V and VI, revealed a significant decrease (approximately 50%, $P<0.05$) in the number of positively labeled cells in OXY+BUP-treated offspring (**Fig. 4J, 4K**). There was also a significant decrease in the thickness ($P<0.01$) of Ctip2-labeled layers and the percent area within this ROI ($P<0.05$) (**Fig. 4L-N**). Total cell counts, within the ROI, of cut-like homobox 1 protein (Cux1), a layer II/III marker, did not differ significantly between the two treatment groups (**Fig. 4O, 4P**). However, a trend towards a decrease in the thickness of Cux1-labeled layers was observed (**Fig. 4Q, 4R**). Additionally, the percent of positively labeled CUX1 cells within the ROI did not differ between treatments (**Fig. 4S**). Lastly, reelin (RELN) a layer I marker was examined. A trend towards reduced RELN$^+$ cells following OXY+BUP treatment was observed relative to controls, however no change was observed in layer thickness (**Fig. 4T-V**). Together our results show a significant influence of maternal opioid exposure due to changes in cortical thickness and ventricular widening. Taken together, we see distinct alterations in cortical layer development, specifically layer V and VI, in OXY+BUP offspring compared to control.

45
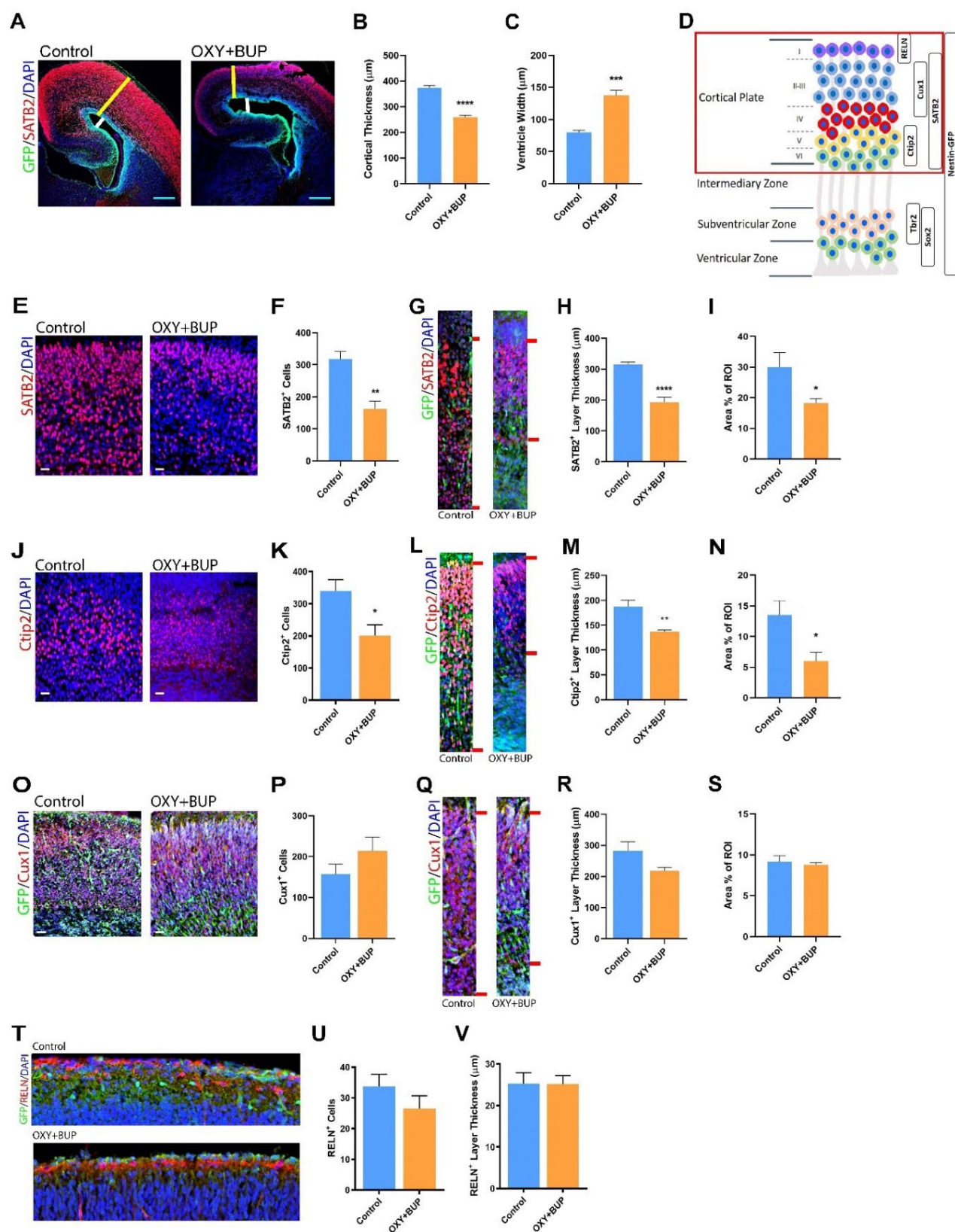
Figure 4. Altered Cortical Development during Prenatal Opioid Exposure

(A) Representative diagram showing cortical layer markers in E18.5 mouse embryos. Red box for emphasis on cortical plate markers. (B) SATB2 and GFP co-labeled, imaged at 4x magnification, of control and OXY+BUP E18.5 brains. Yellow line and white line denote cortical thickness and ventricular width measurements, respectively. (C) Graph showing cortical thickness. (D) Graph showing changes in ventricular width. (E) Representative images showing SATB2 and GFP staining of control and OXY+BUP E18.5 brains. (F) Graph showing SATB2$^+$ total cell counts for ROI. (G) SATB2 staining in E18.5 with red bars denoting measurement (H) graphing the migration of positive cells. (I) Quantification of percent area of SATB2$^+$ cells within ROI. (J) Representative images showing Ctip2 staining of control and OXY+BUP E18.5 brains. (K) Graph showing Ctip2$^+$ cell count. (L) Ctip2 staining in E18.5 with red bars denoting measurement of (M) migration of positive cells. (N) Quantification of percent area of Ctip2$^+$ cells within ROI. (O) Representative images showing Cux1 and GFP staining of control and OXY+BUP E18.5 brains. (P) Graph showing Cux1$^+$ cell count for ROI. (Q) Cux1 staining in E18.5 with red bars denoting measurement of (R) migration of positive cells. (S) Quantification of percent area of Cux1$^+$ cells within ROI. (T) Representative images showing RELN and GFP staining of control and OXY+BUP E18.5 brains. (U) Graph showing RELN$^+$ cell count. (V) Quantification of percent area of Cux1$^+$ cells within ROI. Light blue scale bars are 500µm. White scale bars are 100µm. Data is represented as mean ± SEM, n=2 embryos/litter with 4 litters/treatment group with *p<0.05, **p<0.01, ***P<0.001, two-tailed *t*-test.

Maternal Opioid Substitution Therapy Alters Adolescent Behavior

To determine whether maternal opioid exposure affects the behavior of adolescent offspring, a subset of dams were allowed to give birth and then care for the pups until postnatal day 21 (PND 21), when the pups were weaned and group-housed according to sex with their littermates (**Fig. 5A**). Behavioral testing began at PND 60 and sample collection was carried out at approximately PND 70. Due to the importance of maternal care on adolescent behavior during early postnatal days, we monitored dam behavior as well as offspring survival rates between control and OXY+BUP-treated dams [158]. Maternal care behavior such as offspring care, offspring neglect, and self-care was observed daily. There were no noticeable differences in maternal care behavior during the weaning period, and no differences in offspring survival rates, between the two treatment groups (**Fig. 5B**).
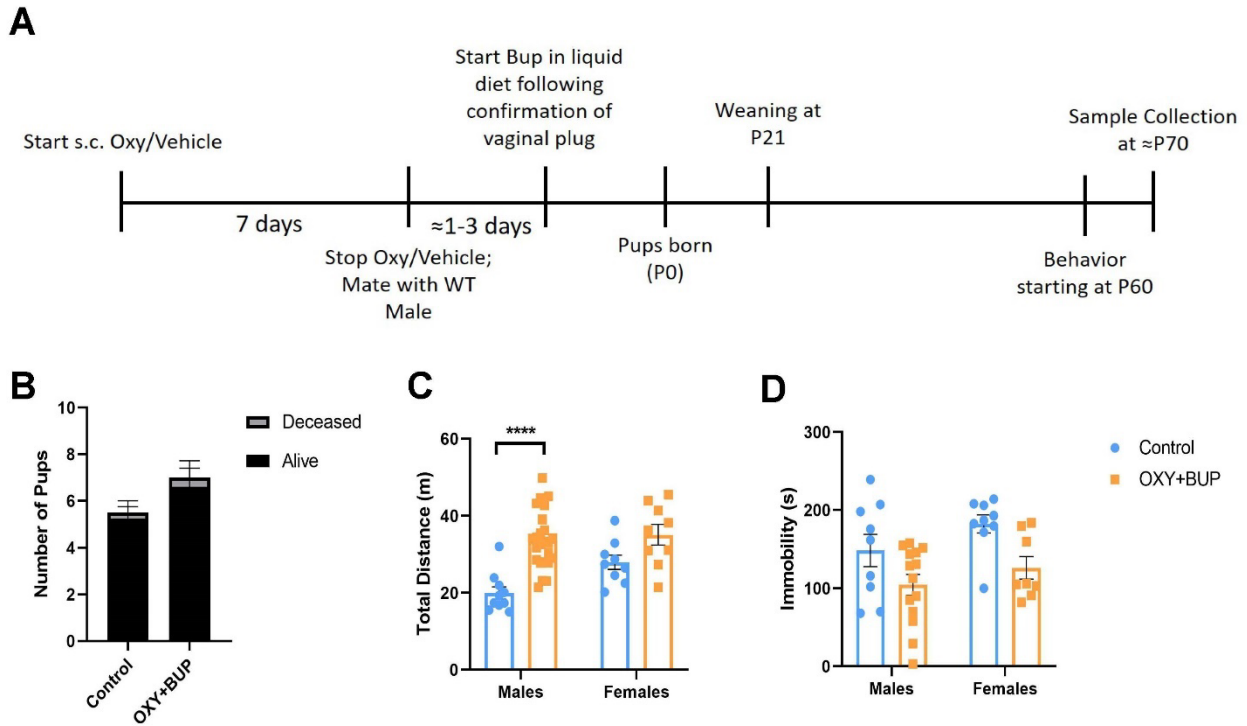
Figure 5. Adolescent Hyperactivity Phenotype in Prenatal Opioid Exposure

(A) Timeline for drug administration, behavior and sample collection for P60 samples. (B) Graph of pup survival following conception, (C) Total distance traveled in open field test, divided into treatment and sex. (E) Total immobility scored from forced swim test divided into treatment and sex. Data is represented as mean ± SEM, n=10-12/sex/treatment group, ****p<0.0001, two-way ANOVA with Tukey's test.

To determine the effects of maternal opioid use on adolescent behavior, we analyzed motor activity in a low-light open field on PND 60. A two-way ANOVA demonstrated a main effect of sex ($F_{(1,48)}$ = 5.203; P=0.0270), treatment ($F_{(1,48)}$ = 25.63; P<0.0001), but no interaction effect of sex X treatment ($F_{(1,48)}$ = 2.553; *n.s.*) on total distance travelled. Tukey's multiple comparisons analyses indicated a significant increase in total distance travelled in the OXY+BUP-treated males relative to control males (P<0.0001; **Fig 5C**), but not OXY+BUP females relative to control males (*n.s.*).Mice were then assessed two days later in the forced swim test (FST), which serves as a measure

of depressive-like behavior in rodents [159]. A two-way ANOVA indicated a main effect of treatment ($F_{(1,36)}$ = 10.27, P=0.0028), but not a main effect of sex ($F_{(1,36)}$ = 3.170; *n.s.*), nor a sex X treatment interaction ($F_{(1,36)}$ = 10.27, *n.s.*) on immobility time (**Fig. 5D**).

Adolescent Brain Changes Following Maternal Opioid Substitution Therapy

Previous studies have demonstrated that opioids, prenatally, can impact the VTA [160]. Given our observations of hyperactivity in adolescents prenatally exposed to OXY+BUP, similar to an ADHD-like phenotype [95], we further investigated potential prenatal opioid-induced structural changes in VTA dopamine neurons (**Fig. 6A**). Robust tyrosine hydroxylase (TH) staining in the VTA was observed and a lower magnification image is provided as an example of the ROI (**Fig. 6B**). A two-way ANOVA indicated a main effect of sex ($F_{(1,32)}$ = 9.791; P=0.0037), treatment ($F_{(1,32)}$ = 48.02 ; P<0.0001), but no sex X treatment interaction ($F_{(1,32)}$ = 0.020 ; *n.s.*) on number of TH+ cells (**Fig. 6C, 6D**). Taken together, these data show that prenatal opioid exposure can increase dopamine neuron ontogenesis within the VTA, which further aligns with an ADHD-like phenotype, in OXY+BUP offspring.
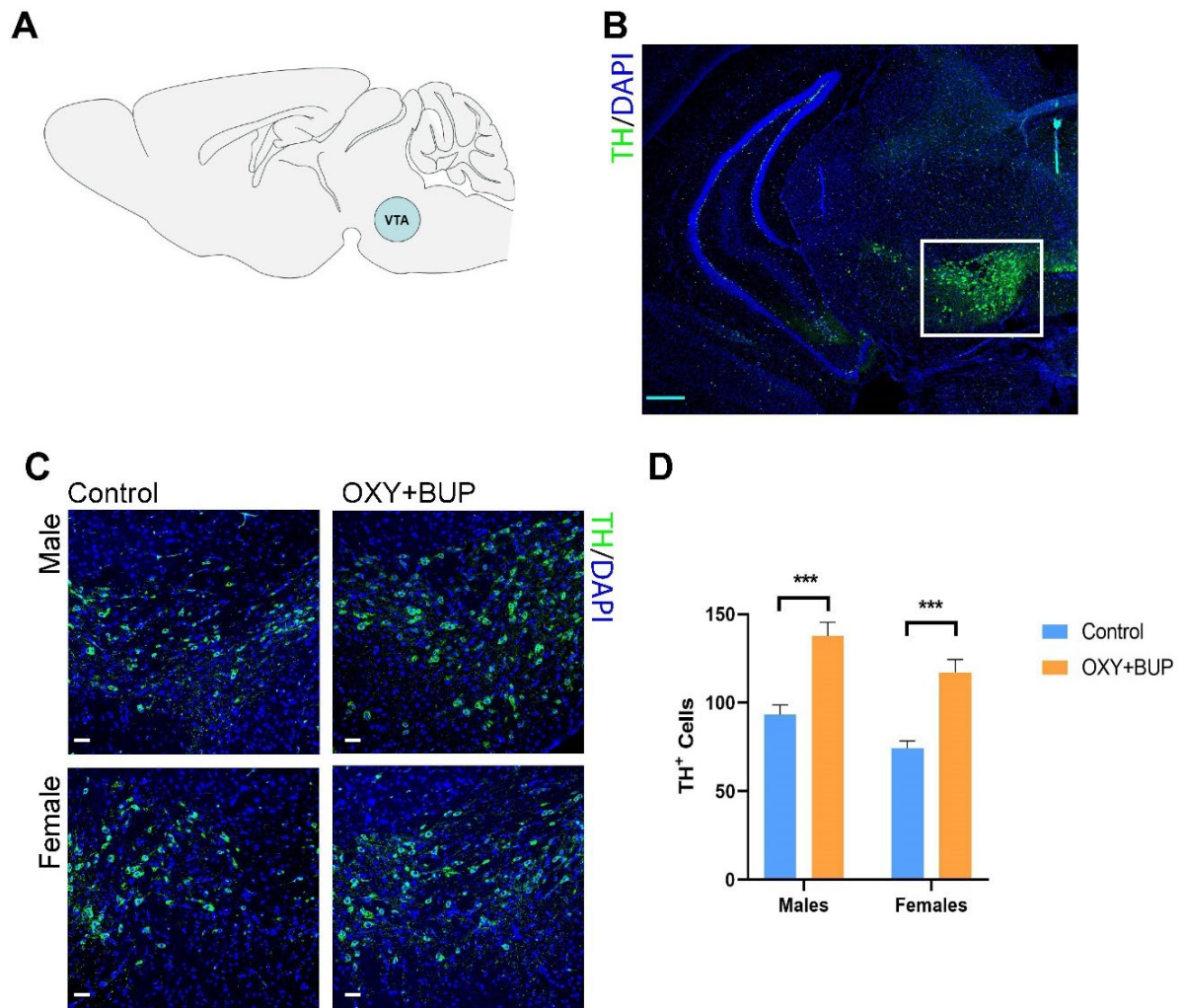
Figure 6. Increased Expression of Dopamine Neurons in Ventral Tegmental Area

(A) Diagram denoting VTA location in an adolescent mouse brain. (B) 4x magnification of TH+ staining for identification of ROI (White box for reference). (C) 20x magnification of both male and female control and OXY+BUP treated sections. (D) Graph showing number of TH+ cells for both groups, divided by sex. Data is represented as mean ± SEM, n=3/sex/treatment group. ***P<0.001, two-way ANOVA with Tukey's test.

DISCUSSION:

To our knowledge, this is the first report of an animal model that is closely translatable to the clinical presentation of maternal opioid use. While previous studies have investigated prenatal opioid exposure, most do not take into account pre-pregnancy opioid use, which can influence the maternal epigenome and gut microbiome and, thus, have additional consequences on pregnancy outcome [149,161,162]. Pregnancy, in our experiments, was confirmed by the presence of vaginal plugs and maternal dam weight. Interestingly, OXY+BUP-treated dams birthed a significantly higher number of male offspring without altering litter sizes. The clinical significance of this phenomena warrants further investigation. Sex ratios have been used as a measurement of population reproductive health and to provide an unbiased assessment of environmental conditions [163]. One study demonstrated that male offspring have an increased risk of developing NOWS; however, the severity of the syndrome was not linked to sex [164].

OXY+BUP-treated offspring exhibited a smaller overall size, compared to controls, which is consistent with clinical presentations [81,83,93,165]. Additionally, our murine model demonstrated an opioid-induced overall reduction in embryo brain size, decreased cortical thickness, and ventricular enlargement. Changes in cortical thickness during development can lead to neurodevelopment disorders such as ADHD, autism, and others [166]; and have been documented in children born from mothers taking opioids during pregnancy [167,168]. Additionally, enlarged ventricles, or ventriculomegaly, are associated with developmental disorders, such as ADHD, autism, learning deficits, and schizophrenia [169,170]. Furthermore, alterations in embryo corticogenesis can lead to several developmental and psychological disorders [17,171]. These cortical alterations could be due to changes in neural stem cell proliferation, differentiation, and/or migration.

To determine which of these developmental processes are impacted by prenatal opioid exposure, we first investigated changes in proliferation and the NS/PC population

50

using Ki67 and Sox2/Tbr2, respectively. We showed a significant decrease in cell proliferation in OXY+BUP-treated offspring relative to controls, but no significant differences in VZ/SVZ Sox2$^+$ neural stem cells or Tbr2$^+$ neural progenitors. Sox2 is upstream of Notch signaling which is critical for promoting proliferation during development [172,173]. Therefore, Notch signaling may be disrupted by prenatal opioid exposure; adversely affecting cell proliferation, without reducing the NSC pool. Future directions may include further characterization to investigate changes in Notch signaling, which affects not only proliferation but also differentiation and migration of cells [174].

We next examined specific changes in cell differentiation and layer thickness in the cortical plate. This is a highly controlled process, which starts with layer I formation and the Cajal-Retzius cells that secrete Reelin [12]. We found a significant reduction in the percent area in OXY+BUP-treated offspring, when compared to controls. Decreased expression of reelin has been associated with memory and learning deficits, and reelin-deficient animal models show behaviors consistent with psychiatric and mood related disorders [16,175]. Further studies to examine the cognitive function of OXY+BUP offspring are warranted.

The thinning of the cortex in OXY+BUP treated offspring required careful consideration of the choice for ROIs analyzed for the subsequent cortical layer markers, and we comprehensively included all factors such as cell count, layer thickness (indicating both cell number and migration distance), and percent area for each marker. In layer II/III, significant differences in Cux1 were not observed. Cux1 is a key transcription factor for corticocortical connections within layers II/III , and more specifically, Cux1 plays a role in late-differentiation dendritogenesis and synaptogenesis [176]. So, while we may not see a reduction in cell number, there could be alterations in the connections formed between cells, such as deficits in dendritic branching, spine or synapse formation, within layers II/III. Magnetic resonance imaging (MRI) studies have shown an underdevelopment of synapse

formation on dendritic spines in ADHD adolescents, compared to healthy controls [177]. Future studies should include looking into the effects of prenatal opioid exposure on dendrite and synapse formation in OXY+BUP-treated offspring.

In layer II-VI, a significant reduction in total number of SATB2+ cells and spread of SATB2-labeled layers were seen within the ROI. SATB2 has been shown to be important for directing pyramidal neurons, during corticogenesis, toward the specification of deep- and upper-layer neurons, which are found in layers V and VI primarily [178]. Indeed, we also saw reductions in layer V-VI, with the reduction of Ctip2+ cells and decreased layer thickness. Together, these data indicate that the development of layers V and VI, deep- or upper-layer neurons, are susceptible to maternal opioid use.

Due to the numerous clinical studies showing development of mental health disorders, including ADHD, learning deficits, and depression in adolescents whose mothers were taking opioids during pregnancy [93,122-124], we investigated the hypothesis that our mice may show differential behaviors during adolescence. Excitingly, we detected increased locomotor activity in the prenatally opioid-exposed offspring, which is consistent with hyperactivity seen in ADHD clinical presentations [95]. More specifically, there was a significant increase in locomotor activity in OXY+BUP-treated males compared to control. These data are consistent with clinical studies that show sexual dimorphisms in adolescent ADHD symptomology, in that males will more often present with hyperactivity and inattention compared to females [127,129].

Previous reports have stated that, following maternal opioid use, there is an increased risk for depression in adolescents [94]. Additionally, one animal study showed that using the FST, young rats, equivalent to 3-5 years in humans, from dams who received BUP alone, starting at E7 and continuing for 14 days, exhibited higher levels of immobility in the FST [179], a measure of depressive-like behaviors. In our own study, however, we showed that OXY+BUP-treated adolescent offspring exhibited less immobility time when

compared to controls, consistent with our observation of elevated motor activity. Interestingly, our results showed a significant reduction in time spent immobile in OXY+BUP-treated offspring compared to control; however, this outcome was not sex-dependent. Future studies need to include assessing other behavioral alterations linked to ADHD including attention and impulsivity [129]. Additionally, how different animal species, age of analysis, and opioid treatment regimens contribute to the discrepancies in the literature requires further investigation.

The intriguing observations made in the behavioral assays prompted an additional analysis of dopaminergic neuron ontogenesis within the VTA, due to the OXY+BUP-induced ADHD-like behavioral phenotype. It has been hypothesized, in multiple studies, that ADHD symptomology is linked to altered function of the dopaminergic system [180,181]. Interestingly, our model showed significant increases in TH^+ immunoreactivity in the VTA in OXY+BUP-treated offspring compared to control. TH is a well-established marker for dopaminergic neurons within the VTA. Previous studies, in animal models of ADHD, showed increases in VTA TH immunoreactivity in adult rats and suggest a hyperfunctioning dopamine hypothesis in ADHD [140,141]. These results further corroborate our own exciting findings of increased dopaminergic neuron ontogenesis within the VTA. The upregulation of dopamine neurons in the VTA could serve as a compensatory mechanism for dopamine deficits in the prefrontal cortex, which have been documented in multiple ADHD studies [134]. Further studies are needed to confirm this hypothesis and can include investigation into behaviors that are affected by the VTA such as motivation, inattention, and impulsivity. To our knowledge, this is the first report showing alterations in dopaminergic neuron ontogenesis, in the VTA, following prenatal opioid exposure, and warrants further investigation.

Previous studies have suggested that MAT is safer than abstinence or withdrawal from opioids during pregnancy [182]. However, based on increasing clinical evidence

75,83,86,93,122, and the results from our preclinical studies, additional clarity is crucially needed to support the safe implementation of BUP MAT during pregnancy. Future studies should incorporate investigation of the effects of abstinence/withdrawal in pregnant dams compared to BUP-treated dams. Overall, this study provides critical evidence that BUP MAT can alter fetal brain development, which can then result in an ADHD-like phenotype in male adolescents. This prenatal exposure can have lifelong implications for offspring by means of learning difficulties due to hyperactivity and, possibly, inattentiveness and altered social behaviors.

SPECIFIC METHODS:

Animals

Nestin-GFP heterozygous offspring were generated by crossing homozygous *Nestin-GFP* females (provided by Dr. Grigori Enikolopov, Stony Brook University) with wild type C57BL/6J males (JAX Stock No. 000664). Mice were genotyped as described previously [58]. All animal experiments were approved by the Institutional Animal Care and Use Committee of the University of Texas Medical Branch and conducted in accordance with the *Guide for the Care and Use of Laboratory Animals*. All animals were maintained on a 12-hour light/dark cycle.

Experimental Design

Female mice, 2-4 months old, were randomly assigned to two groups, control or OXY+BUP, total of n=10-12 dams per group. Females were individually housed and subcutaneously injected with 0.9% NaCl or oxycodone (10 mg/kg) (Sigma, CAT#01378) for seven days, twice per day with eight hours between injections. On the eighth day, wild type males were placed into the cages with the females and all injections ceased. Female

mice were checked twice daily for confirmation of vaginal plug. Once the presence of the vaginal plug was confirmed, which was marked as E0.5, the male was removed from the cage and administration of liquid diet began. The liquid diet used was Ensure High Protein Vanilla (Abbott, Illinois). Control animals received 3 mL of liquid diet alone and OXY+BUP females received 3 mL liquid diet with buprenorphine (Sigma, CAT#B9275) at 18:00 once daily. Buprenorphine was administered in a ramping schedule starting at 0.5 mg/kg and increasing each consecutive day by 0.5 mg/kg until the maximum dose of 4 mg/kg/day was reached. After reaching max dose, 4 mg/kg/day was continued throughout the remainder of the gestation until data collection. The doses chosen for this study were based on human equivalent doses as prescribed in the clinic [183,184]. All diet was made fresh daily and supplied in custom-made food dishes. Weight following confirmation of vaginal plug was monitored daily as well as overall body condition of pregnant females. Brain samples were collected at E18.5 and PND60. For behavior (PND60) and subsequent sample collection (PND70), cessation of liquid diet began on PND0 and dams only had access to standard chow. Pups were counted on PND0 and daily monitoring was conducted by blinded experimenter for overall dam nursing behavior and pup health. Weaning occurred on PND21 and then offspring were group housed until sample collection at PND70.

E18.5 Sample Collection

At E18.5, female dams were placed under anesthesia using isoflurane and underwent cervical decapitation. The abdomen was then opened, and the uterus was removed containing the embryos. All dissections of embryos were performed on ice. Individual embryos were separated from the placenta and photographed for gross size. The brain was then removed from the skull, photographed and placed in 4% paraformaldehyde for a total of 48 hours. Following this, the brain was washed 3 times for

10 minutes in phosphate buffered saline (PBS). For tissue preservation, brains were placed in 15% sucrose with gentle rocking for 12 hours and then moved to 30% sucrose for 24 hours. The brains were then placed in optimal cutting temperature embedding medium (OCT) for 30 minutes and then frozen using 2-methylbutane (Sigma, Milwaukee, WI, CAT#M32631).

Sex Determination and PCR

DNA was extracted from tail samples, collected at the same time as brains, using Qiagen DNeasy Blood & Tissue kit (Qiagen, CAT#69506). DNA was stored at -20° until analysis. PCR was performed as previously described [154]. 10ng DNA was processed using Applied Biosystems Thermocycler (GeneAmp PCR System 9700), with cycling parameters: 94°C for 1 minute, 94°C for 30 sec, 50°C for 30 sec, 72°C for 1 min, repeating steps 2-4 for 30 cycles, followed by 72°C for 1 min and lastly a 4°C hold. Samples were run using gel electrophoresis for 1 hour and developed with ethidium bromide (Thermo Fisher Cat#15585011). Gels were imaged using a LI-COR Odyssey Fc Imaging System.

PND60 Sample Collection

Following behavioral assessments, mice were anesthetized with ketamine and xylazine, 90 mg/kg and 10 mg/kg, respectively. Intra-cardiac perfusion was then performed with 5 mL of phosphate buffered saline (PBS), followed by 30 mL freshly prepared 4% paraformaldehyde (Thermo Fisher Scientific, Waltham, MA). The brains were collected and post fixed for 24 hours in 4% paraformaldehyde at 4° C. They were then transferred to 15% sucrose for 12 hours and then placed in 30% sucrose for 24 hours at 4° C. For cryopreservation, samples were placed in OCT at room temperature for 30 minutes, upon which they were immediately frozen using 2-methylbutane (Sigma, Milwaukee, WI, CAT#M32631).

Open Field and Forced Swim Test Behavioral Analyses

A low-light open field assay assessment of motor activity was conducted with a video-based data capture and analysis software (TopScan, CleverSys, Inc., Reston, VA). All procedures were performed between 8:00 a.m. and 5:00 p.m. Prior to behavior assessments, mice were handled daily by experimenter for three days prior to the experiment for two minutes/day. Body weights were taken daily. Mice were exposed to testing room for a one-hour acclimation. To assess spontaneous motor activity, mice were placed in open field chambers for fifteen minutes and allowed to explore freely. Total distance traveled was scored by the software. Following completion of motor experiments, mice were returned to their home cages for two days without behavior manipulation before undergoing the forced swim test (FST) to investigate depressive-like behavior. The FST was performed as described previously [159]. Mice were recorded for a total of six minutes, and two blinded participants scored the last four minutes of the session, as total time spent immobile. Mobility was defined as any behavior not essential to keeping the animal's head/nose above water.

Immunohistochemistry

Tissues from two offspring/litter and four litters/treatment group (n=8/treatment group) were used for all *in vivo* immunohistochemistry experiments. Tissue was sectioned, coronally, using a Leica cryostat at 30 μm thickness. Animal numbers were randomized for blinded counting. The primary antibodies used for staining of select cortical markers for E18.5 samples were anti-GFP 1:1000 (Aves Lab, Tigard, OR, CAT#GFP-1020), anti-Ki67 (Abcam, Cambridge, MA, CAT#ab15580), anti-Sox2 1:1000 (Abcam, Cambridge, MA, CAT#ab97959), anti-Tbr2 1:1000 (Millipore, Billercia MA CAT#AB15894), anti-RELN 1:1000 (Invitrogen, CAT#PA5-47537), anti-CUX1 1:100 (Atlas Antibodies, St. Louis, MO, CAT#HPA003277), anti-Ctip2 1:300 (Abcam, Cambridge, MA, CAT#ab187668), and anti-

SATB2 1:1000 (Abcam, Cambridge, MA, CAT#ab92446). The primary antibodies used for staining of neuronal populations of P60 samples was anti-TH (Abcam, Cambridge, MA, CAT#ab76442). Primary antibody incubation occurred at 4° C overnight, following which sections were incubated with secondary antibodies (goat anti-chicken 488, CAT#A11039, goat anti-rabbit 568, CAT#A11011 and goat anti-mouse 568, CAT#AB175473). Sections were then washed and incubated with DAPI nuclear stain (Thermo-Fisher, CAT#D1306).

Imaging and Cell Counting

All images were taken on a Nikon A1 Confocal Microscope, utilizing the Nikon EZ-C1 software. Cell counts were performed under blinded conditions using FIJI, the ImageJ software. The settings for counting were rolling ball radius 18.0 pixels, with a threshold of 0-75. The particle size was 50-infinity and the particle circularity was 0.00-1.00. For E18.5 samples, sections were identified using key regions as identifiers, surrounding the cortex. Additionally, for P60 samples, sections spanning bregma -2.92 to -3.52 were counted. Three sections per sample were counted for each antibody.

Statistical Analysis

All behavioral scoring and immunohistochemical analyses were performed under blinded conditions. Power analyses were performed using G*Power 3.1.9.4 to determine the number of mice for the experiments. An n=4 litters were needed for all *in vivo* immunohistochemical experiments, with two offspring/litter for a total of n=8 offspring per treatment group, to provide significance at p<0.05 with an alpha value of 0.80; and an n=12 offspring per sex per treatment group was required for behavioral analyses. A standard two-tailed *t*-test was performed in morphological analyses and embryo gross measurements at E18.5. A two-way, between-subjects ANOVA for the factors of sex and treatment with Tukey's multiple comparisons test used for sex genotyping at E18.5 as well

as for behavior and morphological analyses at PND60. All statistical analyses were performed using GraphPad Prism v8 software.

CHAPTER 3: CHRONIC POLY-DRUG ADMINISTRATION DAMAGES ADULT MOUSE BRAIN NEURAL STEM CELLS[1]

INTRODUCTION

Ethanol and cocaine are two commonly co-abused substances. In a 2007 survey, 96% of cocaine users reported ethanol use within the same month (concurrently), and 85% reported using the two drugs simultaneously [185]. Co-abuse of ethanol and cocaine has been shown to produce psychotic episodes, increase suicidal and homicidal ideation, and enhance symptoms of psychiatric disorders, such as depression [105,108,109,186,187]. Despite these strong negative consequences, cocaine and ethanol are preferentially co-abused and people who report co-abuse show poorer prognosis after treatment and higher risk of relapse [114,115,188]. In clinical studies, individuals report ethanol ameliorates negative side effects of "coming down" after using cocaine, and females generally report stronger euphoric feelings compared to males [117,189]. Aside from clinical studies, very little work has been done evaluating the chronic effect of ethanol and cocaine poly-drug administration on the brain. This presents a large gap in knowledge regarding mechanistic and neuropathological changes that occur in the brain following chronic poly-drug administration, which impedes efforts to develop effective treatments or management strategies.

It is well established that ethanol and cocaine individually contribute to neurodegeneration and negatively affect the adult endogenous neural stem cell population [21,48,96]. Endogenous neural stem cells (NSCs) in the adult brain have gained attention as a potential therapeutic target due to their critical role in maintaining neurogenesis

---

throughout life and possibly mediating brain repair and functional recovery [100,190]. The subventricular zone (SVZ) of the lateral ventricles and the subgranular zone (SGZ) of the dentate gyrus are the two most commonly studied regions of adult NSCs, and individual administration of either cocaine or ethanol affects NSCs in these regions [21,48,96,98]. Furthermore, sustained neurogenesis in the hippocampus is believed to contribute to contextual memory formation [98]. The tanycyte layer (TL) of the third ventricle also contains cells with NSC-like properties [42,43,48]; however, the impact of drugs and ethanol on the cells in this region in relatively unknown. To date, there is a lack of report on the combined use of ethanol and cocaine on any of these NSC populations. Considering the therapeutic implications of adult NSCs in a variety of fields, it is important to evaluate the impact of simultaneous poly-drug use on the NSC populations in order to advance translational efficacy of poly-drug abuse interventions.

To achieve this, we utilized a genetic inducible fate mapping transgenic mouse model to trace the fate of endogenous NSC populations [48,57] in response to chronic ethanol, cocaine, or combination treatment. By developing a novel poly-drug administration paradigm, we investigated the effect of ethanol and cocaine co-use on the fate of NSCs in three regions of interest (SVZ, SGZ, and TL). Responses between male and female mice, in each respective region, were compared to determine if sex altered NSC response to drug treatment. Finally, behavioral tests were conducted to assess memory and homeostatic/hedonic feeding behaviors.

RESULTS

Novel mouse model of chronic cocaine and ethanol co-exposure

Adult Nestin-CreER[T2]:R26R-YFP bi-transgenic mice were used to trace the fate of endogenous NSCs, following tamoxifen induction, in response to chronic ethanol feeding, in a calorically-balanced liquid diet, and/or cocaine administration, via intraperitoneal injections (**Fig. 7A**). Animals with similar ages were used in this study, and males and females were randomly assigned to a treatment group. The age of mice was chosen to represent an adult population of approximately 25-30 years of age [191] (**Fig. 7B**). We were interested in evaluating the impact of poly-drug use in the adult population, as we were interested in the effect poly-drug abuse has on the fully matured brain, which in humans is approximately 25-30 years of age [192,193]. Tamoxifen was administered when animals were 2 months of age, in this study, then 1 month lapsed prior to drug treatment to enable maximum recombination of the GFP transgene, as well as to allow washout of the immediate effects of tamoxifen.

Male mice weighed more than females, however, there were no significant differences among bodyweights of control and treatment groups (**Fig. 7C**). Male mice tended to have higher average daily diet consumption compared to their female counterparts. In the ethanol group, males consumed more diet than females; therefore, males consumed significantly more grams of ethanol per day (**Fig. 7D-E**). However, females in both the ethanol and combination treatment groups consumed more grams of ethanol per kilogram of body weight (**Fig. 7F**). Mice in the control and cocaine groups exhibited similar growth rates in bodyweight; however, in the ethanol and combination groups, both males and females had a significant reduction in gain of bodyweight (**Fig. 7G**).
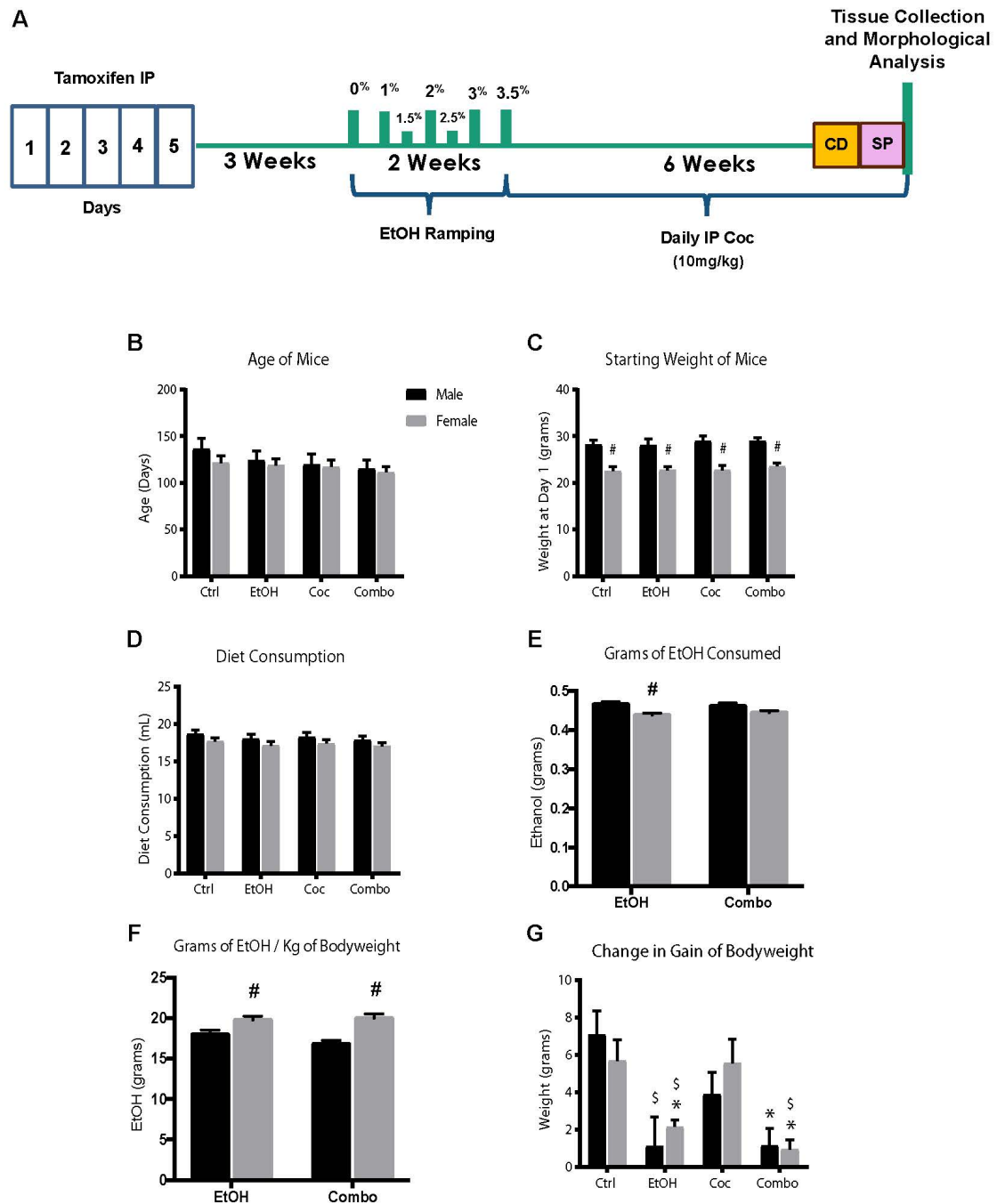
Figure 7. Chronic Drug Treatment Model

(A) Schematic of experimental paradigm. CD, context fear discrimination learning; IP, intraperitoneal; SP, sucrose preference test. **(B)** Average age of mice at the start of experiment. **(C)** Average bodyweight at the start of experiment. **(D)** Average daily diet consumption. **(E)** Average grams of ethanol consumed daily. **(F)** Average grams of ethanol consumed per kilogram of mouse bodyweight. **(G)** Average changes in gain of bodyweight. Values are shown as mean±SEM, #p<0.05 compared to other sex in the same group, *p<0.05 compared to control, \$p<0.05 compared to cocaine; control (Ctrl), ethanol (EtOH), cocaine (Coc), and combination (Combo). Ctrl male n=7, Ctrl female n=13, EtOH male n=10, EtOH female n=13, Coc male n=10, Coc female n=14, Combo male n=10, Combo female n=15.

The metabolism of cocaine in the presence of ethanol produces a unique metabolite, cocaethylene, which is known to be cardiotoxic [194,195]. Thus, liquid chromatography coupled to mass spectrometry (LC-MS) was used to measure cocaine and its metabolites in whole blood at one hour and 24 hours following cocaine injection (**Fig. 8**). There were increased levels of cocaine (Coc), benzoylecgonine (BCE), and cocaethylene (CE) one hour after administration; however, after 24 hours these metabolites were undetectable. Daily intraperitoneal injections of cocaine were used to maintain active cocaine metabolism and blood levels.
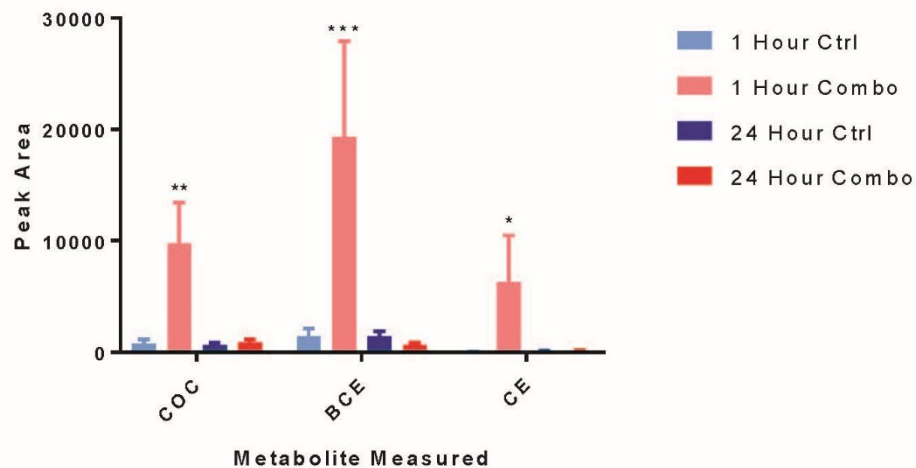
Figure 8. Drug Metabolites Measured Using LC-MS

  Quantification of metabolites measured using LC-MS at two time points. Values are shown as mean ±SEM, **p<0.01, ***p<0.001 compared to control. COC - cocaine, BCE – benzoylecgonine. CE – cocaethylene.

Effect of drug treatment on SVZ NSCs

The SVZ of the rostral lateral ventricle was chosen because it harbors endogenous NSCs and is an area of active neurogenesis in adult mammalian brains [196]. Tamoxifen enabled expression of YFP was enhanced by immunohistochemistry using a green fluorescent protein (GFP) antibody. We examined three phases of NSCs, including NSCs (GFP+) and newly differentiated NSCs which were doublecortin (DCX) positive

(DCX$^+$GFP$^+$) or glial fibrillary acidic protein (GFAP) positive (GFAP$^+$GFP$^+$). Since NSCs also express GFAP, cautions were made to exclude those GFAP$^+$ cells with DAPI-stained nuclei located in the SVZ, and other NSC regions below. DCX is a marker for neuronal lineage and GFAP is for glial lineage. The third phase we examined was total neuronal or astrocyte populations (DCX$^+$ or GFAP$^+$), including those differentiated cells before tamoxifen induction. Cells that were double labeled with GFP and a marker of differentiation (DCX or GFAP) represent newly differentiated cells after induction of YFP expression in Nestin$^+$ cells. Cells that differentiated prior to tamoxifen induction and no longer expressed Nestin would not be co-labeled with GFP. We quantified positively stained cells in the SVZ, particularly focusing on the origin of the rostral migratory stream (oRMS).

There were no differences in GFP$^+$ cells between control male and female mice (**Fig. 9A and 9E**). All drug treatments resulted in a reduction of GFP$^+$ cells (Figure 2). Males and females in the ethanol group had fewer GFP$^+$ cells compared to control and cocaine mice (**Fig. 9A-C, 9E**). Combination treatment had the greatest impact on GFP$^+$ cells (**Fig. 9D-E**). Next, we examined the neurogenic capacity of SVZ NSCs after drug treatment using the DCX antibody. Male and female control mice had the similar number of DCX expressing cells (**Fig. 9A and 9F**). Interestingly, while ethanol decreased total number of DCX$^+$ cells, cocaine did not reduce the DCX$^+$ population (**Fig. 9B-C, 9F**). Combination treatment caused the largest reduction in DCX$^+$ cells (**Fig. 9D and 9F**), which were significantly greater than ethanol alone.

All drug treatments significantly reduced the newly differentiated neurons (DCX$^+$GFP$^+$) (**Fig. 9B-D, 9G**). Combination treatment decreased DCX$^+$GFP$^+$ cells in male
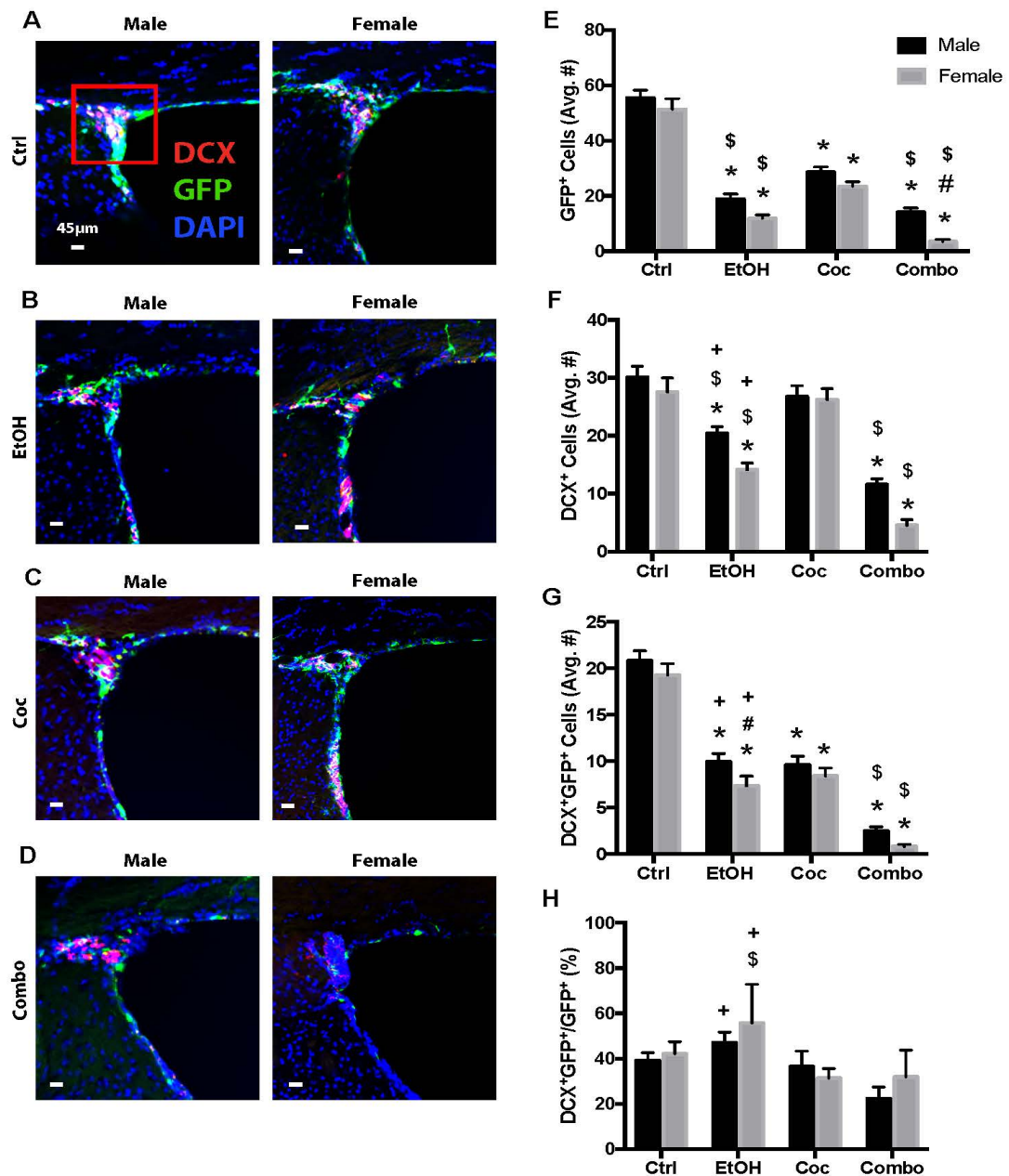
Figure 9. Neural Stem Cell and Neurogenesis in the Subventricular Zone (SVZ)

(A-D) Representative brain images of control (Ctrl), ethanol (EtOH), cocaine (Coc), and combination (Combo) treated mice, respectively, immunostained with stem cell marker (GFP, green), neuronal marker (DCX, red), and merged with nuclear marker DAPI (Bregma 0.5 through 1.08). **(E-H)** Quantification of GFP$^+$, DCX$^+$, DCX$^+$GFP$^+$, and the percentage of DCX$^+$GFP$^+$ over total GFP$^+$ cells in the SVZ and origin of the rostral migratory stream (area inside red square). Values are shown as mean ±SEM, *p<0.05 compared to control, #p<0.05 compared to other sex in the same group, $p<0.05 compared to cocaine group, +p<0.05 compared to combination group, n=3 mice per sex per group. Scale bars, 45µm.

and females (**Fig. 9G**); and both sexes exhibited significantly more severe damage than their ethanol counterparts. In terms of the percentage of GFP$^+$ cells becoming DCX$^+$ (DCX$^+$GFP$^+$/GFP$^+$), none of the treatment groups had a significant change when compared to controls (**Fig. 9H**). However, both sexes in the ethanol group showed significantly higher values than those in the combination group.

To further verify a reduction in neurogenesis, the olfactory bulb of control and combination mice were stained for GFP and mature neuronal marker, NeuN (**Fig. 10**).
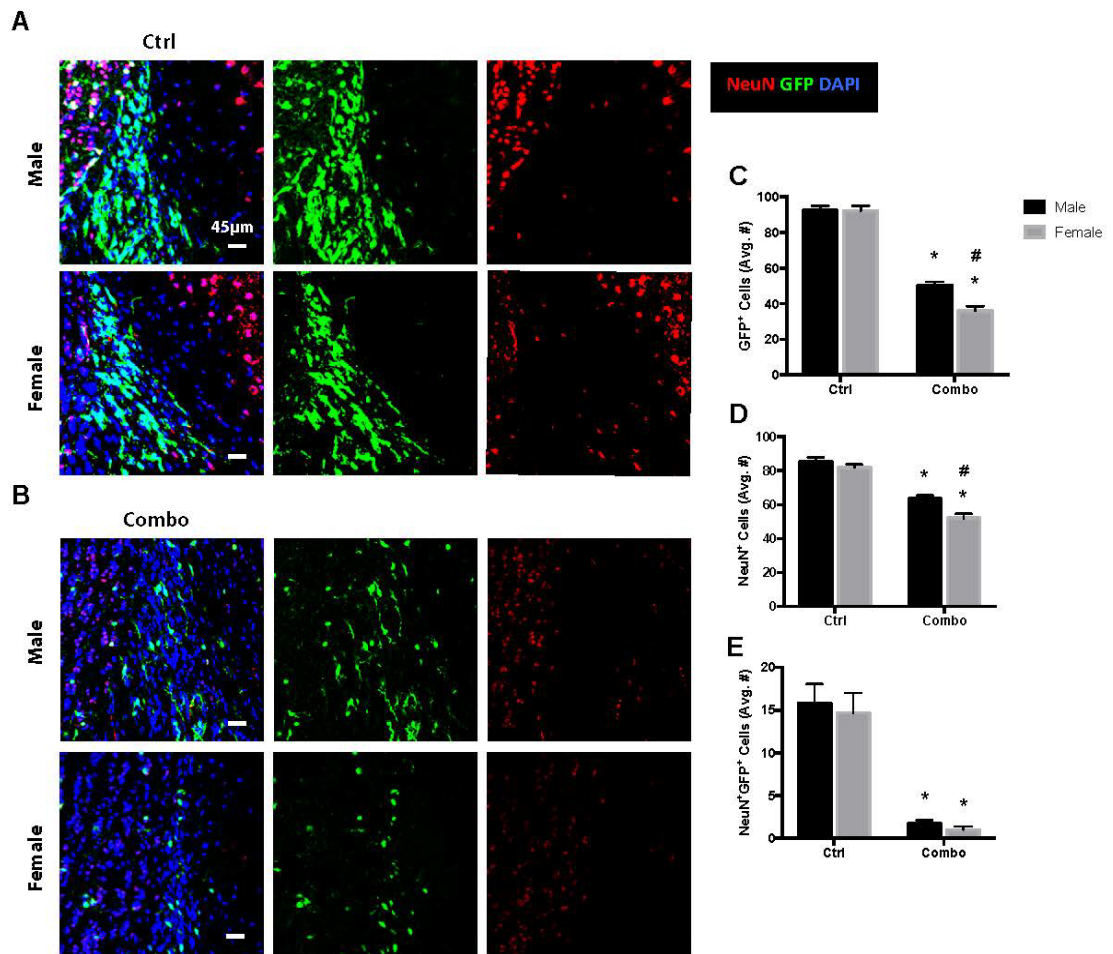
Figure 10. Neurogenesis in the Olfactory Bulb

(A-B) Representative brain images of control (Ctrl), and combination (Combo) treated mice, respectively, immunostained with stem cell marker (GFP, green), neuronal marker (NeuN, red), and merged with nuclear maker DAPI. **(C-D)** Quantification of GFP$^+$, NeuN$^+$, NeuN$^+$GFP cells in the olfactory bulb. Values are shown as mean ±SEM, *p<0.05 compared to control, #p<0.05 compared to other sex in the same group, n=3 mice per sex per group. Scale bars, 45μm.

There was a significant decrease in both GFP$^+$ and NeuN$^+$ cells in the combination group, which was more pronounced in the females (**Fig. 10A-D**). Additionally, there was a dramatic reduction in NeuN$^+$GFP$^+$ cell populations compared to control.

We further assessed the effect of drug consumption on astroglial differentiation in the oRMS by using GFAP as a glial marker. No significant differences were found in the number of GFAP$^+$, GFAP$^+$GFP$^+$, or the percentage of GFP$^+$ cells becoming GFAP$^+$ (GFAP$^+$GFP$^+$/GFP$^+$) between males and females in control mice (**Fig. 11E-G**). Cocaine had no effect on the total population of GFAP$^+$ cells; however, ethanol and combination treatment significantly reduced this population (**Fig. 11A-E**). All treatments reduced the newly differentiated GFAP$^+$GFP$^+$ cells (**Fig. 11B-D, 11F**). Both males and females in the ethanol and combinations groups had significantly fewer cells than those in the cocaine group. There were no significant changes among the groups with regards to the percentage of GFP$^+$ cells becoming GFAP$^+$ (**Fig. 11G**).

In summary, these data show the NSCs in the SVZ are sensitive to chronic ethanol and cocaine treatment but were most sensitive to the combination drug treatment. Additionally, female NSCs (GFP$^+$) are more sensitive to combination drug treatment when compared to males. Migratory neurons (DCX$^+$) and astrocytes (GFAP$^+$) present before tamoxifen induction were not affected by cocaine treatment but are sensitive to combination drug treatment. Newly differentiated neurons and astrocytes (DCX$^+$GFP$^+$ and GFAP$^+$GFP$^+$) seem to be the most vulnerable to combination drug treatment.
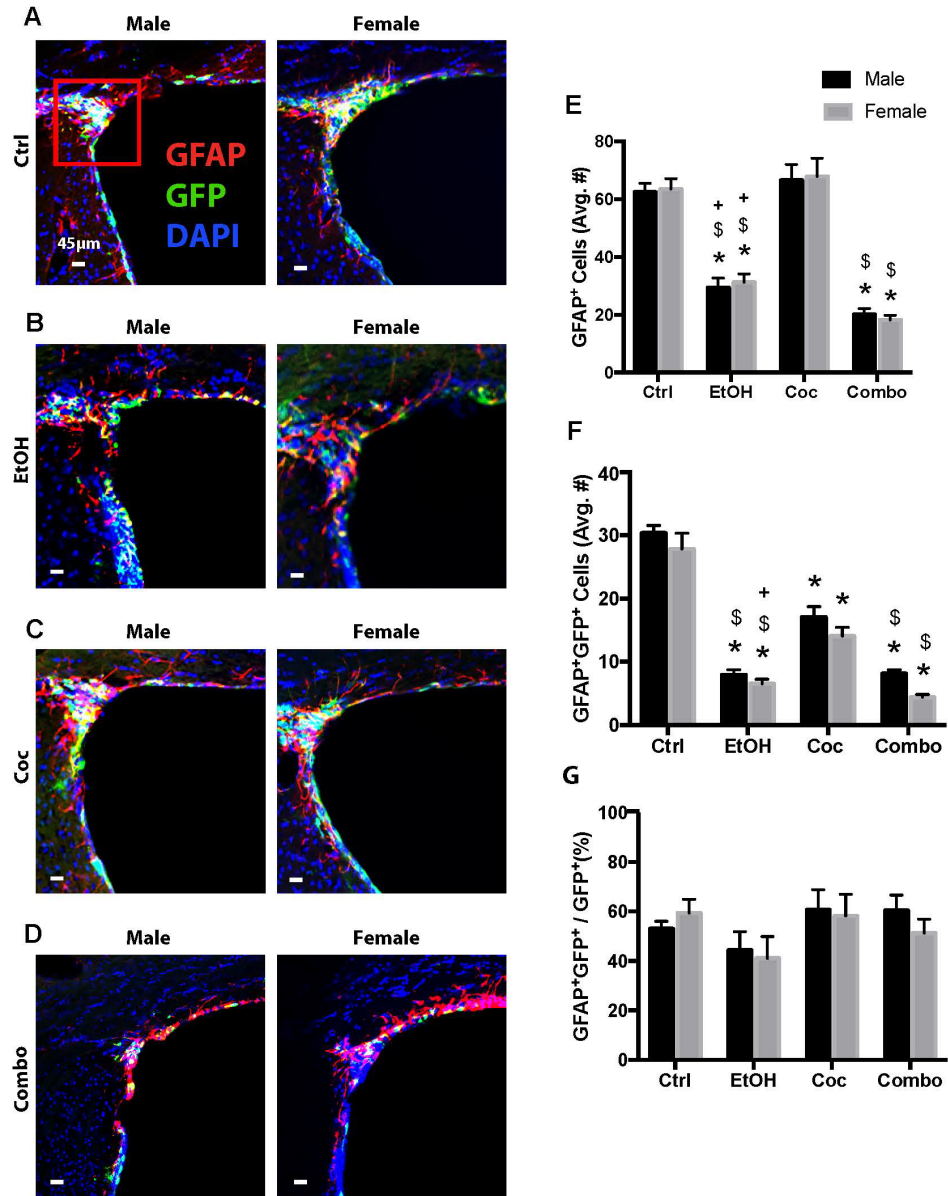
Figure 11. Astrogliogenesis in the SVZ

(A-D) Representative brain images of control (Ctrl), ethanol (EtOH), cocaine (Coc), and combination (Combo) treated mice, respectively, immunostained with stem cell marker (GFP, green), astrocyte marker (GFAP, red), and merged with nuclear maker DAPI (Bregma 0.5 through 1.08). **(E-G)** Quantification of GFAP[+], GFAP[+]GFP[+], and the percentage of GFAP[+]GFP[+] over total GFP^{+} cells in the SVZ and origin of the rostral migratory stream (area inside red square). Values are shown as mean ±SEM, *$p < 0.05$ compared to control, [#]$p < 0.05$ compared to other sex in the same group, [$]$p < 0.05$ compared to cocaine group, [+]$p < 0.05$ compared to combination group, n=3 mice per sex per group. Scale bars, 45μm.

Effect of drug treatment on SGZ NSCs

Next, we examined the SGZ in the dentate gyrus of the dorsal hippocampus, given its role in active adult neurogenesis and cognitive function [21]. Control males seemed to have fewer GFP^{+} cells compared to control females (**Fig. 12A, 12E**). Ethanol reduced GFP^{+} cells in both males and females however, cocaine did not significantly impact the number of GFP^{+} cells (**Fig. 12B-C, 12E**). Interestingly, there was a change in the morphology of many GFP^{+} cells, showing loss of arborization in both cocaine and combination groups (**Fig. 12C**). Combination treatment almost completely depleted GFP^{+} cells in males and females (**Fig. 12B, 12D, 12E**).

Furthermore, ethanol, cocaine and combination treatment significantly reduced DCX^{+} cells in female mice (**Fig. 12B-D, 12F**). Males in the cocaine group did not show reduction in DCX^{+} cells, whereas males in the ethanol and combination groups had a significant decrease (**Fig. 12B-D, 12F**). Female mice in the ethanol and cocaine groups had significantly fewer DCX+ cells compared to their male counterparts (**Fig. 12B-C, 12F**). Although control female mice tended to have more GFP^{+} cells, they had significantly fewer DCX[+]GFP^{+} cells compared to control males (**Fig. 12G**). All drug treatments reduced DCX[+]GFP[+] cell populations in both male and female mice (**Fig. 12G**). Cocaine significantly reduced the percentage of NSCs differentiating into neurons (DCX[+]GFP[+]/GFP[+]) in female mice, while combination treatment significantly reduced this percentage in males (**Fig. 12H**).

Figure 12. Neural Stem Cell and Neurogenesis in the Subgranular Zone (SGZ)

(A-D) Representative brain images of control (Ctrl), ethanol (EtOH), cocaine (Coc), and combination (Combo) treated mice, respectively, stained with stem cell marker (GFP green), neuronal marker (DCX red), and merged with nuclear maker DAPI (Bregma 0.5 through 1.08). White boxes represent increased magnification of selected cells as seen on the right side of panel. **(E-H)** Quantification of GFP⁺, DCX⁺, DCX⁺GFP⁺, and the percentage of DCX⁺GFP⁺ over total GFP⁺ cells, in the SGZ. Values are shown as mean ±SEM, *p<0.05 compared to control, #p<0.05 compared to other sex in the same group, $p<0.05 compared to cocaine group, +p<0.05 compared to combination group, n=3 mice per sex per group. Scale bars, 45μm.

In summary, combination drug treatment almost completely obliterated NSCs, newly differentiated neurons and total DCX^{+} immature neurons in the SGZ of both males and females. Newly differentiated neurons are most susceptible to drug treatment, and the SGZ neurons of female mice are more sensitive to cocaine compared to males.

Effect of drug treatment on TL NSCs

We also evaluated the TL of the third ventricle because this region harbors a subpopulation of cells known as tanycytes which possess NSC-like characteristics and is becoming known as a new neurogenic niche [42,43]. In this study, there was little evidence of newly differentiating neurons in the adult TL, therefore our primary focus was on GFP[+] and GFAP[+] cell populations. Control male and female mice had similar numbers of GFP[+] and GFAP^{+} cells; whereas males had more GFAP[+]GFP[+] (**Fig. 13A, 13E-G**). Ethanol and combination treatment reduced GFP^{+} cells in the TL in males and females (**Fig. 13E**). Cocaine did not significantly alter female GFP[+] cell populations compared to control; however, males had a decrease (**Fig. 13C, 13E**). In all three treatment groups there was a noticeable change in morphology of GFP^{+} cells, with loss of arborization and flattening of cells (**Fig. 13B-D**). Ethanol and cocaine reduced total GFAP^{+} cells in males and females (**Fig. 13F**). Interestingly, combination treatment did not impact the total GFAP[+] population in this region (**Fig. 13D, 13E**). As shown in Figure 5G, ethanol reduced the GFAP[+]GFP[+] population in males and females. Cocaine, on the other hand, decreased GFAP[+]GFP^{+} cells in males, but increased these cells in females. Combination treatment reduced GFAP[+]GFP^{+} cells in both males and females. Despite the reduction of GFAP[+]GFP^{+} cells in male cocaine-treated mice (**Fig. 13G**), they had showed an increase in the percentage

of GFP⁺ cells becoming GFAP⁺ cells (**Figure 13H**). Males in the combination group had a

reduction in this percentage compared to both cocaine and control mice (**Fig. 13H**).

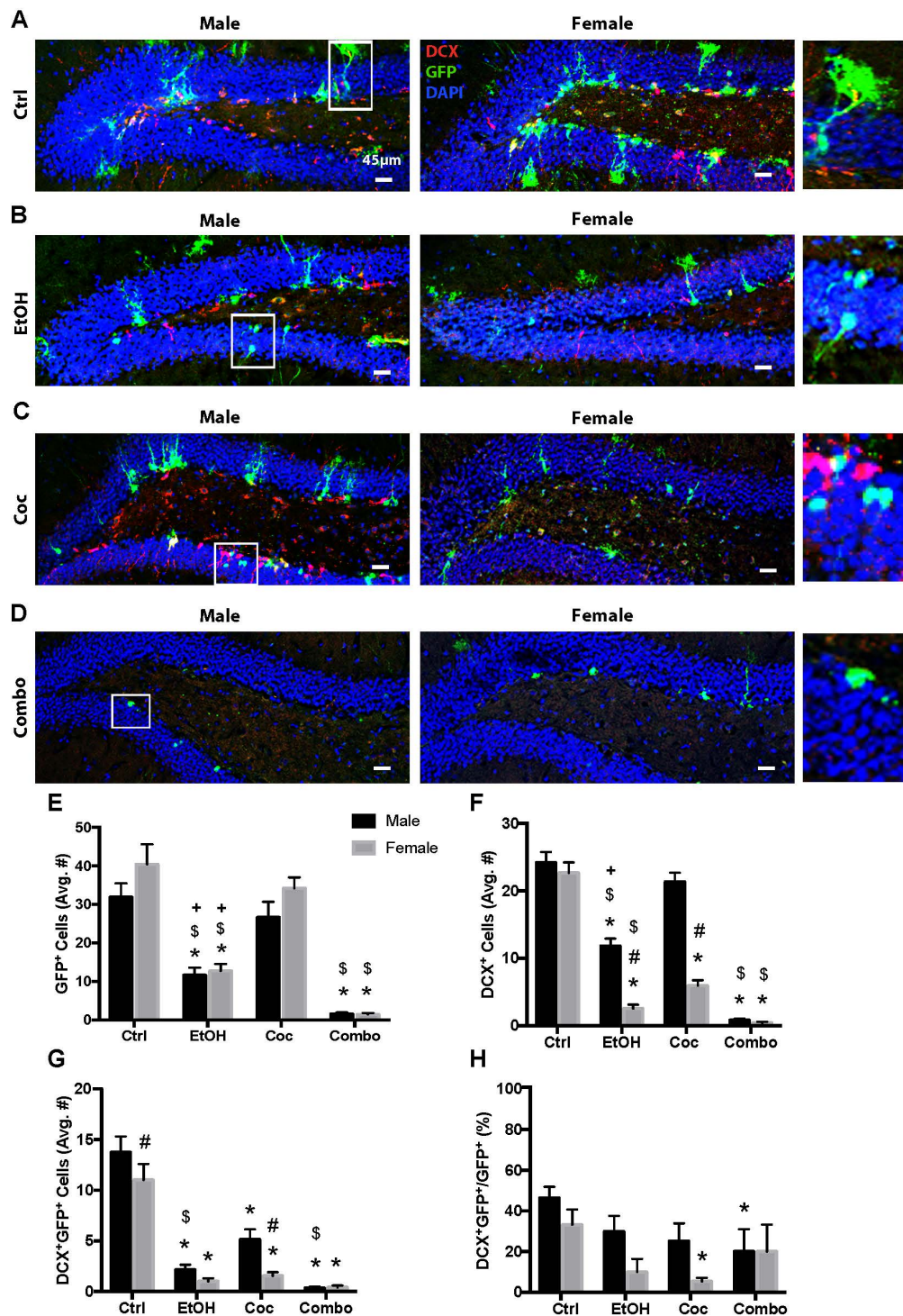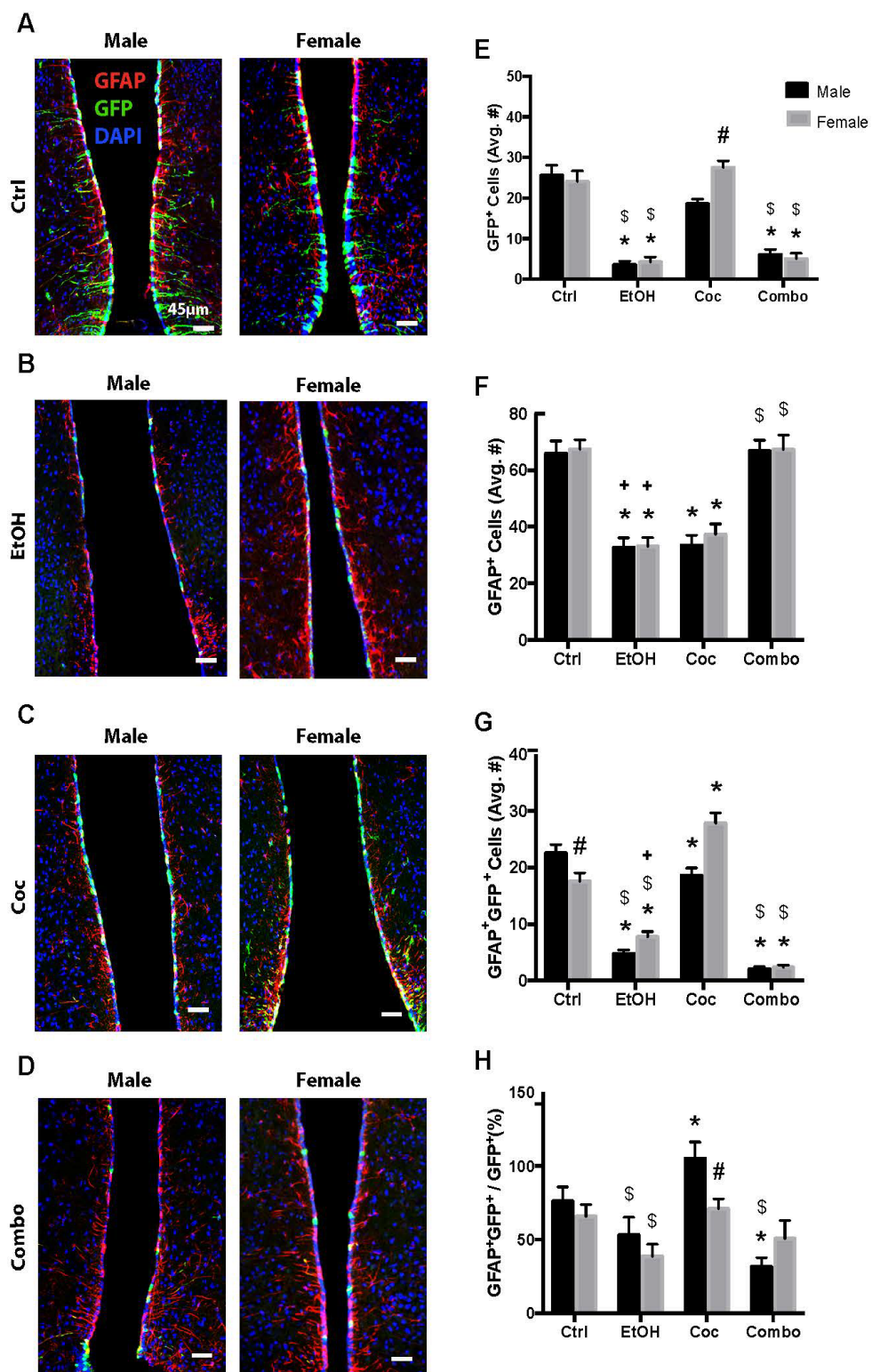**Figure 13. Neural Stem Cell and Astrogliogenesis in the Tanycyte Layer (TL)**

(A-D) Representative brain images of control (Ctrl), ethanol (EtOH), cocaine (Coc), and combination (Combo) treated mice, respectively, stained with stem cell marker (GFP green), astrocyte marker (GFAP red), and merged with nuclear maker DAPI (Bregma 0.5 through 1.08). **(E-H)** Quantification of GFP^+, $GFAP^+$, $GFAP^+GFP^+$, and the percentage of $GFAP^+GFP^+$ over total GFP^+ cells, in the SGZ. Values are shown as mean ±SEM, *$p<0.05$ compared to control, #$p<0.05$ compared to other sex in the same group, $p<0.05$ compared to cocaine group, +$p<0.05$ compared to combination group, n=3 mice per sex per group. Scale bars, 45μm.

Effect of drug treatment on animal behavior

To determine whether single and poly-drug chronic administration altered behavioral outcomes, we conducted a fear conditioning contextual discrimination test for cognitive function, and a sucrose preference test for hedonic behavior.

Context fear discrimination learning has been related to hippocampal neurogenesis and function [35]. Here we found that all four groups of animals gradually increased the time of freezing in the shock context (**Fig. 14A-B**). Control and ethanol groups reached a mean discrimination ratio above 0.5 by day 3, but it took 4 days for cocaine and combination groups to discriminate (**Fig. 14C**). Compared to the control, there was a decreasing trend in the mean ratio after drug treatment on day 4, albeit statistically insignificant. A further analysis on the performance of each individual mouse revealed that the control group (n= 20) had only 10% of mice unable to discriminate (i.e., ratio $\leq$ 0.5), which was increased to 20% in the ethanol group, 40% in cocaine, and 26% in combination (**Fig. 14D, 14E**). In addition, females of both cocaine and combination groups tended to perform worse than males.
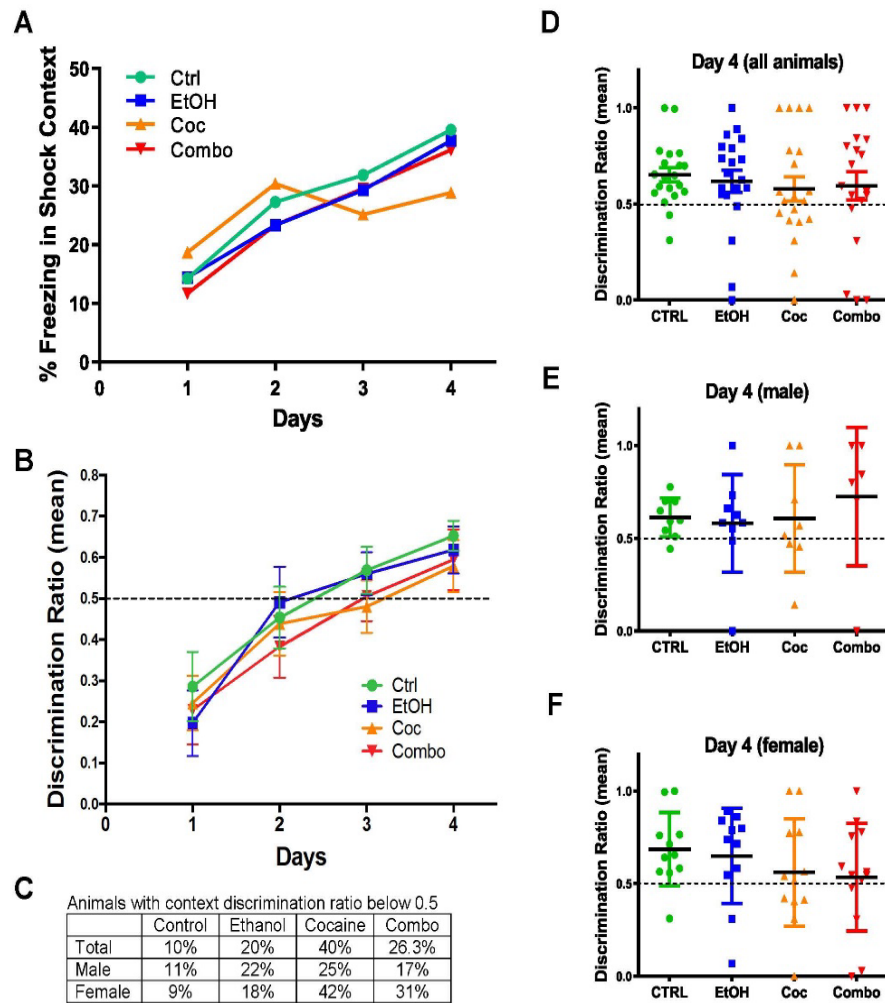
Figure 14. Context Fear Discrimination Learning Paradigm

(A-B) Analysis of percent freezing (b) and discrimination ratio (c) for each treatment group from day 1-4. **(C)** Chart comparing the percentage of male and female in each treatment group with a discrimination ratio below 0.5. **(D-F)** plots of the discrimination ratio for individual animal in each group on day 4. Control (Ctrl) n=20, ethanol (EtOH) n=20, cocaine (Coc) n=20, and combination (Combo) n=19. Values are shown as mean ±SEM.

Furthermore, to determine if changes in the tanycyte layer correlated with changes in hedonic behavior, we conducted a modified form of the sucrose preference task (**Fig. 15**). It has been shown that hypothalamic tanycytes play a role in glucose-sensing via G protein coupled receptors and glucose transporters [54,197], suggesting alterations of

tanycytes may affect feeding-related behaviors based on communication between these cells and the arcuate nucleus of the hypothalamus [47]. In our modified sucrose preference paradigm, mice had access to two bottles of their respective diets, which were identical in every way except one bottle had a percentage of sucrose replacing the equivalent amount of maltose-dextrin (**Fig. 15A**).
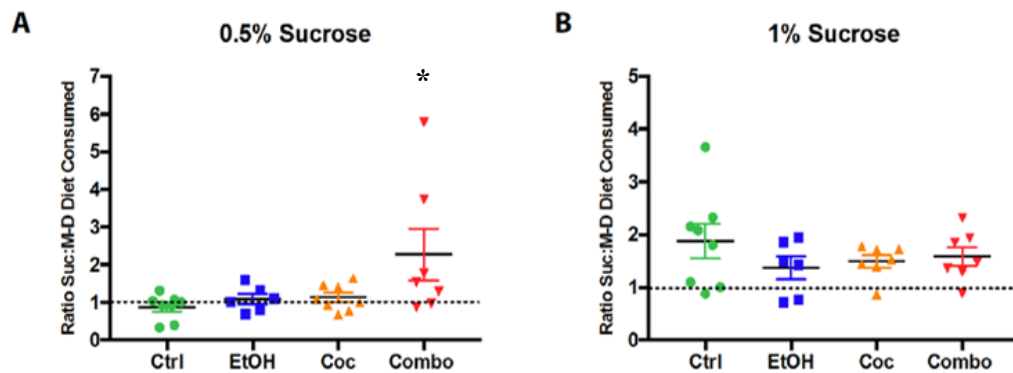
Figure 15. Modified Sucrose Preference Test

> **(A-B)** Analysis of sucrose to maltose-dextrin diet consumed at 0.5% sucrose and 1% sucrose. Control (Ctrl) n=6, ethanol (EtOH) n=6, cocaine (Coc) n=8, and combination (Combo) n=6, *$p < 0.05$ compared to control.

In this way, mice were tested on their preference for sucrose over maltose-dextrin, since the diet was calorically balanced. As shown in Figure 9B, control, ethanol and cocaine groups did not show preference for sucrose diet at 0.5% sucrose, but the combination group consumed approximately 62% more sucrose diet. As expected, increasing sucrose to 1% led all groups to exhibit sucrose-preference; however, there are no significant differences among groups (**Fig. 15B**). This data suggests that combination mice were able to detect a difference in sugar substitution at a lower concentration than other groups. Although preliminary, this behavioral study suggested a potential role of

hypothalamic tanycytes and the effect of poly-drug use on hedonic feeding-related behaviors.

DISCUSSION

This study employs a novel poly-drug administration paradigm using a genetic inducible fate-mapping rodent model to study the effects of chronic ethanol and cocaine co-administration on NSCs and their progeny, and to assess behavioral outcomes following poly-drug administration. To the best of our knowledge, this is the first study to report findings from a chronic poly-drug administration of ethanol and cocaine. Additionally, the primary advantage of this model is the ability to trace a distinct population of NSCs over time, in response to treatment, and characterize behavioral changes. Along this line, we found that chronic treatment of poly-drugs caused more severe damage on NSCs than ethanol alone, while cocaine led to only mild or no damage of NSCs. Single and combined drug treatments all significantly reduced neurogenesis and females were more vulnerable. Chronic exposure to cocaine and poly-drugs tend to alter some cognitive function and hedonic behavior, respectively. However, the severity of drug induced NSC damage did not correlate completely with the changes of these behaviors.

Previously, we have characterized the blood ethanol concentration (BEC) following ethanol liquid diet consumption compared to control [48]. We found that BEC was highly variable and did not correlate with behavioral changes. Peak BEC occurs 1-2 hours following feeding which is a measure of acute intoxication[198]. In our study, mice were given ad libitum access to the ethanol liquid diet and did most of their feeding in the first few hours of the dark cycle. Therefore, during the day, BEC could vary drastically. However, mice still exhibited behavioral changes, due to chronic consumption of an ethanol diet.

The main goal of this study was to evaluate the effect of co-administration of ethanol and cocaine on NSCs in the adult mouse brain. It has been well established that

ethanol interacts with cocaine to form cocaethylene [110,199]. Typically, cocaine is metabolized by carboxylesterase-1 to produce the inactive metabolite BCE. In the presence of ethanol, carboxylesterase metabolizes cocaine, into cocaethylene. It has also been shown that ethanol does not change cocaine pharmacokinetics, suggesting that the enhanced effect on NSCs seen in poly-drug use here could be attributed to a synergistic effect of both drugs taken simultaneous and/or the cocaethylene metabolite [200]. Future experiments will be focused on understanding the direct effect of cocaethylene on NSCs.

In the SVZ, female NSCs were more sensitive to the toxic effects of poly-drug treatment, which also caused the most dramatic reduction of newly differentiated neurons. It is important to note that the female mice in this study were free cycling. While we acknowledge that the estrous cycle and sex hormones play a role in NSC behavior [201], free cycling females were included to increase the translational value of our findings. Furthermore, poly-drug treatment was almost equally detrimental to NSCs and newly differentiated neurons in both the SVZ and SGZ; however, neurons that differentiated before tamoxifen induction were more sensitive to poly-drug treatment in the SGZ. One limitation in our study was the lack of a NSC proliferation marker, which would have established if the lack of differentiation was due to truly reduced differentiation versus an overall reduction in the number of progenitor cells. Previous work in our lab with chronic administration of ethanol alone also produced sex- and region dependent effects and resulted in a much more dramatic impairment of NSCs in the SVZ as well as high mortality and adverse health events [48]. This discrepancy is most likely due to the higher dose of ethanol (4%) used in our previous study as compared to the 3.5% in this study. The lower dosing of ethanol in this study was critically important in order to observe subtle effects of ethanol alone as well as evaluate the synergistic effect of poly-drug use.

Interestingly, we did not observe a correlation between context discrimination performance and degree of NSC loss and neurogenesis in the SGZ of the hippocampus.

It is well established that adult NSCs contribute to spatial learning and memory [202,203]; however, these studies were conducted with selective ablation or suppression of NSCs growth. In our study the brain was grossly affected by cocaine and ethanol administration which may influence neurocircuitry in the hippocampus and the amygdala [204]. The latter may not have been sufficiently impaired following combined administration and was able to produce a compensatory fear response, explaining the maintained performance in the task. It is of interest in future studies to conduct more refined and challenging behavioral tests to better isolate brain functions associated with neurogenic regions.

A reduction in hypothalamic NSCs was detected in the TL following combination treatment; however, the reduction was not quite as dramatic as that seen in the SGZ or SVZ. Further investigation would be beneficial to determine if there are protective factors in the microenvironment surrounding the TL. Another noteworthy finding was that, despite significant reduction of new astrocytic differentiation, the total number of astrocytes (GFAP$^+$) were unaffected in the TL following combination treatment. The heightened resiliency of astrocyte populations in the TL warrants further investigation into the mechanisms of resilience. To interrogate whether changes in the TL affected hedonic feeding-related behavior we conducted a modified sucrose preference test and found that the combination group exhibited an increased sensitivity to this hedonic stimulation. While it has been demonstrated that hypothalamic tanycytes have a glucose-sensing function, their role in poly-drug use and feeding-related behaviors remains ambiguous [54,204]. Our modified sucrose preference test thus offers a new way for further dissecting and understanding their roles in regulating hedonic preference in the context of drug abuse. Furthermore, a study conducted by Jones and colleagues in 2006 shows that there were sex-dependent differences on ethanol and cocaine induced taste aversions [205]. The TL presents a unique opportunity into examining how hypothalamic tanycytes communicate signals from cerebrospinal fluid to the hypothalamus.

While this study provides important information on the neuropathology of poly-drug exposure, one limitation was that drug administration was involuntary; therefore, conclusions about drug dependency cannot be drawn. In order to accurately control confounding variables such as dosing and caloric intake, mice were not given a choice between ethanol or control diet, and cocaine was administered via daily intraperitoneal injections. While this treatment paradigm provides a well-controlled dosing scheme, there can be no assessment of drug seeking. It is of interest to evaluate drug-seeking and dependency in this model in future studies

Endogenous adult NSCs are significantly impacted following chronic ethanol and cocaine co-exposure in a regional and sex-dependent manner. Given the adverse effects of neurodegeneration in substance using populations, targeting NSCs regeneration and neurogenic repair may be a promising approach to improve clinical efficacy of treatments and patient quality of life.

SPECIFIC METHODS

Animals

Nestin-CreERT[2]:R26R-YFP bi-transgenic male and female mice were generated by crossing the C57BL/6-Tg(Nes-cre/ERT2)KEisc/J strain with the B6.129X1-Gt(ROSA)26Sortm1(EYFP)Cos/J strain (both obtained from the Jackson Laboratory), and have been described elsewhere [57]. Mice were genotyped by PCR using genomic DNA from tail snip to confirm presence of Cre and YFP trans-genes. Upon induction, tamoxifen will allow for constitutive expression of enhanced yellow fluorescent protein (eYFP) in all *nestin* expressing cells of adult mice. *Nestin* is an intermediate filament protein expressed in quiescent and proliferative neural stem cells. Tamoxifen was administered

intraperitoneally for a total of 5 days at 75mg/kg. Female mice were free cycling during the duration of this study. All animal experiments were approved by the Institutional Animal Care and Use Committee of the University of Texas Medical Branch and conducted in accordance with the *Guide for the Care and Use of Laboratory Animals*, and maintained on a 12-hour light/dark cycle.

Experimental design

Mice, 3-4 months old, were randomly assigned using the "randomize" (RAND) function in Microsoft Excel to one of four groups: control (male n=7, female n=13), cocaine (male n=10, female n=14), ethanol (male n=10, female n=13), or combination (male n=10, female n=15). Mice in each group were age and sex matched to control for variability. Following randomized group assignment, mice were individually housed and given *ad libitum* access to water and a Lieber-DeCarli liquid diet containing complete nutrients for rodents (Dyets Inc., Bethlehem, PA, CAT #710260) as previously described [50]. Calorically-matched feeding was done in which ethanol calories replaced the equivalent calories of maltose-dextrin in the diet for ethanol and combination mice. The amount of ethanol in the liquid diet was slowly increased from 1% to 3.5% over the course of two weeks. Mice in the ethanol and combination groups were maintained on 3.5% ethanol liquid diet for a total of 8 weeks, while mice in the control and cocaine groups were given calorie balanced liquid diet without ethanol. Cocaine treatment was given over a total of 6 weeks (Figure 1A). The 8-week treatment course was chosen as a chronic paradigm [206]. All diet was made fresh daily. Each day, between 9:00-11:00am, the feeding bottles were removed from the cage, the remaining liquid diet was measured and subtracted from the original diet administered. Blood ethanol concentrations (BEC) following chronic liquid diet consumption were monitored as described before [48]. On the first day of 3.5% ethanol in diet, the combination and cocaine mice received daily 10mg/kg intraperitoneal injections

(i.p.) of (−)-Cocaine (National Institute on Drug Abuse), dissolved in 0.9% NaCl, every day for six weeks. Mice in the control and ethanol group received vehicle injection of 20μL of 0.9% saline. Animals were weighed once a week. All data presented represents ±SEM.

Analysis of Cocaine & Metabolites Using LC-MS

An Agilent 1260 HPLC system with a binary gradient pump, autosampler and column oven (50°C) was used for the chromatographic separation. An Agilent SB-C18 1.8uM 2.1 X 50mm column was used. Mobile phase A was water + 0.1% formic acid and mobile phase B acetonitrile + 0.1% formic acid. A flow rate 500 μL/min was used. The gradient with a total run time of 12 minutes 0-1min 98% A, 1-7min a linear gradient to 35% A, 7-7.1 min to 2% A, 7.1-9min 2% A, 9-9.1 min 98% A, 9.1-12min 98% A. The injection volume was set to 10 μL.

A SCIEX QTRAP 6500 system with Turbo V source with ESI probe was used. The target compounds were detected in positive polarity. The ion source parameters were optimized for the new LC conditions using the Compound Optimization (FIA) function in Analyst® software and are as follows: Curtain gas (40), CAD set to high, Ionspray voltage 4500, Temperature 50C, GS1 50, GS2 50, DP ranged from 76-81 volts, CE ranged from 27-41 volts, CXP ranged from 10-16 volts. Two characteristic MRM transitions were monitored for each analyte, and 1 MRM transition for each internal standard.

Behavioral assessment

Context fear discrimination learning was conducted as we described previously [35]. All procedures were carried out between 7:00 a.m. and 6:00 p.m. Each day before testing, mice were allowed to acclimate to the testing room for 1 hour. Control (n=20), ethanol (n=20), cocaine (n=20), and combination (n=19) were exposed to the shock context on training day (Day 0), before being returned to their home cage. Starting Day 1 through the

rest of the experiment, mice were placed in both the shock (Context A) and a safe (Context B) context. Animals were randomly selected from each group and the order of context presented was randomized each day to avoid animals adjusting to the schedule. There was no foot shock in Context B. Percent freezing was recorded in each context. Because contextual fear-discrimination is a hippocampal-dependent task, it measures an animal's ability to distinguish between two environmental contexts. Each context used a standard mouse fear conditioning chamber (MedAssociates). Context A had no modifications to the chamber with light and fan. Context B also had a grid floor, however it also contained cardboard inserts, vanilla extract, and the chamber light and fan were shut off. Mice spend equal amounts of time in both chambers and were randomly assigned to which context they would experience first. A four-hour interval was left in between contexts for each subject on each day of testing. Chambers were cleaned with 70% ethanol in between each subject. Digital video-based data capture and analysis with FreezeFrame software (Actimetrics) was used to assess freezing behavior. Discrimination ratios (% freezing in Context A ÷ % freezing in Context A+B) were calculated for each group on each test day.

Sucrose preference task

In order to assess if changes observed in cell populations in the TL correlated with behavioral changes, a sucrose preference test was employed. Mice were given two bottles, one containing only maltose-dextrin, the other containing the substituted percentage of sucrose. In order to assess if drug treatment affected taste preference for sucrose compared to maltose-dextrin, sucrose was increased in the liquid diets of control (n=6), ethanol (n=8), cocaine (n=6), and combination (n=8) mice over the course of 4 days. Sucrose was increased incrementally every 2 days from 0.5% to 1%. The equivalent amount of maltose-dextrin was removed from the liquid diet corresponding to the amount of sucrose added in order to maintain the caloric balance of the diets. Diet consumption

83

was measured daily and used to calculate the ratio of sucrose:maltose-dextrin consumption.

Immunohistochemistry

At the termination of the experiments, mice were anesthetized with ketamine/xylazine (90mg/kg and 10mg/kg), and blood samples were collected prior to perfusion with 5 mL PBS and 30 mL of cold 4% paraformaldehyde via an intra-cardial injection. Mouse brains were collected, post-fixed in 4% paraformaldehyde for 1 day at 4°C, and then infiltrated with 30% sucrose for 5 days at 4°C before embedding in OCT media. Tissue from three mice per treatment group was serially sectioned, coronally, at a thickness of 30µm using a Leica cryostat machine. Every fifth section was collected on the same slide with four sections per slide, and five slides per region (each slide covered a distance of 480 µm). Therefore, for every region and each cell marker, four tissue sections were counted spanning a distance of 480 µm. Slides were randomized for staining and double blinded for stereology using anonymous identification numbers. Detection of induced-YPF was enhanced by immunohistochemical staining with chicken anti-GFP antibodies (Aves Labs, Tigard, OR, CAT# GFP-1020). Additionally, sections were incubated with antibodies against GFAP (Thermo Fisher Scientific, Waltham, MA, CAT#PA110019), DCX (San Francisco, CA, Abcam, CAT#ab18723), or NeuN (Millipore, Billercia MA CAT#MAB377). Following primary antibody incubation at 4°C overnight, sections were incubated with AlexaFluor secondary antibodies (goat-anti-chicken 488, CAT#A11039; goat-anti-rabbit 568, CAT#A11011; and goat-anti-mouse 568 CAT#AB175473).

Imaging and Cell Counting

All images were acquired on a Nikon D-ECLIPSE C1 Confocal Microscope, using the Nikon EZ-C1 3.91 software. Stereology was performed as previously described [207]. Blinded cell counting was performed using either NIS Elements or ImageJ software. Positive identification of cells was based on both immunostaining and morphological characteristics, and only DAPI$^+$ nucleated cell profiles were counted. The SVZ of the lateral ventricle was counted from bregma 0.50mm through 1.08mm, the origin of the rostral migratory stream was counted from bregma 1.5mm through 2mm, and both the SGZ of the hippocampus and the TL of the third ventricle were counted from bregma -1.58mm through -2.16mm. Four sections (both hemispheres) from each region, spanning a total of 480µm longitudinally, were counted for each antibody. Average total positive cells were performed using triplicate mice for each region and antibody.

Statistical Analysis

The number of mice required for analysis was calculated based on our previous results and power analyses using G*Power 3.1.7. An n=3 was needed to provide statistical significance at $p<0.05$ with a power of 0.80 for the histological data, and an n=11 for behavioral analysis based on pilot studies. For morphological analyses, 2-way ANOVA (effects of treatment and sex) with a post hoc Tukey test assisted by GraphPad Prism v7 software were applied to analyze the effects of treatment on brain cells both individually and combined. A 2-way ANOVA was conducted to analyze morphological alterations in the olfactory bulb. Each group had three mice being used for each immunostaining, a p value less than 0.05 was considered statistically significant and a p value greater than 0.05 but less than 0.1 was considered a trend. Context discrimination and sucrose preference was analyzed using a 2-way repeated measures ANOVA (effects of treatment and sex) with a post hoc Tukey's test.

CHAPTER 4: SUMMARY AND FUTURE DIRECTIONS

CHAPTER 2 CONCLUSIONS AND FUTURE DIRECTIONS

Chapter 2 investigated the effects of maternal OUD treated with BUP MAT on fetal brain development and adolescent behavior. There was a significant decrease in overall embryo, as shown by decreases in CRL and body width, and brain size. Studies using magnetic resonance imaging (MRI) have shown children diagnosed with ADHD, have significantly smaller overall brain size, than matched healthy controls [126]. There were also significant impairments in cortical layer development, due to decreases in cell proliferation, differentiation, and migration. More specifically, we showed significant impairments in the development of layers V and VI, which are primarily deep-layer neuronal populations [208].

Furthermore, we show significant behavioral alterations, specifically a hyperactive behavioral phenotype, in male OXY+BUP-treated offspring at PND60. OXY+BUP-treated male offspring had significantly increased locomotor behavior, as well as, decreased immobility in the FST. Hyperactivity is a common phenotype of ADHD and due to the prevalence of ADHD diagnoses in offspring following maternal opioid use in clinical cases [93], we wanted to explore changes in the VTA. Excitingly, we showed a significant increase in dopaminergic neuronal ontogenesis, in male and female OXY+BUP-treated offspring compared to control. Further studies should also include looking at changes in the PFC of OXY+BUP adolescent animals including; sustained decreases in cortical thickness and ventriculomegaly. Changes in cortical thickness have been linked to a worse clinical outcome in children diagnosed with ADHD [130]. Studies also show significant decreases in the corpus callosum in ADHD patients, compared to healthy controls [126,131,132].

Future directions for this project include investigating the role of abstinence during pregnancy. Current standard treatment of care recommends MAT as the safer alternative and against withdrawal during pregnancy, due to a higher risk of relapse [182]. However,

based on our studies showing significant changes in brain development and the impacts on adolescent behavior, more studies need to investigate the impact of withdrawal, possibly in a supervised setting, over MAT.

Further behavioral paradigms that would be interesting to probe would be alterations in attention and impulsivity, such as the 5-choice serial response task, and altered social behaviors. These behaviors have been linked to ADHD [124,209,210], and clinical cases have shown a high correlation between MAT and ADHD [93]. Furthermore, in our own model we are showing a hyperactive phenotype, therefore characterization into ADHD-like behaviors following maternal BUP MAT is warranted. Future experiments can also investigate self-administration studies in OXY+BUP-treated offspring. Multiple clinical studies have shown that prenatal exposure to opioids can lead to a greater likelihood for the development of addiction in young offspring [124,211,212]. There has also been many studies showing positive correlations between ADHD patients and drug addiction, where ADHD patients are more likely to become addicted to drugs of abuse [213-215].

Future studies also need to include investigation into the mechanistic implications for alterations in dopamine neuron ontogenesis. More specifically, the posed hypothesis, that increased TH immunoreactivity in the VTA is due to dopamine hypofunction in the PFC, needs investigation. Experiments could include looking at changes in dopamine neuron activity, using electrophysiology, and changes in dopamine release from the VTA to the PFC using microdialysis and neuronal tracers. Also, studies could include looking at the dopamine transporter (DAT) and dopamine 4 receptor (D4R), which have been linked to ADHD [132,216]. Additionally, polymorphisms of D4R have been linked to ADHD [132,139]. Further studies can probe for expression level changes, of DAT or D4R, using qRT-PCR and Western blotting from tissue samples of our BUP MAT model.

CHAPTER 3 CONCLUSIONS AND FUTURE DIRECTIONS

Poly-drug use represents a significant problem due to the additive or synergistic effects when two drugs of abuse are combined. This project highlighted this by showing a significant increase in NPC loss following combined administration of cocaine and alcohol, which was greater than either drug alone (**Illustration 4**). We also showed significant reductions in neurogenesis and astrogliogenesis in the combined drug group. Preliminary behavioral results, looking into sucrose preference, showed a heightened sensitivity to sucrose in the combination group, compared to single drug administration.

SVZ	Male	Female
NSPC Survival	↓	↓↓
Neurogenesis	↓↓	↓↓
Astrogliogenesis	↓	↓

SGZ	Male	Female
NSPC Survival	↓↓	↓↓
Neurogenesis	↓↓	↓↓
Astrogliogenesis	↓↓	↓↓

TL	Male	Female
NSPC Survival	↓↓	↓↓
Neurogenesis	—	—
Astrogliogenesis	↓	↑
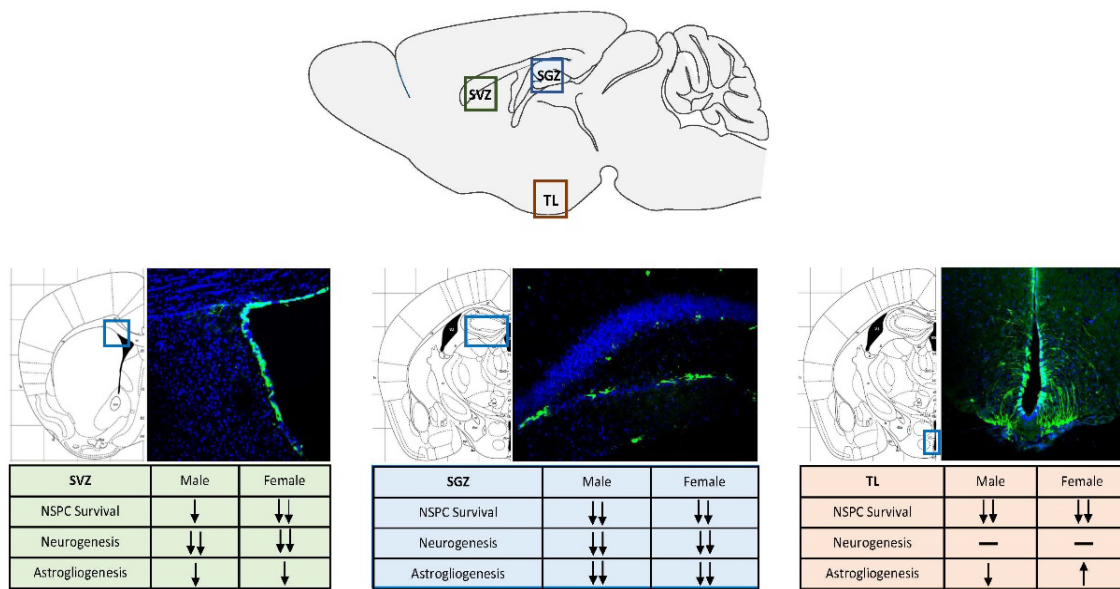
Illustration 4: Neural Progenitor Cell Response to Combined Drug Use in Neurogenic Regions. NPCs are labeled by green fluorescent protein (GFP), nuclei stained with DAPI showing the representative neurogenic regions. SVZ – subventricular zone. SGZ – subgranular zone, TL – tanycyte layer.

Future directions for this project should include investigation into the mechanism of cocaethylene in precipitating the detrimental effects seen in the combination group. Cocaethylene is only produced when cocaine and ethanol are consumed simultaneously. This is because ethanol inhibits the canonical hydrolysis of cocaine and,

instead, induces carboxylesterase 1 (CES1) which metabolizes cocaine into cocaethylene [119,217,218]. Cocaethylene, similar to cocaine, inhibits dopamine reuptake; and has been shown to have greater euphoric properties than cocaine due to an additive effect following alcohol and cocaine use [219,220].

Cocaethylene, metabolized by CES1 which is found in low levels in the brain [49,221], has been studied primarily for the effects on the heart, and has been shown to be ten times more cardio-toxic than cocaine [104,222,223]. This is due, in part, to the fact that the half-life of cocaethylene is three times longer than cocaine, so effects are sustained for longer periods of time. Additionally, one study has shown cocaethylene can have negative effects on the brain, specifically a loss in righting reflex following intracerebroventricular (ICV) administration [119]. Further research, specifically into the neurotoxic effects of cocaethylene, have yet to be done. Future directions for investigation also include determining whether cocaethylene is independently neurotoxic to NPCs and if the production of cocaethylene can precipitate an addictive phenotype greater than cocaine or ethanol alone.

Additional future investigations include probing the behavioral alterations we see in this model. Multiple groups have shown the important role of tanycytes in nutrient-sensing [50-52]. More specifically, htNSCs have been shown to have taste receptors, similar to those found on the tongue, which could be driving the increased sensitivity to sucrose we see in the behavioral paradigm [54]. Binge eating and drug use is of concern and one group has shown that Agouti-related peptide (Agrp) neurons are key regulators of binge eating following alcohol intake [224]. Additionally, another study showed that following insult with monosodium glutamate (MSG), there is an increased proliferation of Agrp neurons [44]. Due to the proximity of htNSCs to the arcuate nucleus, and therefore Agrp neurons, it would be interesting to see if the impact of combined drug use affects the arcuate nucleus more directly, and related eating behaviors.

Overall, the work presented in this dissertation provides multiple models in which to study the role of drugs of abuse on endogenous neural stem cells and neurogenesis, in the adult and developing brain. Not only that, but this work also stresses the direct effect of drugs of abuse on the brain and this critical cell population. Further studies are needed to explore the mechanistic implications behind these alterations, in order to better drive development of therapies and interventions for individuals with adult or prenatal drug exposure.

References

1   Schlagal, C. R. & Wu, P. Tipsy neural stem cells: chronic effects of alcohol on the
        brain. *Neural Regen Res* **14**, 67-68, doi:10.4103/1673-5374.243702 (2019).

2   Zhao, X. & Moore, D. L. Neural stem cells: developmental mechanisms and
        disease modeling. *Cell Tissue Res* **371**, 1-6, doi:10.1007/s00441-017-2738-1
        (2018).

3   Brazel, C. Y., Romanko, M. J., Rothstein, R. P. & Levison, S. W. Roles of the
        mammalian subventricular zone in brain development. *Prog Neurobiol* **69**, 49-69,
        doi:10.1016/s0301-0082(03)00002-9 (2003).

4   Hill, M. A. Carnegie Stages. *Embryology* (2020).

5   Schoenwolf, G. C. B. S. B. B. P. R. F.-W. P. H. & Philippa, H.   (2015).

6   Sadler, T. W. Embryology of neural tube development. *Am J Med Genet C Semin
        Med Genet* **135C**, 2-8, doi:10.1002/ajmg.c.30049 (2005).

7   Ishikawa, Y., Yamamoto, N., Yoshimoto, M. & Ito, H. The primary brain vesicles
        revisited: are the three primary vesicles (forebrain/midbrain/hindbrain) universal
        in vertebrates? *Brain. Behav. Evol.* **79**, 75-83, doi:10.1159/000334842 (2012).

8   O'Rahilly, R. & Muller, F. Ventricular system and choroid plexuses of the human
        brain during the embryonic period proper. *Am J Anat* **189**, 285-302,
        doi:10.1002/aja.1001890402 (1990).

9   Morest, D. K. & Silver, J. Precursors of neurons, neuroglia, and ependymal cells
        in the CNS: what are they? Where are they from? How do they get where they are
        going? *Glia* **43**, 6-18, doi:10.1002/glia.10238 (2003).

10   Kriegstein, A. & Alvarez-Buylla, A. The glial nature of embryonic and adult neural stem cells. *Annu Rev Neurosci* **32**, 149-184, doi:10.1146/annurev.neuro.051508.135600 (2009).

11   Gilmore, E. C. & Herrup, K. Cortical development: layers of complexity. *Curr. Biol.* **7**, R231-234, doi:10.1016/s0960-9822(06)00108-4 (1997).

12   Villar-Cerviño, V. & Marín, O. Cajal-Retzius cells. *Curr. Biol.* **22**, R179, doi:10.1016/j.cub.2012.01.016 (2012).

13   D'Arcangelo, G. The reeler mouse: anatomy of a mutant. *Int Rev Neurobiol* **71**, 383-417, doi:10.1016/s0074-7742(05)71016-3 (2005).

14   Larkum, M. E., Petro, L. S., Sachdev, R. N. S. & Muckli, L. A Perspective on Cortical Layering and Layer-Spanning Neuronal Elements. *Front Neuroanat* **12**, 56, doi:10.3389/fnana.2018.00056 (2018).

15   Abdel Razek, A. A., Kandell, A. Y., Elsorogy, L. G., Elmongy, A. & Basett, A. A. Disorders of cortical formation: MR imaging features. *AJNR Am J Neuroradiol* **30**, 4-11, doi:10.3174/ajnr.A1223 (2009).

16   Fatemi, S. H. Reelin mutations in mouse and man: from reeler mouse to schizophrenia, mood disorders, autism and lissencephaly. *Mol Psychiatry* **6**, 129-133, doi:10.1038/sj.mp.4000129 (2001).

17   Pang, T., Atefy, R. & Sheen, V. Malformations of cortical development. *Neurologist* **14**, 181-191, doi:10.1097/NRL.0b013e31816606b9 (2008).

18   Rubenstein, J. L. Annual Research Review: Development of the cerebral cortex: implications for neurodevelopmental disorders. *J Child Psychol Psychiatry* **52**, 339-355, doi:10.1111/j.1469-7610.2010.02307.x (2011).

19   Hadjivassiliou, G. *et al.* The application of cortical layer markers in the evaluation of cortical dysplasias in epilepsy. *Acta Neuropathol* **120**, 517-528, doi:10.1007/s00401-010-0686-x (2010).

20   Altman, J.   (Science, 1962).

21   Kempermann, G., Song, H. & Gage, F. H. Neurogenesis in the Adult Hippocampus. *Cold Spring Harb Perspect Biol* **7**, a018812, doi:10.1101/cshperspect.a018812 (2015).

22   Sierra, A., Encinas, J. M. & Maletic-Savatic, M. Adult human neurogenesis: from microscopy to magnetic resonance imaging. *Front Neurosci* **5**, 47, doi:10.3389/fnins.2011.00047 (2011).

23   Gage, F. H. Neurogenesis in the adult brain. *J Neurosci* **22**, 612-613 (2002).

24   Brancaccio, M., Pivetta, C., Granzotto, M., Filippis, C. & Mallamaci, A. Emx2 and Foxg1 inhibit gliogenesis and promote neuronogenesis. *Stem Cells* **28**, 1206-1218, doi:10.1002/stem.443 (2010).

25   Obernier, K. & Alvarez-Buylla, A. Neural stem cells: origin, heterogeneity and regulation in the adult mammalian brain. *Development* **146**, doi:10.1242/dev.156059 (2019).

26   Wang, Y. Z., Plane, J. M., Jiang, P., Zhou, C. J. & Deng, W. Concise review: Quiescent and active states of endogenous adult neural stem cells: identification and characterization. *Stem Cells* **29**, 907-912, doi:10.1002/stem.644 (2011).

27   Kawai, H. *et al.* Area-Specific Regulation of Quiescent Neural Stem Cells by Notch3 in the Adult Mouse Subependymal Zone. *J Neurosci* **37**, 11867-11880, doi:10.1523/JNEUROSCI.0001-17.2017 (2017).

28   Martínez-Cerdeño, V. & Noctor, S. C. Neural Progenitor Cell Terminology. *Front Neuroanat* **12**, 104, doi:10.3389/fnana.2018.00104 (2018).

29   Noctor, S. C., Martinez-Cerdeño, V. & Kriegstein, A. R. Neural stem and progenitor cells in cortical development. *Novartis Found Symp* **288**, 59-73; discussion 73-58, 96-58 (2007).

30   Carpentier, P. A. & Palmer, T. D. Immune influence on adult neural stem cell regulation and function. *Neuron* **64**, 79-92, doi:10.1016/j.neuron.2009.08.038 (2009).

31   Wang, W. *et al.* Mitochondrial DNA damage level determines neural stem cell differentiation fate. *J Neurosci* **31**, 9746-9751, doi:10.1523/JNEUROSCI.0852-11.2011 (2011).

32   Gould, E. How widespread is adult neurogenesis in mammals? *Nat Rev Neurosci* **8**, 481-488, doi:10.1038/nrn2147 (2007).

33   Goncalves, J. T., Schafer, S. T. & Gage, F. H. Adult Neurogenesis in the Hippocampus: From Stem Cells to Behavior. *Cell* **167**, 897-914, doi:10.1016/j.cell.2016.10.021 (2016).

34   Guo, W. *et al.* Ablation of Fmrp in adult neural stem cells disrupts hippocampus-dependent learning. *Nat Med* **17**, 559-565, doi:10.1038/nm.2336 (2011).

35   Cortez, I. *et al.* Aged dominant negative p38α MAPK mice are resistant to age-dependent decline in adult-neurogenesis and context discrimination fear conditioning. *Behav Brain Res* **322**, 212-222, doi:10.1016/j.bbr.2016.10.023 (2017).

36   Ming, G. L. & Song, H. Adult neurogenesis in the mammalian brain: significant answers and significant questions. *Neuron* **70**, 687-702, doi:10.1016/j.neuron.2011.05.001 (2011).

37   Miller, J. A. *et al.* Conserved molecular signatures of neurogenesis in the hippocampal subgranular zone of rodents and primates. *Development* **140**, 4633-4644, doi:10.1242/dev.097212 (2013).

38   Onksen, J. L., Brown, E. J. & Blendy, J. A. Selective deletion of a cell cycle checkpoint kinase (ATR) reduces neurogenesis and alters responses in rodent models of behavioral affect. *Neuropsychopharmacology* **36**, 960-969, doi:10.1038/npp.2010.234 (2011).

39   Alvarez-Buylla, A. & Garcia-Verdugo, J. M. Neurogenesis in adult subventricular zone. *J Neurosci* **22**, 629-634 (2002).

40   Horstmann, E. [The fiber glia of selacean brain]. *Z Zellforsch Mikrosk Anat* **39**, 588-617 (1954).

41   Millhouse, O. E. A Golgi study of third ventricle tanycytes in the adult rodent brain. *Z Zellforsch Mikrosk Anat* **121**, 1-13 (1971).

42   Robins, S. C. *et al.* α-Tanycytes of the adult hypothalamic third ventricle include distinct populations of FGF-responsive neural progenitors. *Nat Commun* **4**, 2049, doi:10.1038/ncomms3049 (2013).

43   Haan, N. *et al.* Fgf10-expressing tanycytes add new neurons to the appetite/energy-balance regulating centers of the postnatal and adult hypothalamus. *J Neurosci* **33**, 6170-6180, doi:10.1523/jneurosci.2437-12.2013 (2013).

44   Yulyaningsih, E. *et al.* Acute Lesioning and Rapid Repair of Hypothalamic Neurons outside the Blood-Brain Barrier. *Cell Rep* **19**, 2257-2271, doi:10.1016/j.celrep.2017.05.060 (2017).

45   Zhang, Y. *et al.* Hypothalamic stem cells control ageing speed partly through exosomal miRNAs. *Nature* **548**, 52-57, doi:10.1038/nature23282 (2017).

46   Zhang, Y., Liu, G., Yan, J., Li, B. & Cai, D. Metabolic learning and memory formation by the brain influence systemic metabolic homeostasis. *Nat Commun* **6**, 6704, doi:10.1038/ncomms7704 (2015).

47   Lee, D. A. *et al.* Tanycytes of the hypothalamic median eminence form a diet-responsive neurogenic niche. *Nat Neurosci* **15**, 700-702, doi:10.1038/nn.3079 (2012).

48   McGrath, E. L. *et al.* Spatial and Sex-Dependent Responses of Adult Endogenous Neural Stem Cells to Alcohol Consumption. *Stem Cell Reports*, doi:10.1016/j.stemcr.2017.10.007 (2017).

49   McGrath, E. L. *et al.* Chronic poly-drug administration damages adult mouse brain neural stem cells. *Brain Res*, 146425, doi:10.1016/j.brainres.2019.146425 (2019).

50   Rodríguez, E. M. *et al.* Hypothalamic tanycytes: a key component of brain-endocrine interaction. *Int Rev Cytol* **247**, 89-164, doi:10.1016/s0074-7696(05)47003-5 (2005).

51   Prevot, V. *et al.* The versatile tanycyte: a hypothalamic integrator of reproduction and energy metabolism. *Endocr Rev*, doi:10.1210/er.2017-00235 (2018).

52   Parkash, J. *et al.* Semaphorin7A regulates neuroglial plasticity in the adult hypothalamic median eminence. *Nat Commun* **6**, 6385, doi:10.1038/ncomms7385 (2015).

53   Recabal, A., Caprile, T. & García-Robles, M. L. A. Hypothalamic Neurogenesis as an Adaptive Metabolic Mechanism. *Front Neurosci* **11**, 190, doi:10.3389/fnins.2017.00190 (2017).

54   Benford, H. *et al.* A sweet taste receptor-dependent mechanism of glucosensing in hypothalamic tanycytes. *Glia* **65**, 773-789, doi:10.1002/glia.23125 (2017).

55   Lee, A. A. & Owyang, C. Sugars, Sweet Taste Receptors, and Brain Responses. *Nutrients* **9**, doi:10.3390/nu9070653 (2017).

56   Hancock, A., Priester, C., Kidder, E. & Keith, J. R. Does 5-bromo-2'-deoxyuridine (BrdU) disrupt cell proliferation and neuronal maturation in the adult rat hippocampus in vivo? *Behav Brain Res* **199**, 218-221, doi:10.1016/j.bbr.2008.11.050 (2009).

57   Lagace, D. C. *et al.* Dynamic contribution of nestin-expressing stem cells to adult neurogenesis. *J Neurosci* **27**, 12623-12629, doi:10.1523/jneurosci.3812-07.2007 (2007).

58   Mignone, J. L., Kukekov, V., Chiang, A. S., Steindler, D. & Enikolopov, G. Neural stem and progenitor cells in nestin-GFP transgenic mice. *J Comp Neurol* **469**, 311-324, doi:10.1002/cne.10964 (2004).

59   Yau, S. Y., Gil-Mohapel, J., Christie, B. R. & So, K. F. Physical exercise-induced adult neurogenesis: a good strategy to prevent cognitive decline in

neurodegenerative diseases? *Biomed Res Int* **2014**, 403120, doi:10.1155/2014/403120 (2014).

60   Brandhorst, S. *et al.* A Periodic Diet that Mimics Fasting Promotes Multi-System Regeneration, Enhanced Cognitive Performance, and Healthspan. *Cell Metab* **22**, 86-99, doi:10.1016/j.cmet.2015.05.012 (2015).

61   DiFeo, G. & Shors, T. J. Mental and physical skill training increases neurogenesis via cell survival in the adolescent hippocampus. *Brain Res* **1654**, 95-101, doi:10.1016/j.brainres.2016.08.015 (2017).

62   United States. Department of, H. & Human, S. *Facing addiction in America : the Surgeon General's report on alcohol, drugs and health*. (U.S. Department of Health & Human Services, 2016).

63   Schuchat, A., Houry, D. & Guy, G. P., Jr. New Data on Opioid Use and Prescribing in the United States. *JAMA* **318**, 425-426, doi:10.1001/jama.2017.8913 (2017).

64   SAMHSA.   (https://www.samhsa.gov/data/sites/default/files/NSDUH-FFR1-2016/NSDUH-FFR1-2016.htm, 2016).

65   Association, A. P. Diagnostic and statistical manual of mental disorders (5th ed.). (2013).

66   SAMHSA. Key Substance Use and Mental Health Indicators in the United States: Results from the 2018 National Survey on Drug Use and Health. (2018).

67   Cortazzo, M. H., Copenhaver, D., Fishman, S.M. 36 - Major Opioids and Chronic Opioid Therapy. *Practical Management of Pain (Fifth Edition)*, Pages 495-507.e493 (2014).

68   Enga, R. M., Jackson, A., Damaj, M. I. & Beardsley, P. M. Oxycodone physical

       dependence and its oral self-administration in C57BL/6J mice. *Eur J Pharmacol*

       789, 75-80, doi:10.1016/j.ejphar.2016.07.006 (2016).

69   Bostrom, E., Simonsson, U. S. & Hammarlund-Udenaes, M. In vivo blood-brain

       barrier transport of oxycodone in the rat: indications for active influx and

       implications for pharmacokinetics/pharmacodynamics. *Drug Metab Dispos* **34**,

       1624-1631, doi:10.1124/dmd.106.009746 (2006).

70   Koons, A. L., Rayl Greenberg, M., Cannon, R. D. & Beauchamp, G. A. Women

       and the Experience of Pain and Opioid Use Disorder: A Literature-based

       Commentary. *Clin Ther* **40**, 190-196, doi:10.1016/j.clinthera.2017.12.016 (2018).

71   Desai, R. J., Hernandez-Diaz, S., Bateman, B. T. & Huybrechts, K. F. Increase in

       prescription opioid use during pregnancy among Medicaid-enrolled women.

       Obstet Gynecol **123**, 997-1002, doi:10.1097/AOG.0000000000000208 (2014).

72   Coyle, M. G., Brogly, S. B., Ahmed, M. S., Patrick, S. W. & Jones, H. E.

       Neonatal abstinence syndrome. *Nat Rev Dis Primers* **4**, 47, doi:10.1038/s41572-

       018-0045-0 (2018).

73   Patrick, S. W., Davis, M. M., Lehman, C. U. & Cooper, W. O. Increasing

       incidence and geographic distribution of neonatal abstinence syndrome: United

       States 2009 to 2012. *J Perinatol* **35**, 667, doi:10.1038/jp.2015.63 (2015).

74   Gibson, K. S., Stark, S., Kumar, D. & Bailit, J. L. The relationship between

       gestational age and the severity of neonatal abstinence syndrome. *Addiction* **112**,

       711-716, doi:10.1111/add.13703 (2017).

75   Jansson, L. M. & Velez, M. Neonatal abstinence syndrome. *Curr Opin Pediatr*
       24, 252-258, doi:10.1097/MOP.0b013e32834fdc3a (2012).

76   Dematteis, M. *et al.* Recommendations for buprenorphine and methadone therapy
       in opioid use disorder: a European consensus. *Expert Opin Pharmacother* **18**,
       1987-1999, doi:10.1080/14656566.2017.1409722 (2017).

77   Guille, C. & Aujla, R. Developmental Consequences of Prenatal Substance Use in
       Children and Adolescents. *J Child Adolesc Psychopharmacol* **29**, 479-486,
       doi:10.1089/cap.2018.0177 (2019).

78   Klaman, S. L. *et al.* Treating Women Who Are Pregnant and Parenting for Opioid
       Use Disorder and the Concurrent Care of Their Infants and Children: Literature
       Review to Support National Guidance. *J Addict Med* **11**, 178-190,
       doi:10.1097/ADM.0000000000000308 (2017).

79   Wilder, C. M. & Winhusen, T. Pharmacological Management of Opioid Use
       Disorder in Pregnant Women. *CNS Drugs* **29**, 625-636, doi:10.1007/s40263-015-
       0273-8 (2015).

80   Blum, K. *et al.* Introducing "Precision Addiction Management (PAM. *Open
       Access J Behav Sci Psychol* **1**, 1-4 (2018).

81   Ross, E. J., Graham, D. L., Money, K. M. & Stanwood, G. D. Developmental
       consequences of fetal exposure to drugs: what we know and what we still must
       learn. *Neuropsychopharmacology* **40**, 61-87, doi:10.1038/npp.2014.147 (2015).

82   Parikh, R., Hussain, T., Holder, G., Bhoyar, A. & Ewer, A. K. Maternal
       methadone therapy increases QTc interval in newborn infants. *Arch Dis Child
       Fetal Neonatal Ed* **96**, F141-143, doi:10.1136/adc.2009.181701 (2011).

83   Binder, T. & Vavrinková, B. Prospective randomised comparative study of the effect of buprenorphine, methadone and heroin on the course of pregnancy, birthweight of newborns, early postpartum adaptation and course of the neonatal abstinence syndrome (NAS) in women followed up in the outpatient department. *Neuro Endocrinol Lett* **29**, 80-86 (2008).

84   Gupta, M., Mulvihill, A. O., Lascaratos, G., Fleck, B. W. & George, N. D. Nystagmus and reduced visual acuity secondary to drug exposure in utero: long-term follow-up. *J Pediatr Ophthalmol Strabismus* **49**, 58-63, doi:10.3928/01913913-20110308-01 (2012).

85   Gill, A. C. *et al.* Strabismus in infants of opiate-dependent mothers. *Acta Paediatr* **92**, 379-385 (2003).

86   Broussard, C. S. *et al.* Maternal treatment with opioid analgesics and risk for birth defects. *Am J Obstet Gynecol* **204**, 314.e311-311, doi:10.1016/j.ajog.2010.12.039 (2011).

87   Rothman, K. J. & Fyler, D. C. Sex, birth order, and maternal age characteristics of infants with congenital heart defects. *Am J Epidemiol* **104**, 527-534, doi:10.1093/oxfordjournals.aje.a112326 (1976).

88   Yazdy, M. M., Mitchell, A. A., Tinker, S. C., Parker, S. E. & Werler, M. M. Periconceptional use of opioids and the risk of neural tube defects. *Obstet Gynecol* **122**, 838-844, doi:10.1097/AOG.0b013e3182a6643c (2013).

89   Wouldes, T. A. & Woodward, L. J. Maternal methadone dose during pregnancy and infant clinical outcome. *Neurotoxicol Teratol* **32**, 406-413, doi:10.1016/j.ntt.2010.01.007 (2010).

90   Tran, T. H., Griffin, B. L., Stone, R. H., Vest, K. M. & Todd, T. J. Methadone, Buprenorphine, and Naltrexone for the Treatment of Opioid Use Disorder in Pregnant Women. *Pharmacotherapy* **37**, 824-839, doi:10.1002/phar.1958 (2017).

91   Winhusen, T. *et al.* Design considerations for point-of-care clinical trials comparing methadone and buprenorphine treatment for opioid dependence in pregnancy and for neonatal abstinence syndrome. *Contemp Clin Trials* **39**, 158-165, doi:10.1016/j.cct.2014.08.009 (2014).

92   Zedler, B. K. *et al.* Buprenorphine compared with methadone to treat pregnant women with opioid use disorder: a systematic review and meta-analysis of safety in the mother, fetus and child. *Addiction* **111**, 2115-2128, doi:10.1111/add.13462 (2016).

93   Azuine, R. E. *et al.* Prenatal Risk Factors and Perinatal and Postnatal Outcomes Associated With Maternal Opioid Exposure in an Urban, Low-Income, Multiethnic US Population. *JAMA Netw Open* **2**, e196405, doi:10.1001/jamanetworkopen.2019.6405 (2019).

94   Lester, B. M. & Lagasse, L. L. Children of addicted women. *J Addict Dis* **29**, 259-276, doi:10.1080/10550881003684921 (2010).

95   Sandtorv, L. B. *et al.* Symptoms Associated With Attention Deficit/Hyperactivity Disorder and Autism Spectrum Disorders in School-Aged Children Prenatally Exposed to Substances. *Subst Abuse* **12**, 1178221818765773, doi:10.1177/1178221818765773 (2018).

96   Crews, F. T. & Nixon, K. Alcohol, neural stem cells, and adult neurogenesis. *Alcohol Res Health* **27**, 197-204 (2003).

97   Sudai, E. *et al.* High cocaine dosage decreases neurogenesis in the hippocampus and impairs working memory. *Addict Biol* **16**, 251-260, doi:10.1111/j.1369-1600.2010.00241.x

10.1111/j.1369-1600.2010.00241.x. Epub 2010 Aug 23. (2011).

98   Xu, C., Loh, H. H. & Law, P. Y. Effects of addictive drugs on adult neural stem/progenitor cells. *Cell Mol Life Sci* **73**, 327-348, doi:10.1007/s00018-015-2067-z (2016).

99   Rachael A. Olsufka, H. P., Jessica S. Newton, Kimberly Nixon. Alcohol Effects on Adult Neural Stem Cells – A Novel Mechanism of Neurotoxicity and Recovery in Alcohol Use Disorders. *Stem Cells in Birth Defects Research and Developmental Toxicology* (2018).

100   Crews, F. T. Alcohol-related neurodegeneration and recovery: mechanisms from animal models. *Alcohol Res Health* **31**, 377-388 (2008).

101   Noonan, M. A., Bulin, S. E., Fuller, D. C. & Eisch, A. J. Reduction of adult hippocampal neurogenesis confers vulnerability in an animal model of cocaine addiction. *J Neurosci* **30**, 304-315, doi:10.1523/JNEUROSCI.4256-09.2010 (2010).

102   Noonan, M. A., Choi, K. H., Self, D. W. & Eisch, A. J. Withdrawal from cocaine self-administration normalizes deficits in proliferation and enhances maturity of adult-generated hippocampal neurons. *J Neurosci* **28**, 2516-2526, doi:10.1523/JNEUROSCI.4661-07.2008 (2008).

103   Weiss, F. *et al.* Compulsive drug-seeking behavior and relapse. Neuroadaptation, stress, and conditioning factors. *Ann N Y Acad Sci* **937**, 1-26 (2001).

104   Wilson, L. D., Jeromin, J., Garvey, L. & Dorbandt, A. Cocaine, ethanol, and cocaethylene cardiotoxity in an animal model of cocaine and ethanol abuse. *Acad Emerg Med* **8**, 211-222 (2001).

105   Garlow, S. J., Purselle, D. C. & Heninger, M. Cocaine and alcohol use preceding suicide in African American and white adolescents. *J Psychiatr Res* **41**, 530-536, doi:10.1016/j.jpsychires.2005.08.008 (2007).

106   McCance-Katz, E. F., Kosten, T. R. & Jatlow, P. Concurrent use of cocaine and alcohol is more potent and potentially more toxic than use of either alone--a multiple-dose study. *Biol Psychiatry* **44**, 250-259 (1998).

107   Bolla, K. I., Funderburk, F. R. & Cadet, J. L. Differential effects of cocaine and cocaine alcohol on neurocognitive performance. *Neurology* **54**, 2285-2292 (2000).

108   Goldstein, R. Z. *et al.* Severity of neuropsychological impairment in cocaine and alcohol addiction: association with metabolism in the prefrontal cortex. *Neuropsychologia* **42**, 1447-1458, doi:10.1016/j.neuropsychologia.2004.04.002 (2004).

109   Salloum, I. M., Daley, D. C., Cornelius, J. R., Kirisci, L. & Thase, M. E. Disproportionate lethality in psychiatric patients with concurrent alcohol and cocaine abuse. *Am J Psychiatry* **153**, 953-955, doi:10.1176/ajp.153.7.953 (1996).

110   Althobaiti, Y. S. & Sari, Y. Alcohol Interactions with Psychostimulants: An Overview of Animal and Human Studies. *J Addict Res Ther* **7**, doi:10.4172/2155-6105.1000281 (2016).

111   Wise, R. A. Neural mechanisms of the reinforcing action of cocaine. *NIDA Res Monogr* **50**, 15-33 (1984).

112   Valenzuela, C. F.   (1997).

113   Deitrich, R. A., Dunwiddie, T. V., Harris, R. A. & Erwin, V. G. Mechanism of action of ethanol: initial central nervous system actions. *Pharmacol Rev* **41**, 489-537 (1989).

114   Lyne, J., O'Donoghue, B., Clancy, M., Kinsella, A. & O'Gara, C. Concurrent cocaine and alcohol use in individuals presenting to an addiction treatment program. *Ir J Med Sci* **179**, 233-237, doi:10.1007/s11845-009-0385-6 (2010).

115   Schmitz, J. M., Bordnick, P. S., Kearney, M. L., Fuller, S. M. & Breckenridge, J. K. Treatment outcome of cocaine-alcohol dependent patients. *Drug Alcohol Depend* **47**, 55-61 (1997).

116   Di Sclafani, V. *et al.* Abstinent chronic crack-cocaine and crackcocaine/alcohol abusers evidence normal hippocampal volumes on MRI despite persistent cognitive impairments. *Addict Biol* **3**, 261-270, doi:10.1080/13556219872074 (1998).

117   Graziani, M., Nencini, P. & Nisticò, R. Genders and the concurrent use of cocaine and alcohol: Pharmacological aspects. *Pharmacol Res* **87**, 60-70, doi:10.1016/j.phrs.2014.06.009 (2014).

118   Henning, R. J. & Wilson, L. D. Cocaethylene is as cardiotoxic as cocaine but is less toxic than cocaine plus ethanol. *Life Sci* **59**, 615-627 (1996).

119   Wilson, D. M. *et al.* The interaction of dopamine, cocaine, and cocaethylene with ethanol on central nervous system depression in mice. *Pharmacol Biochem Behav* **57**, 73-80 (1997).

120   Nixon, K. & Crews, F. T. Binge ethanol exposure decreases neurogenesis in adult rat hippocampus. *J Neurochem* **83**, 1087-1093 (2002).

121   Jones, H. E., Kaltenbach, K., Benjamin, T., Wachman, E. M. & O'Grady, K. E. Prenatal Opioid Exposure, Neonatal Abstinence Syndrome/Neonatal Opioid Withdrawal Syndrome, and Later Child Development Research: Shortcomings and Solutions. *J Addict Med* **13**, 90-92, doi:10.1097/ADM.0000000000000463 (2019).

122   Hunt, R. W., Tzioumi, D., Collins, E. & Jeffery, H. E. Adverse neurodevelopmental outcome of infants exposed to opiate in-utero. *Early Hum Dev* **84**, 29-35, doi:10.1016/j.earlhumdev.2007.01.013 (2008).

123   Sundelin Wahlsten, V. & Sarman, I. Neurobehavioural development of preschool-age children born to addicted mothers given opiate maintenance treatment with buprenorphine during pregnancy. *Acta Paediatr* **102**, 544-549, doi:10.1111/apa.12210 (2013).

124   Nygaard, E., Slinning, K., Moe, V. & Walhovd, K. B. Behavior and Attention Problems in Eight-Year-Old Children with Prenatal Opiate and Poly-Substance Exposure: A Longitudinal Study. *PLoS One* **11**, e0158054, doi:10.1371/journal.pone.0158054 (2016).

125   Blum, K. *et al.* Attention-deficit-hyperactivity disorder and reward deficiency syndrome. *Neuropsychiatr Dis Treat* **4**, 893-918, doi:10.2147/ndt.s2627 (2008).

126   Curatolo, P., D'Agati, E. & Moavero, R. The neurobiological basis of ADHD. *Ital J Pediatr* **36**, 79, doi:10.1186/1824-7288-36-79 (2010).

127   Arnett, A. B., Pennington, B. F., Willcutt, E. G., DeFries, J. C. & Olson, R. K. Sex differences in ADHD symptom severity. *J Child Psychol Psychiatry* **56**, 632-639, doi:10.1111/jcpp.12337 (2015).

128   Gaub, M. & Carlson, C. L. Gender differences in ADHD: a meta-analysis and critical review. *J Am Acad Child Adolesc Psychiatry* **36**, 1036-1045, doi:10.1097/00004583-199708000-00011 (1997).

129   Mowlem, F. D. *et al.* Sex differences in predicting ADHD clinical diagnosis and pharmacological treatment. *Eur Child Adolesc Psychiatry* **28**, 481-489, doi:10.1007/s00787-018-1211-3 (2019).

130   Shaw, P. *et al.* Longitudinal mapping of cortical thickness and clinical outcome in children and adolescents with attention-deficit/hyperactivity disorder. *Arch Gen Psychiatry* **63**, 540-549, doi:10.1001/archpsyc.63.5.540 (2006).

131   Shaw, P. & Rabin, C. New insights into attention-deficit/hyperactivity disorder using structural neuroimaging. *Curr Psychiatry Rep* **11**, 393-398, doi:10.1007/s11920-009-0059-0 (2009).

132   Swanson, J. M. *et al.* Etiologic subtypes of attention-deficit/hyperactivity disorder: brain imaging, molecular genetic and environmental factors and the dopamine hypothesis. *Neuropsychol Rev* **17**, 39-59, doi:10.1007/s11065-007-9019-9 (2007).

133   Pliszka, S. R. The neuropsychopharmacology of attention-deficit/hyperactivity

       disorder. *Biol Psychiatry* **57**, 1385-1390, doi:10.1016/j.biopsych.2004.08.026

       (2005).

134   Brennan, A. R. & Arnsten, A. F. Neuronal mechanisms underlying attention

       deficit hyperactivity disorder: the influence of arousal on prefrontal cortical

       function. *Ann N Y Acad Sci* **1129**, 236-245, doi:10.1196/annals.1417.007 (2008).

135   Arnsten, A. F. The Emerging Neurobiology of Attention Deficit Hyperactivity

       Disorder: The Key Role of the Prefrontal Association Cortex. *J Pediatr* **154**, I-

       S43, doi:10.1016/j.jpeds.2009.01.018 (2009).

136   Madras, B. K., Miller, G. M. & Fischman, A. J. The dopamine transporter and

       attention-deficit/hyperactivity disorder. *Biol Psychiatry* **57**, 1397-1409,

       doi:10.1016/j.biopsych.2004.10.011 (2005).

137   Volkow, N. D. *et al.* Depressed dopamine activity in caudate and preliminary

       evidence of limbic involvement in adults with attention-deficit/hyperactivity

       disorder. *Arch Gen Psychiatry* **64**, 932-940, doi:10.1001/archpsyc.64.8.932

       (2007).

138   Schonwald, A. Update: attention deficit/hyperactivity disorder in the primary care

       office. *Curr Opin Pediatr* **17**, 265-274,

       doi:10.1097/01.mop.0000156983.71532.eb (2005).

139   Casey, B. J., Nigg, J. T. & Durston, S. New potential leads in the biology and

       treatment of attention deficit-hyperactivity disorder. *Curr Opin Neurol* **20**, 119-

       124, doi:10.1097/WCO.0b013e3280a02f78 (2007).

140   Viggiano, D., Grammatikopoulos, G. & Sadile, A. G. A morphometric evidence for a hyperfunctioning mesolimbic system in an animal model of ADHD. *Behav Brain Res* **130**, 181-189, doi:10.1016/s0166-4328(01)00423-5 (2002).

141   Papa, M. *et al.* A rostro-caudal dissociation in the dorsal and ventral striatum of the juvenile SHR suggests an anterior hypo- and a posterior hyperfunctioning mesocorticolimbic system. *Behav Brain Res* **130**, 171-179, doi:10.1016/s0166-4328(01)00421-1 (2002).

142   Carboni, E., Silvagni, A., Valentini, V. & Di Chiara, G. Effect of amphetamine, cocaine and depolarization by high potassium on extracellular dopamine in the nucleus accumbens shell of SHR rats. An in vivo microdyalisis study. *Neurosci Biobehav Rev* **27**, 653-659, doi:10.1016/j.neubiorev.2003.08.008 (2003).

143   Beckstead, R. M., Domesick, V. B. & Nauta, W. J. Efferent connections of the substantia nigra and ventral tegmental area in the rat. *Brain Res* **175**, 191-217, doi:10.1016/0006-8993(79)91001-1 (1979).

144   Hnasko, T. S., Hjelmstad, G. O., Fields, H. L. & Edwards, R. H. Ventral tegmental area glutamate neurons: electrophysiological properties and projections. *J Neurosci* **32**, 15076-15085, doi:10.1523/JNEUROSCI.3128-12.2012 (2012).

145   Luo, S. X. & Huang, E. J. Dopaminergic Neurons and Brain Reward Pathways: From Neurogenesis to Circuit Assembly. *Am J Pathol* **186**, 478-488, doi:10.1016/j.ajpath.2015.09.023 (2016).

146   Pignatelli, M. & Bonci, A. Role of Dopamine Neurons in Reward and Aversion: A Synaptic Plasticity Perspective. *Neuron* **86**, 1145-1157, doi:10.1016/j.neuron.2015.04.015 (2015).

147   Duvarci, S. *et al.* Impaired recruitment of dopamine neurons during working memory in mice with striatal D2 receptor overexpression. *Nat Commun* **9**, 2822, doi:10.1038/s41467-018-05214-4 (2018).

148   Fischer, G. *et al.* Treatment of opioid-dependent pregnant women with buprenorphine. *Addiction* **95**, 239-244, doi:10.1046/j.1360-0443.2000.95223910.x (2000).

149   Byrnes, E. M. & Vassoler, F. M. Modeling prenatal opioid exposure in animals: Current findings and future directions. *Front Neuroendocrinol* **51**, 1-13, doi:10.1016/j.yfrne.2017.09.001 (2018).

150   Jones, H. E., Jansson, L. M. & O'Grady, K. E. Maternal treatment with opioid analgesics and risk for birth defects: additional considerations. *Am J Obstet Gynecol* **205**, e12; author reply e12-13, doi:10.1016/j.ajog.2011.04.026 (2011).

151   J.L.R., R.   (J Child Psychol Psychiatry, 2012).

152   Vaswani, A. R. *et al.* Correct setup of the substantia nigra requires Reelin-mediated fast, laterally-directed migration of dopaminergic neurons. *Elife* **8**, doi:10.7554/eLife.41623 (2019).

153   Tomasi, D. & Volkow, N. D. Functional connectivity of substantia nigra and ventral tegmental area: maturation during adolescence and effects of ADHD. *Cereb Cortex* **24**, 935-944, doi:10.1093/cercor/bhs382 (2014).

154   Dhakal, P. & Soares, M. J. Single-step PCR-based genetic sex determination of rat tissues and cells. *Biotechniques* **62**, 232-233, doi:10.2144/000114548 (2017).

155 Atlas, A. D. M. B. (https://developingmouse.brain-map.org/experiment/siv?id=100054035&imageId=101103312&initImage=nissl, 2008).

156 Miller, J. A. *et al.* Transcriptional landscape of the prenatal human brain. *Nature* **508**, 199-206, doi:10.1038/nature13185 (2014).

157 Gaspard, N. *et al.* An intrinsic mechanism of corticogenesis from embryonic stem cells. *Nature* **455**, 351-357, doi:10.1038/nature07287 (2008).

158 Richter, S. H., Kästner, N., Loddenkemper, D. H., Kaiser, S. & Sachser, N. A Time to Wean? Impact of Weaning Age on Anxiety-Like Behaviour and Stability of Behavioural Traits in Full Adulthood. *PLoS One* **11**, e0167652, doi:10.1371/journal.pone.0167652 (2016).

159 Can, A. *et al.* The mouse forced swim test. *J Vis Exp*, e3638, doi:10.3791/3638 (2012).

160 Sithisarn, T. *et al.* The Effects of Perinatal Oxycodone Exposure on Behavioral Outcome in a Rodent Model. *Front Pediatr* **5**, 180, doi:10.3389/fped.2017.00180 (2017).

161 Wachman, E. M. & Farrer, L. A. The genetics and epigenetics of Neonatal Abstinence Syndrome. *Semin Fetal Neonatal Med* **24**, 105-110, doi:10.1016/j.siny.2019.01.002 (2019).

162 Buffington, S. A. *et al.* Microbial Reconstitution Reverses Maternal Diet-Induced Social and Synaptic Deficits in Offspring. *Cell* **165**, 1762-1775, doi:10.1016/j.cell.2016.06.001 (2016).

163   Terrell, M. L., Hartnett, K. P. & Marcus, M. Can environmental or occupational hazards alter the sex ratio at birth? A systematic review. *Emerg Health Threats J* **4**, 7109, doi:10.3402/ehtj.v4i0.7109 (2011).

164   Charles, M. K. *et al.* Male Sex Associated With Increased Risk of Neonatal Abstinence Syndrome. *Hosp Pediatr* **7**, 328-334, doi:10.1542/hpeds.2016-0218 (2017).

165   Kandall, S. R., Albin, S., Dreyer, E., Comstock, M. & Lowinson, J. Differential effects of heroin and methadone on birth weights. *Addict Dis* **2**, 347-355 (1975).

166   Silk, T. J. *et al.* Cortical morphometry in attention deficit/hyperactivity disorder: Contribution of thickness and surface area to volume. *Cortex* **82**, 1-10, doi:10.1016/j.cortex.2016.05.012 (2016).

167   Walhovd, K. B. *et al.* Volumetric cerebral characteristics of children exposed to opiates and other substances in utero. *Neuroimage* **36**, 1331-1344, doi:10.1016/j.neuroimage.2007.03.070 (2007).

168   Monnelly, V. J. *et al.* Prenatal methadone exposure is associated with altered neonatal brain development. *Neuroimage Clin* **18**, 9-14, doi:10.1016/j.nicl.2017.12.033 (2018).

169   Gilmore, J. H. *et al.* Outcome in children with fetal mild ventriculomegaly: a case series. *Schizophr Res* **48**, 219-226, doi:10.1016/s0920-9964(00)00140-7 (2001).

170   Lyall, A. E. *et al.* Prenatal isolated mild ventriculomegaly is associated with persistent ventricle enlargement at ages 1 and 2. *Early Hum Dev* **88**, 691-698, doi:10.1016/j.earlhumdev.2012.02.003 (2012).

171   Ben-Reuven, L. & Reiner, O. Dynamics of cortical progenitors and production of subcerebral neurons are altered in embryos of a maternal inflammation model for autism. *Mol Psychiatry*, doi:10.1038/s41380-019-0594-y (2019).

172   Bani-Yaghoub, M. *et al.* Role of Sox2 in the development of the mouse neocortex. *Dev Biol* **295**, 52-66, doi:10.1016/j.ydbio.2006.03.007 (2006).

173   Andersson, E. R., Sandberg, R. & Lendahl, U. Notch signaling: simplicity in design, versatility in function. *Development* **138**, 3593-3612, doi:10.1242/dev.063610 (2011).

174   Fuss, B., Josten, F., Feix, M. & Hoch, M. Cell movements controlled by the Notch signalling cascade during foregut development in Drosophila. *Development* **131**, 1587-1595, doi:10.1242/dev.01057 (2004).

175   Stranahan, A. M., Erion, J. R. & Wosiski-Kuhn, M. Reelin signaling in development, maintenance, and plasticity of neural networks. *Ageing Res Rev* **12**, 815-822, doi:10.1016/j.arr.2013.01.005 (2013).

176   Cubelos, B. *et al.* Cux1 and Cux2 regulate dendritic branching, spine morphology, and synapses of the upper layer neurons of the cortex. *Neuron* **66**, 523-535, doi:10.1016/j.neuron.2010.04.038 (2010).

177   Stanley, J. A. *et al.* Evidence of developmental alterations in cortical and subcortical regions of children with attention-deficit/hyperactivity disorder: a multivoxel in vivo phosphorus 31 spectroscopy study. *Arch Gen Psychiatry* **65**, 1419-1428, doi:10.1001/archgenpsychiatry.2008.503 (2008).

178 Britanova, O. *et al.* Satb2 is a postmitotic determinant for upper-layer neuron specification in the neocortex. *Neuron* **57**, 378-392, doi:10.1016/j.neuron.2007.12.028 (2008).

179 Wu, C. C. *et al.* Treadmill exercise alleviated prenatal buprenorphine exposure-induced depression in rats. *Neurochem Int* **110**, 91-100, doi:10.1016/j.neuint.2017.09.012 (2017).

180 Russell, V. A. Overview of animal models of attention deficit hyperactivity disorder (ADHD). *Curr Protoc Neurosci* **Chapter 9**, Unit9.35, doi:10.1002/0471142301.ns0935s54 (2011).

181 Lou, H. C. *et al.* ADHD: increased dopamine receptor availability linked to attention deficit and low neonatal cerebral blood flow. *Dev Med Child Neurol* **46**, 179-183, doi:10.1017/s0012162204000313 (2004).

182 Committee on Obstetric Practice, A. S. o. A. M. Opioid Use and Opioid Use Disorder in Pregnancy. **711** (2017).

183 Nair, A. B. & Jacob, S. A simple practice guide for dose conversion between animals and human. *J Basic Clin Pharm* **7**, 27-31, doi:10.4103/0976-0105.177703 (2016).

184 Jones, H. E. *et al.* Treatment of opioid-dependent pregnant women: clinical and research issues. *J Subst Abuse Treat* **35**, 245-259, doi:10.1016/j.jsat.2007.10.007 (2008).

185 Midanik, L. T., Tam, T. W. & Weisner, C. Concurrent and simultaneous drug and alcohol use: results of the 2000 National Alcohol Survey. *Drug Alcohol Depend* **90**, 72-80, doi:10.1016/j.drugalcdep.2007.02.024 (2007).

186   Velasquez, M. M., von Sternberg, K., Mullen, P. D., Carbonari, J. P. & Kan, L. Y. Psychiatric distress in incarcerated women with recent cocaine and alcohol abuse. *Womens Health Issues* **17**, 264-272, doi:10.1016/j.whi.2007.02.005 (2007).

187   Salloum, I. M., Douaihy, A., Ndimbie, O. K. & Kirisci, L. Concurrent alcohol and cocaine dependence impact on physical health among psychiatric patients. *J Addict Dis* **23**, 71-81, doi:10.1300/J069v23n02_05 (2004).

188   Mengis, M. M., Maude-Griffin, P. M., Delucchi, K. & Hall, S. M. Alcohol use affects the outcome of treatment for cocaine abuse. *Am J Addict* **11**, 219-227, doi:10.1080/10550490290087992 (2002).

189   Magura, S. & Rosenblum, A. Modulating effect of alcohol use on cocaine use. *Addict Behav* **25**, 117-122 (2000).

190   Mandyam, C. D. & Koob, G. F. The addicted brain craves new neurons: putative role for adult-born progenitors in promoting recovery. *Trends Neurosci* **35**, 250-260, doi:10.1016/j.tins.2011.12.005 (2012).

191   Dutta, S. & Sengupta, P. Men and mice: Relating their ages. *Life Sci* **152**, 244-248, doi:10.1016/j.lfs.2015.10.025 (2016).

192   Sowell, E. R. *et al.* Mapping cortical change across the human life span. *Nat Neurosci* **6**, 309-315, doi:10.1038/nn1008 (2003).

193   Arain, M. *et al.* Maturation of the adolescent brain. *Neuropsychiatr Dis Treat* **9**, 449-461, doi:10.2147/NDT.S39776 (2013).

194   Cittadini, F. *et al.* Genetic and toxicologic investigation of Sudden Cardiac Death in a patient with Arrhythmogenic Right Ventricular Cardiomyopathy (ARVC)

under cocaine and alcohol effects. *Int J Legal Med* **129**, 89-96, doi:10.1007/s00414-014-1119-5 (2015).

195   O'Leary, M. E. Inhibition of HERG potassium channels by cocaethylene: a metabolite of cocaine and ethanol. *Cardiovasc Res* **53**, 59-67 (2002).

196   Lim, D. A. & Alvarez-Buylla, A. Adult neural stem cells stake their ground. *Trends Neurosci* **37**, 563-571, doi:10.1016/j.tins.2014.08.006 (2014).

197   Lazutkaite, G., Soldà, A., Lossow, K., Meyerhof, W. & Dale, N. Amino acid sensing in hypothalamic tanycytes via umami taste receptors. *Mol Metab* **6**, 1480-1492, doi:10.1016/j.molmet.2017.08.015 (2017).

198   Grahame, N. J. & Grose, A. M. Blood alcohol concentrations after scheduled access in high-alcohol-preferring mice. *Alcohol* **31**, 99-104 (2003).

199   Bunney, E. B., Appel, S. B. & Brodie, M. S. Electrophysiological effects of cocaethylene, cocaine, and ethanol on dopaminergic neurons of the ventral tegmental area. *J Pharmacol Exp Ther* **297**, 696-703 (2001).

200   Fowler, J. S. *et al.* Alcohol intoxication does not change [11C]cocaine pharmacokinetics in human brain and heart. *Synapse* **12**, 228-235, doi:10.1002/syn.890120308 (1992).

201   Ponti, G., Farinetti, A., Marraudino, M., Panzica, G. & Gotti, S. Sex Steroids and Adult Neurogenesis in the Ventricular-Subventricular Zone. *Front Endocrinol (Lausanne)* **9**, 156, doi:10.3389/fendo.2018.00156 (2018).

202   Zhang, C. L., Zou, Y., He, W., Gage, F. H. & Evans, R. M. A role for adult TLX-positive neural stem cells in learning and behaviour. *Nature* **451**, 1004-1007, doi:10.1038/nature06562 (2008).

203   Imayoshi, I. *et al.* Roles of continuous neurogenesis in the structural and functional integrity of the adult forebrain. *Nat Neurosci* **11**, 1153-1161, doi:10.1038/nn.2185 (2008).

204   Antoniadis, E. A. & McDonald, R. J. Amygdala, hippocampus and discriminative fear conditioning to context. *Behav Brain Res* **108**, 1-19 (2000).

205   Jones, J. D., Busse, G. D. & Riley, A. L. Strain-dependent sex differences in the effects of alcohol on cocaine-induced taste aversions. *Pharmacol Biochem Behav* **83**, 554-560, doi:10.1016/j.pbb.2006.03.017 (2006).

206   Bertola, A., Mathews, S., Ki, S. H., Wang, H. & Gao, B. Mouse model of chronic and binge ethanol feeding (the NIAAA model). *Nat Protoc* **8**, 627-637, doi:10.1038/nprot.2013.032 (2013).

207   Coggeshall, R. E. & Lekan, H. A. Methods for determining numbers of cells and synapses: a case for more uniform standards of review. *J Comp Neurol* **364**, 6-15, doi:10.1002/(SICI)1096-9861(19960101)364:1<6::AID-CNE2>3.0.CO;2-9 (1996).

208   Hevner, R. F. Layer-specific markers as probes for neuron type identity in human neocortex and malformations of cortical development. *J Neuropathol Exp Neurol* **66**, 101-109, doi:10.1097/nen.0b013e3180301c06 (2007).

209   Semrud-Clikeman, M. The role of inattention and social perception and performance in two subtypes of ADHD. *Arch Clin Neuropsychol* **25**, 771-780, doi:10.1093/arclin/acq074 (2010).

210   Carpenter Rich, E., Loo, S. K., Yang, M., Dang, J. & Smalley, S. L. Social functioning difficulties in ADHD: association with PDD risk. *Clin Child Psychol Psychiatry* **14**, 329-344, doi:10.1177/1359104508100890 (2009).

211   Bennett, D., Bendersky, M. & Lewis, M. Preadolescent health risk behavior as a function of prenatal cocaine exposure and gender. *J Dev Behav Pediatr* **28**, 467-472, doi:10.1097/DBP.0b013e31811320d8 (2007).

212   Loeber, R., Burke, J. D., Lahey, B. B., Winters, A. & Zera, M. Oppositional defiant and conduct disorder: a review of the past 10 years, part I. *J Am Acad Child Adolesc Psychiatry* **39**, 1468-1484, doi:10.1097/00004583-200012000-00007 (2000).

213   Wilens, T. E. The nature of the relationship between attention-deficit/hyperactivity disorder and substance use. *J Clin Psychiatry* **68 Suppl 11**, 4-8 (2007).

214   Wilens, T. E. *et al.* Do individuals with ADHD self-medicate with cigarettes and substances of abuse? Results from a controlled family study of ADHD. *Am J Addict* **16 Suppl 1**, 14-21; quiz 22-13, doi:10.1080/10550490601082742 (2007).

215   Davis, C., Cohen, A., Davids, M. & Rabindranath, A. Attention-deficit/hyperactivity disorder in relation to addictive behaviors: a moderated-mediation analysis of personality-risk factors and sex. *Front Psychiatry* **6**, 47, doi:10.3389/fpsyt.2015.00047 (2015).

216   Cinque, S. *et al.* Behavioral Phenotyping of Dopamine Transporter Knockout Rats: Compulsive Traits, Motor Stereotypies, and Anhedonia. *Front Psychiatry* **9**, 43, doi:10.3389/fpsyt.2018.00043 (2018).

217 Laizure, S. C., Mandrell, T., Gades, N. M. & Parker, R. B. Cocaethylene metabolism and interaction with cocaine and ethanol: role of carboxylesterases. *Drug Metab Dispos* **31**, 16-20, doi:10.1124/dmd.31.1.16 (2003).

218 Landry, M. J. An overview of cocaethylene, an alcohol-derived, psychoactive, cocaine metabolite. *J Psychoactive Drugs* **24**, 273-276, doi:10.1080/02791072.1992.10471648 (1992).

219 Jatlow, P. Cocaethylene: pharmacologic activity and clinical significance. *Ther Drug Monit* **15**, 533-536 (1993).

220 Hearn, W. L. *et al.* Cocaethylene: a unique cocaine metabolite displays high affinity for the dopamine transporter. *J Neurochem* **56**, 698-701, doi:10.1111/j.1471-4159.1991.tb08205.x (1991).

221 Wang, D. *et al.* Human carboxylesterases: a comprehensive review. *Acta Pharm Sin B* **8**, 699-712, doi:10.1016/j.apsb.2018.05.005 (2018).

222 Wilson, L. D. *et al.* Cocaethylene causes dose-dependent reductions in cardiac function in anesthetized dogs. *J Cardiovasc Pharmacol* **26**, 965-973 (1995).

223 Qiu, Z. & Morgan, J. P. Differential effects of cocaine and cocaethylene on intracellular Ca2+ and myocardial contraction in cardiac myocytes. *Br J Pharmacol* **109**, 293-298 (1993).

224 Cains, S., Blomeley, C., Kollo, M., Racz, R. & Burdakov, D. Agrp neuron activity is required for alcohol-induced overeating. *Nat Commun* **8**, 14014, doi:10.1038/ncomms14014 (2017).

Vita

NAME: Caitlin Reese Schlagal

BIOGRAPHICAL:

Birthdate: 17 April 1994

Birthplace: San Antonio, Texas

Mother: Donna Sue Schlagal

Father: Russell Mark Schlagal

Email: crschlag@utmb.edu

EDUCATION:

Incarnate Word University (05/2014-05/2016): Bachelor of Science – Biology, Minor – Chemistry

Tarleton State University (08/2012-12/2013)

Earl Warren High School (08/2008-05/2012): High School Degree

PUBLISHED ARTICLES IN PEER-REVIEWED JOURNALS (*denotes co-first author)

1. **Schlagal C.R.,** Xu, P., Dunn, T.J., Felsing, D.E., Merritt, C.M., Fox, R.G., Buffington, S.A., Cunningham, K.A., Wu, P. Prenatal Opioid Exposure Affects Fetal Neurodevelopment and Contributes to Hyperactive Phenotype in Adolescence. Nature Communications. *Under Review*.

2. Song, W., Ding, H., Dunn, T.J., Gao, J., Allende-Labastida, J., **Schlagal, C.R.**, Sowers, J.L., Ning, G., Feng, S., Wu, P. Subacute Metformin Treatment Leads to Better Functional Recovery after Spinal Cord Injury. Journal of Neurotrauma. *Under Review*.

3. Xu P., Shan C., Dunn T.J., Xie X., Gao J., Allende Labastida J., Zou J., Villarreal P.P., **Schlagal C.R.,** Yu Y., Vargas G., Rossi S.L., Vasilakis N., Shi P.Y., Weaver S.C., Wu P. Role of microglia in the vertical transmission of Zika virus from mother to fetal brain. PLOS Neglected Tropical Diseases.

4. **Schlagal C.R.,** Wu P. Alcohol and Cocaine Combined Substance Use on Adult Neurogenesis and Tanycyte Layer. Brain Plasticity.

5. McGrath E.L.*, **Schlagal C.R.***, Cortez I., Gao J., Dunn T.J., Fox R., Stutz S., Hommel, J.D., Dineley K.T., Cunningham K.A., Kaphalia B.S., Wu P. Chronic poly-drug administration damages adult mouse brain neural stem cells. Brain Research.

6. **Schlagal C.R.,** Wu P. Tipsy Neural Stem Cells: Chronic effects of Alcohol on the Brain. Neural Regeneration Research. doi:10.4103/1673-5374.243702

7. Wang L., **Schlagal C.R.**, Gao J., Hao Y., Dunn T.J., McGrath E.L., Allende Labastida J., Yu Y., Feng S., Liu S., Wu P. Oligodendrocyte Differentiation from Human Neural Stem Cells: a Novel Role for c-Src. Neurochemistry International. https://doi.org/10.1016/j.neuint.2018.07.006

CURRENT GRANT SUPPORT AND SCHOLARSHIPS

5T32DA007287-23 (NEW)- National Institute on Drug Abuse
"Neural and Pharmacological Mechanisms of Abused Drugs"
Caitlin Schlagal
Amount per year: $33,471

COMMITTEE RESPONSIBILITIES:

1. Task Force Leader for the Texas Bay Area Council on Drugs and Alcohol (2017-present)

2. Social Media Scientific Advisor for the Gulf Coast Community Coalition (2018-present)

TEACHING/MENTORING EXPERIENCE:

Taught research laboratory skills to undergraduate mentees and helped lead them through a short-term independent project. Facilitated neuroscience anatomy wet labs for medical students.

Undergraduate Mentees:

Naazneen Ibtehaj

Permanent address: 8447 Timber Loche
 San Antonio, TX 78250

This dissertation was typed by Caitlin R. Schlagal.